EPA-650/2-74-102
OCTOBER 1974

Environmental Protection Technology Series

PARTICULATE SIZING TECHNIQUES FOR CONTROL DEVICE EVALUATION

Office of Research and Development
U.S. Environmental Protection Agency
Washington, DC 20460

EPA-650/2-74-102

PARTICULATE SIZING TECHNIQUES FOR CONTROL DEVICE EVALUATION

by

W. B. Smith, K. M. Cushing, and J. D. McCain

Southern Research Institute
2000 Ninth Avenue South
Birmingham, Alabama 35205

Contract No. 68-02-0273
ROAP No. 21ADM-011
Program Element No. 1AB012

EPA Project Officer: D. B. Harris

Control Systems Laboratory
National Environmental Research Center
Research Triangle Park, North Carolina 27711

Prepared for

OFFICE OF RESEARCH AND DEVELOPMENT
U.S. ENVIRONMENTAL PROTECTION AGENCY
WASHINGTON, D.C. 20460

October 1974

This report has been reviewed by the Environmental Protection Agency and approved for publication. Approval does not signify that the contents necessarily reflect the views and policies of the Agency, nor does mention of trade names or commercial products constitute endorsement or recommendation for use.

TABLE OF CONTENTS

		Page
List of Figures		iv
Sections		
I	Conclusions	1
II	Introduction	3
	A. Inertial Methods	4
	B. Diffusional Methods	5
	C. Optical Particle Counters	6
III	Experimental Methods For Measuring Particle Size Distributions For Control Device Evaluation	9
	A. Impactors	9
	B. Optical & Diffusional Methods	14
IV	Field & Laboratory Evaluation Of Various Inertial Particle Sizing Devices	26
	A. Field Tests	26
	B. Laboratory Tests	29
	C. Cascade Impactor Data Reduction	60
V	Appendix A - Impactor Operating Techniques	66
	A. Impactor Selection	66
	B. Sampling Time	67
	C. Collection Substrates & Adhesives	67
	D. Multipoint Dampling	71
	E. Impactor Orientation	71
	F. Heating Impactor	72
	G. Probes	72
	H. Balance Requirements	72
	I. Sampling Configurations	73
	J. Preparing the Impactors	77
	K. Taking the Sample	79
	L. Disassembling the Impactor	80
	M. Data Logging	81
	N. Cascade Impactor Data Reduction	81
	Appendix B - Extractive Sampling	104
	Appendix C - Diffusional Particle Sizing	109
	A. Experimental Procedure	109
	B. Data Analysis	111
	Appendix D - Optical Techniques	116
	References	118

LIST OF FIGURES & TABLES

Figure No.	Title	Page No.
1a	Parallel Plate Diffusion Battery. The batteries have 12 or 100 channels, 0.1 x 10 x 48 cm	7
1b	Penetration Curves for Monodisperse Aerosols. (100 channels, 0.1 x 10 x 48 cm)	7
Table I	Size Fractionating Points of Some Commercial Cascade Impactors for Unit Density Spheres	10
2	Optical and Diffusional Sizing Systems	15
3	Fractional Loss Rate of Monodisperse Aerosols by Coagulation (by Haberl & Fusco[11])	18
4	Calibration Curve for Climet Optical Particle Counter. Polystyrene latex (PSL) spheres were used as standards	18
5	Correlation of Optical and Sedimentation Diameters. Data acquired using fly ash obtained from a coal-fired boiler	21
6	Particle Size Distribution At Inlet And Outlet of Electrostatic Precipitator At The Effluent of a Coal-Fired Power Boiler	25
7	Schematic Representation of the Vibrating Orifice Aerosol Generator	30
8	Ammonium Fluorescein Aerosol Particles Generated Using The Vibrating Orifice Generator. The Particle Diameters are 5.4 μm	33
9	Percentage Wall Loss vs. Particle Size Andersen Stack Sampler (0.5 acfm, 25°C, 29.60" Hg)	36

LIST OF FIGURES & TABLES

Figure No.	Title	Page No.
10	Percentage Wall Loss vs. Particle Size. Brink Cascade Impactor (0.03 acfm, 25°C, 29.60" Hg)	37
11	Percentage Wall Loss vs. Particle Size. University of Washington (Pilat) Impactor (0.5 acfm, 25°C, 29.60" Hg)	38
12	Stage Collection Efficiency vs. Particle Size. First Stage - University of Washington (Pilat) Impactor (0.5 acfm, 25°C, 29.60" Hg)	39
13	Stage Collection Efficiency vs. Particle Size. Second Stage - University of Washington (Pilat) Impactor (0.5 acfm, 25°C, 29.60" Hg)	40
14	Stage Collection Efficiency vs. Particle Size. First Stage - Andersen Stack Sampler (0.5 acfm, 25°C, 29.60" Hg)	41
15	Stage Collection Efficiency vs. Particle Size. Second Stage - Andersen Stack Sampler (0.5 acfm, 25°C, 29.60" Hg)	42
16	Stage Collection Efficiency vs. Particle Size. Third Stage - Andersen Stack Sampler (0.5 acfm, 25°C, 29.60" Hg)	43
17	Stage Collection Efficiency vs. Particle Size. Fourth Stage - Andersen Stack Sampler (0.5 acfm, 25°C, 29.60" Hg)	44
18	Stage Collection Efficiency vs. $\sqrt{\Psi}$ Andersen Stack Sampler - Glass Fiber Filter Substrates (0.5 acfm, 25°C, 29.60" Hg)	46
19	Stage Collection Efficiency vs. $\sqrt{\Psi}$ Brink Cascade Impactor - Bare Collection Plates (0.03 acfm, 25°C, 29.60" Hg)	47
20	Stage Collection Efficiency vs. $\sqrt{\Psi}$ Brink Cascade Impactor - Glass Fiber Filter Substrates (0.03 acfm, 25°C, 29.60" Hg)	48

LIST OF FIGURES & TABLES

Figure No.	Title	Page No.
21	Stage Collection Efficiency vs. $\sqrt{\Psi}$ Brink Cascade Impactor - Greased Plates 90.03 acfm, 25°C, 29.60" Hg)	49
22	Stage Collection Efficiency vs. $\sqrt{\Psi}$ University of Washington (Pilat) Impactor (0.5 acfm, 25°C, 29.60" Hg)	50
23	Stage Collection Efficiency vs. Particle Size. Brink C2 (Externally Mounted) Cyclone (0.03 acfm, 25°C, 29.60" Hg)	52
24	Stage Collection Efficiency vs. Particle Size. Brink C3 (Inline) Cyclone (0.03 acfm, 25°C, 29.60" Hg)	53
25	Stage Collection Efficiency vs. Particle Size. Andersen Cyclone Precollector (0.5 acfm, 25°C, 29.60" Hg)	54
26	Stage Collection Efficiency vs. Particle Size. McCrone Cyclone T2A - 0.13" H_2O	55
27	Stage Collection Efficiency vs. Particle Size. McCrone Cyclone T2A - 1.00" H_2O	56
28	Stage Collection Efficiency vs. Particle Size. McCrone Cyclone T2B - 0.80" H_2O	57
29	Stage Collection Efficiency vs. Particle Size. McCrone T2B - 20.0" H_2O	58
Table II	Environmental Research Corporation Tag Sampler (Greased Plates)	59
30	Stage Collection Efficiency for a Brink Cascade Impactor with a Pre-collector Cyclone	61
31	Simulated Impactor Tests: a) Input "true" distribution, b) Calculated distribution (Picknett method), c) Calculated distribution (D_{50} method)	62

LIST OF FIGURES & TABLES

Figure No.	Title	Page No.
32	Simulation of a Continuous Particle Size Distribution	64
33	Impactor Tests Using a Known Particle Size Distribution	65
A1	Nomograph For Selecting Nozzles For Iso-kinetic Sampling	68
A2	Sampling Time Determination For Total Mass Collection of 25 Milligrams	69
A3	The Original Brink Impactor System, BMS-11, Set-up for out of stack sampling	74
A4	An Improved Method of Flow Control for the Brink Impactor using a calibrated orifice flowmeter	75
A5	The typical Andersen or Pilat setup using calibrated orifice and dry gas meter	78
A6	Form used for logging field test data	82
B1	Extraction and Dilution system for out of stack flue gas sampling	105
B2	Diffusional Adsorption Apparatus for Removal of H_2O From Sample Aerosol	108
C1	Diffusion battery and condensation nuclei counter lay-out for fine particle sizing	110
C2	Nomograph for determining fine particle size distribution using diffusion battery data	113
C3	Experimental diffusion battery data to be used in conjunction with Figure C2 in determining fine particle size distribution	114

I. CONCLUSIONS

In this study, three techniques were used to measure particle size distributions in industrial plant environments under a variety of conditions. Cascade impactors were primarily used in the particle size range from 0.5 to 20 μm, diffusion batteries and CN counters in the size range from 0.01 to 0.2 μm, and optical counters in the range from 0.3 μm to 2 μm. In addition, laboratory tests were performed on several impactors and cyclones to measure their stage collection efficiencies. An Institute-built vibrating orifice aerosol generator was used in our calibration work.

It was found that when used properly, and with extreme care, cascade impactors can give reliable particle size information. No single impactor was versatile enough, however, to make accurate measurements under the extreme variations in grain loading which occur between inlets and outlets on control devices, or from site to site. Low flow rate impactors were found to be most useful in the case of high grain loadings, while high flow rate impactors are more convenient in low grain loading situations.

With the exception of the first stage of the University of Washington Mark III Source Test Cascade Impactor, all of the impactor stages tested had stage collection efficiencies which agreed fairly well with the theory of Rantz and Wong. Wall losses were significant, explaining the fact that cascade impactors normally give grain loadings about 30% lower than those measured using the EPA method five.

Diffusional sizing was found to be practical with diluted samples, although the procedure is tedious and requires extensive sampling times. This method is most accurate and useful on sources where the particle size distribution and number concentration are relatively stable.

The dilution system which was used with the diffusional and optical sizing systems was reliable and linear over a wide range of dilution ratios. Typical dilution factors varied from

30 to 300 at control device outlets to 200-1000 at the inlets.

Although emphasis was not placed on the use of optical particle counters during this project, they proved valuable because their useful size ranges overlapped with that of the cascade impactors. This allowed for a check on the quality of the impactor size distribution measurements. In general, the particle size distributions and fractional efficiencies calculated from optical data and impactor data were in good agreement.

The system used in this study has proven the feasibility of measuring particle size distributions in stack gases, and fractional efficiencies, from 0.01 μm to 15 μm. We believe that this first generation system represents a viable package which can be improved and will continue to be useful in making these extremely important measurements related to the control of fine particles.

II. INTRODUCTION

In the last few years, the emphasis on particulate control has shifted toward the fine particle size range. Fine particles are defined as particles which have diameters of less than 3 μm. These particles present special problems because they remain in the atmosphere for much longer periods of time and because they follow the gas stream into the depths of the respiratory system where a large percentage is deposited. Fine particles are more difficult to control than large particles and contribute more to the scattering of light in the visible range. In contrast, large particles are collected with higher efficiency by most particulate control devices, and those particles which penetrate the control device tend to settle out of the atmosphere more quickly. For example, the terminal, or settling, velocity of a 10 μm diameter particle of unit density is 0.3 cm/sec., while that of a 1 μm diameter particle is 0.003 cm/sec. Although most of the mass emitted from a particular pollution source may consist of large particles, in general, the largest number of particles is in the fine particle range. Thus, high mass collection efficiency does not always imply high number collection efficiency.

The work described in this report consists mainly of developing, improving, and evaluating experimental techniques and equipment for measuring fine particle size distirbutions and the fractional efficiency (efficiency as a function of particle size) of pollution control devices. Laboratory tests have been performed to evaluate commercial sizing instruments and to find the optimum operating conditions for these instruments. A number of field tests were performed which allowed additional evaluation of the various instruments in harsh industrial environments and which were extremely useful in developing practical sampling techniques and procedures for making particle size distribution measurements.

In order to determine fractional efficiency of particulate control devices, measurements must be made of the size and concentration of particles suspended in the flue gas at both the inlet and outlet of the devices. In making these measurements, one encounters a wide variety of testing conditions. Flue gas temperature, pressure, moisture content, and the physical properties of the particulate vary widely from device to device. Concentrations vary by orders of magnitude from inlet to outlet, and from one control device to another. Because of this complexity and range of testing conditions, and the limited useful size range of individual testing devices, more than one instrument is required to give complete information on the particle size distribution, even at a single site.

Instruments which seem to show the most promise for use in measuring particle size distributions under plant conditions are: inertial sizing devices, diffusion batteries with condensation nuclei counters, optical particle counters, opacity monitors, and electrical particle counters. The initial goal of this study was the evaluation of inertial devices, but diffusional and optical techniques were also used during many tests and considerable insight was gained into their usefulness as part of a complete particle sizing package. Thus, this paper summarizes our work on all three techniques.

A. Inertial Methods

Impactors, impingers, cyclones, and centrifuges have been used for many years for sampling and estimation of particle size. Because of its compact arrangement, the cascade impactor has generally been found to be the most suitable inertial device for mass distribution measurements of pollution emission sources. In most cases, the impactors can be inserted directly into the duct or flue, thus eliminating many condensation and sample loss problems which occur when probes are used.

Early work on impactors was done by May[1] and published in 1945. A cascade impactor similar to the one described by May has been manufactured for a number of years in England by C. F. Casella and Company. During the 1950's, Andersen,[2] and Brink[3] both developed cascade impactors for special applications and a considerable amount of theoretical and experimental work with cascade impactors was done during this period. Much of this early work was guided by the extensive empirical and theoretical studies conducted by Rantz and Wong[4] and published in 1952. Pilat[5] has provided a concise background of work on cascade impactors and a description of the development of modern devices that are suitable for air pollution research.

Existing impactors will yield information leading to a particle size distribution over the range in diameter from 0.3 μm to 15 μm. Since the amount of particulate mass collected depends upon the particulate concentration and volume of gas sampled, the design flow rate is an important consideration in selecting an impactor for a particular test situation.

Cyclones normally are most useful in sizing particles which are larger than 10 μm and in collecting more total mass than impactors. For sub-micron work, cyclones are useful as precollectors to prevent large particles from entering the system.

B. Diffusional Methods

Liu *et al*[6] have developed an electrical sizing device for sub-micron particles, and Pilat[7] is developing a low pressure impactor for sizing of particles down to 0.02 μm. Neither of these devices, however, has been used for fractional efficiency measurements. The only practical means, other than electron microscopy, for sizing particles in the 0.005 to 0.2 μm diameter size range is with diffusion batteries. A diffusion battery consists of a number of long, narrow, parallel channels, or a cluster of small bore parallel tubes. Variations in length and number of channels (or tubes) and in the aerosol flow rate are

used as a means of measuring the number of particles in a selected size range. As the aerosol moves, in streamline flow, through the channels, the random Brownian motion of a particle causes it to be displaced from its original position in the air flow streamline. The most probable displacement from a streamline is zero, but the root mean square displacement is proportioned to the square root of the travel time. Consequently, some of the particles are displaced sufficiently to reach the walls of the battery. It is assumed that once a particle contacts the battery wall, it will adhere. Therefore, only a fraction of the influent particles appear at the effluent from the battery. Because particle diffusivities increase with decreasing particle size, the extent of the penetration of the battery will depend on the particle size. The penetration of the battery can be measured with a condensation-nuclei (CN) counter. Figure 1a shows a typical diffusion battery geometry used in the work to be described in this paper. Figure 1b shows the penetration characteristics. For reasons to be discussed in the next section, extractive sampling is necessary for diffusional sizing.

C. Optical Particle Counters

Photoelectric or optical particle counters function on the principle of light scattering. Each particle in a continuous flowing sample stream is passed through a small illuminated volume. Light scattered by the particle is imaged on the surface of a photodetector during the time the particle is illuminated. The intensity of the scattered light is a function of particle size and index of refraction. Photoelectric particle counters will give reliable information if the concentration of particles is such that the probability of illuminating more than one particle at a time is low. Typically, this restriction places

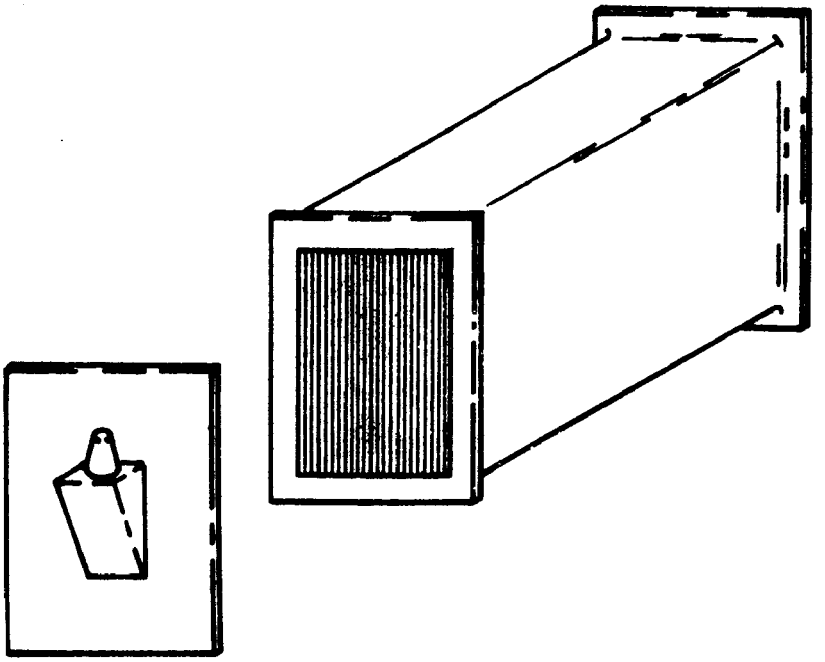

Figure 1a. Parallel Plate Diffusion Battery. The batteries have 12 or 100 channels, 0.1 x 10 x 48 cm.

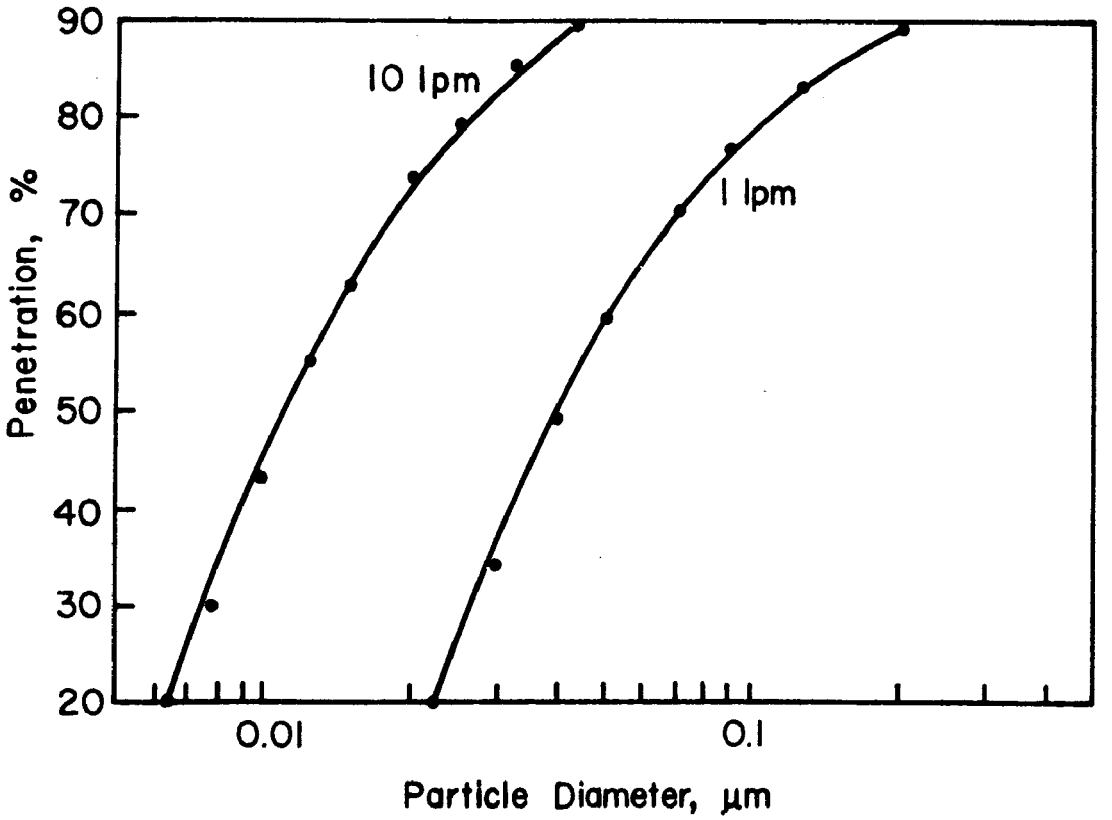

Figure 1b. Penetration Curves for Monodisperse Aerosols. (100 channels, 0.1 x 10 x 48 cm).

an upper limit of about 300 particles/cm^3 for instruments providing size information down to diameters of 0.3 μm, the practical lowest sensitivity for optical sizing. Thus, optical particle counters are effective in the same size regime as inertial sizing devices. Advantages are real-time readout and particle size data that are directly related to atmospheric visibility and plume opacity. Disadvantages are the necessity to dilute the sample to number concentrations less than 300/cm^3 and the dependence of the calibration upon the index of refraction.

By using all three of the techniques mentioned above, inertial, optical, and diffusional sizing, data can be obtained over the size range from 0.005 μm to about 20 μm diameter with some overlap. In the next section, the experimental methods with results will be described in more detail and the shortcomings of the instrumentation in the present stage of development will be discussed. Appendices are included which outline the actual procedures used for making particle size measurements in essentially "cook book" fashion. These appendices also include instruction, charts, and computer programs for data reduction.

III. EXPERIMENTAL METHODS FOR MEASURING PARTICLE SIZE DISTRIBUTIONS FOR CONTROL DEVICE EVALUATION

A. Impactors

1. General considerations in selecting the best impactor for a specific test condition -

Table I shows some characteristics of several commercially available inertial classifiers. It is usually impractical to use the same impactor at the inlet and outlet of a pollution control device for efficiency measurements because of the difference in particle concentration. For example, if a sampling time of thirty minutes is adequate at the inlet (control device efficiency of 99% is assumed), for the same amount of sample to be collected, approximately 3,000 minutes sampling time would be required at the outlet. Although the flow rates are somewhat variable, they cannot be adjusted enough to compensate for this difference without creating other problems. Extremely high flow rates result in particle bounce and in scouring of impacted particles from the lower stages of the impactor where the jet velocities become extremely high. Short sampling times may result in atypical samples being obtained as a result of momentary fluctuations in the particle concentrations or size distribution within the duct. A practical solution might be to choose, for example, to sample at the inlet with a Brink impactor and at the outlet with an Andersen. The sampling times are then adjusted to those times that are required to collect a weighable sample of small particles on the fine particle (lower) stages without accumulating so much mass on the upper stages that overloading and reentrainment occur.

2. Specific techniques used in this study -

The actual extraction of a size-fractionated sample from a gas stream using cascade impactors is a well established

Table I

Size Fractionating Points of Some Commercial Cascade Impactors for Unit Density Spheres

Stage	Modified Brink	Andersen Mark III	U. of W. (Pilat)	E.R.C. Tag
	0.85 LPM	14 LPM	14 LPM	14 LPM
Cyc	18.0 μm			
0	11.0			11.1 μm
1	6.29	14.0 μm	39.0 μm	7.7
2	3.74	8.71	15.0	5.5
3	2.59	5.92	6.5	4.0
4	1.41	4.00	3.1	2.8
5	0.93	2.58	1.65	2.0
6	0.56	1.29	0.80	1.3
7		0.80	0.49	0.9
8		0.51		0.6

procedure at this time,[1,5,7] and is summarized in Appendix A. The following paragraphs deal in general terms, mainly with the unexpected or non-ideal behavior encountered. Section IV contains specific information describing our evaluation of several commercial impactors.

- Wall Losses - Particles are lost within an impactor by diffusion and impaction on the walls and jets. Lundgren,[8] and Gussman et al[9] have shown that the losses per stage can amount to as much material as is collected by the stage. For fractional efficiency measurements, wall losses might not have a large effect on the accuracy if the percentage of losses are the same in the impactors used at the inlet and outlet. With mass concentration measurements, however, uncorrected errors of this magnitude could completely void the data. Measurements of mass concentrations taken with impactors during this study have consistently produced results about 70% as large as those obtained by the non-sizing, standard techniques.

- Reentrainment - All the particles that strike a collection stage do not stick. A technique used to enhance the retention of particles at the original impaction site which is gaining wide acceptance is coating the substrates or collection stages with a suitable viscous grease. In using grease, however, proper precautions must be taken to prevent loss of mass due to the evaporation of the volatile evaporents. One approach that was found to be satisfactory was to make a 10 to 15% suspension of Dow Corning high vacuum silicone grease in benzene. After placing a drop of this suspension on the collecting surface and allowing the benzene to evaporate, the coated substrates are baked for about an hour at 400°F and desiccated until actually used. In at least one case, anomolous weight losses were attributed to the hot grease flowing from the substrates when the impactor was operated in a horizontal position within a hot duct. As yet, no coating suitable for use at temperatures over 400°F has been found.

Even with greased substrates, significant scouring and loss of material occurs on the last stages when the jet velocities are too high. Experimentally, the value of about 65 m/sec has been established as the maximum velocity obtainable without reentrainment or grease erosion using greased substrates, and about 35 m/sec using ungreased substrates. In effect, these phenomena place upper limits on the flow rates at which an impactor may be operated to obtain a valid particle size distribution.

The Andersen Stack Sampler uses glass fiber filters as impaction substrates. These filters seem to be a satisfactory alternative to greased substrates in minimizing particle bounce and reentrainment. Glass fiber substrates have also been used with the Brink impactor at high temperatures.

- Weighing Accuracy - To achieve an accuracy of about 20% in control device penetration measurements, the mass loading in the chosen size intervals must be measured to an accuracy of about 10% at both the inlet and outlet of the control device. If the mass collected in the large particle size ranges is kept reasonably low, to avoid reentrainment, this means that a weighing accuracy of 10 to 30 μg is required for the small particle size ranges where much less mass is collected.

Techniques which have been used to minimize problems in weighing accuracy are: to reduce the tare weight of the collection stages by using light weight inserts made of aluminum foil, stainless steel shim stock, or glass fiber filter material; to purposely bias the sample against large particles by pointing the nozzle downstream; or to use cyclone precollectors to remove large particles prior to the sample entering the impactor.

The use of lightweight substrates and cyclone precollectors is becoming more common. This technique gives the maximum weighing accuracy and still permits isokinetic sampling. The capture efficiency of the precollector cyclone must be taken

into account when doing data analysis, however, or the results will not be representative of the true aerosol for large particle sizes.

- Isokinetic Sampling - If the velocity of the aerosol stream entering the impactor nozzle is the same as the velocity at the stream in the duct, the sampling is said to be "isokinetic." If the sampling velocity is too high, large particles having greater inertia cannot follow the streamlines into the nozzle. In this case, the sample would be biased against large particles. If the sampling velocity is lower than the stream velocity, particles with higher inertia will be oversampled, again biasing the results. Isokinetic sampling is necessary for particles having aerodynamic diameters greater than above 3 to 5 μm.

A selection of nozzles having different bores is available for each impactor so that for a unique flow rate, several velocities may be achieved at the inlet of the impactor. Once a particular sampling velocity is chosen, however, it cannot be changed during a test because the fractionation points at each collection stage would change. Since the velocity is fixed during a test, any fluctuations in gas velocity with time or position within the duct will introduce measurement errors in the data on the larger particles.

- Shape of Particles - The most common parameter used in describing particle size is the aerodynamic diameter. This is the diameter of a sphere of unit density which has the same settling velocity as the particle.

The Stokes or physical diameter may also be used to describe a particle size. This is the diameter of a sphere having the same density and terminal velocity as the particle.

- Density of Particles - Collection efficiencies for cascade impactors are calculated using the equations developed

by Rantz and Wong.[4] The cut points (D_{50})* may be determined for unit spheres (as was done in Table I) and corrected for density as required, or calculated for spheres having the estimated density of the aerosol particles. An "average" density can be calculated from true particle volume-weight data taken with a helium picnometer for a representative sample. If the chemical composition of the particles is known, the bulk density may be used. In some cases, the aerodynamic diameter may be the only information needed and density is not a factor.

The validity of size information based on an average density depends upon the uniformity of the density from particle to particle. A mixture of particles having very different densities could cause large errors in size distributions.

B. Optical and Diffusional Methods

1. Dilution

Because of the concentration limits for operating optical counters (300 particles/cm^3) and condensation nuclei (CN) counters (10^5 particles/cm^3), problems with condensation in the sampling lines, and losses due to agglomeration during the measurement process, it is necessary to dry and dilute the sample aerosol before it reaches these devices. The sampling and dilution problem is simplified; however, in the particle size range of interest here (0.02 - 2 μm diameter) because isokinetic sampling is not required.

Figure 2 shows schematically the testing configuration for optical and diffusional sizing. The sample is introduced at the apex of a perforated cone and clean dilution air is pumped

---

*D_{50} is the particle diameter for which a particular stage has a collection efficiency of 50%.

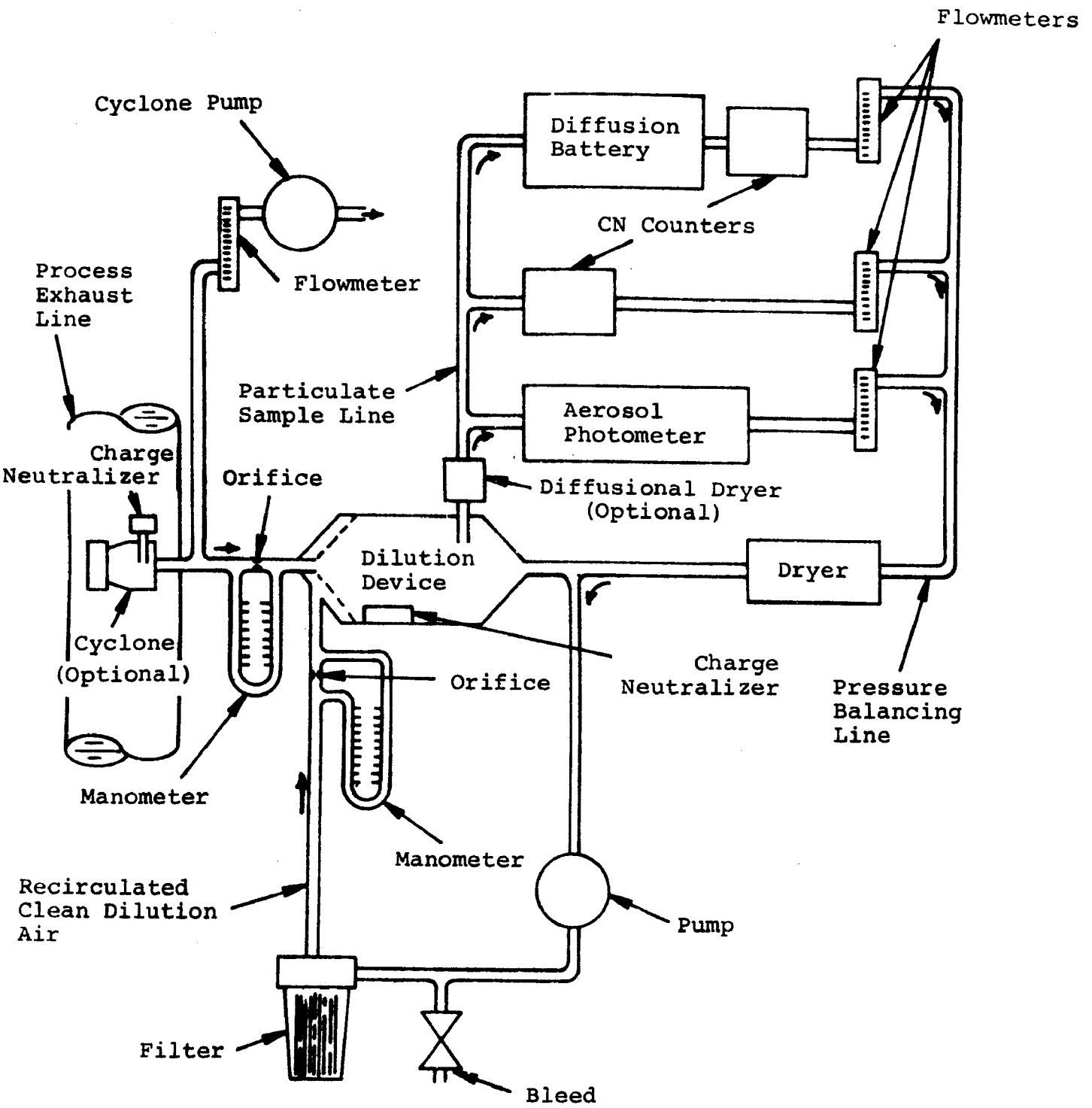

Figure 2. Optical and Diffusional Sizing System

through the perforations, creating a highly turbulent mixing zone. In verifying the performance of the diluter in the laboratory using test aerosols, it was found that the calculated and measured dilution factors agree to within the uncertainty in measuring the sample and dilution air flow rates. The concentration was found to be uniform for sampling points from wall to wall across the body of the diluter.

Drying is accomplished simultaneously with dilution by recirculating the filtered dilution air through condensers and drying tubes. In this way, the concentrations of water and other condensable vapors in the gas stream are reduced by approximately the same fraction as the particle concentration. If drying were not performed, the sample aerosol would be below the dew point for many applications and condensation would occur in the sampling lines. When the duct is below atmospheric pressure, and cool ambient air leaks into the port, it is often necessary to heat the probe to avoid condensation before the sample reaches the diluter.

Plugging of the sample metering orifice can be a problem, even when condensation does not occur. To prevent this, a cyclone precollector with a D_{50} of about 2 μm is used to eliminate large particles. Typical sample flow rates are from 0.1 lpm to 5 lpm with cyclone flow rates of about 14 lpm.

Ström[10] has done experiments to determine the significance of particle losses in sample lines. Two mechanisms were considered: 1. settling in horizontal lines, and 2. impaction at the bends. For Ström's particular system (8 m of horizontal and 8 m of vertical stainless tubing 16.8 mm in diameter, with three 90° elbows, Reynold's No. $\geq$ 2000), 90% of the particles of 15 μm diameter were lost, 30-50% of the 8 μm diameter, and almost none having diameters less than 2 μm. Diffusional losses in the probes and sample lines used in our work are estimated to be

about 98% at 0.001 μm diameter, 25% at 0.005 μm diameter and 12% of the 0.01 μm diameter. Thus, losses in the sampling lines used in this work are probably not significant for particles having diameters between about 0.005 μm and 2 μm.

Figure 3, after Haberl and Fusco,[11] shows the losses due to coagulation at various particle sizes and concentrations for monodisperse aerosols. The loss rate of a particular size, in this case, is inversely proportional to the concentration. Because of the long residence time in diffusion battery sizing, significant losses can occur if the concentration is not reduced by dilution.

2. Optical Sizing

Procedures applicable to measurement of particle sizes and concentration by light scattering have been reviewed by Hodkinson,[12] and more recently by Berglund.[13] In addition, Berglund compared the actual response of three commercially available optical particle counters with experiment using particles with different indices of refraction.

The basic operating principle for optical particle counters is the scattering of light by individual particles as they pass through a small viewing volume; the scattered light being measured by a photomultiplier tube.

A Climet Particle Analyzer, Model No. CI-201 was used in this study. This instrument uses "near forward" light scattering to obtain particle size information. The view volume is the volume shared by the focused light beam and aerosol stream. The view volume is located at one focus of an elliptical mirror, and the photomultiplier at the other. The amplitude of the scattered light pulses is related to the particle size

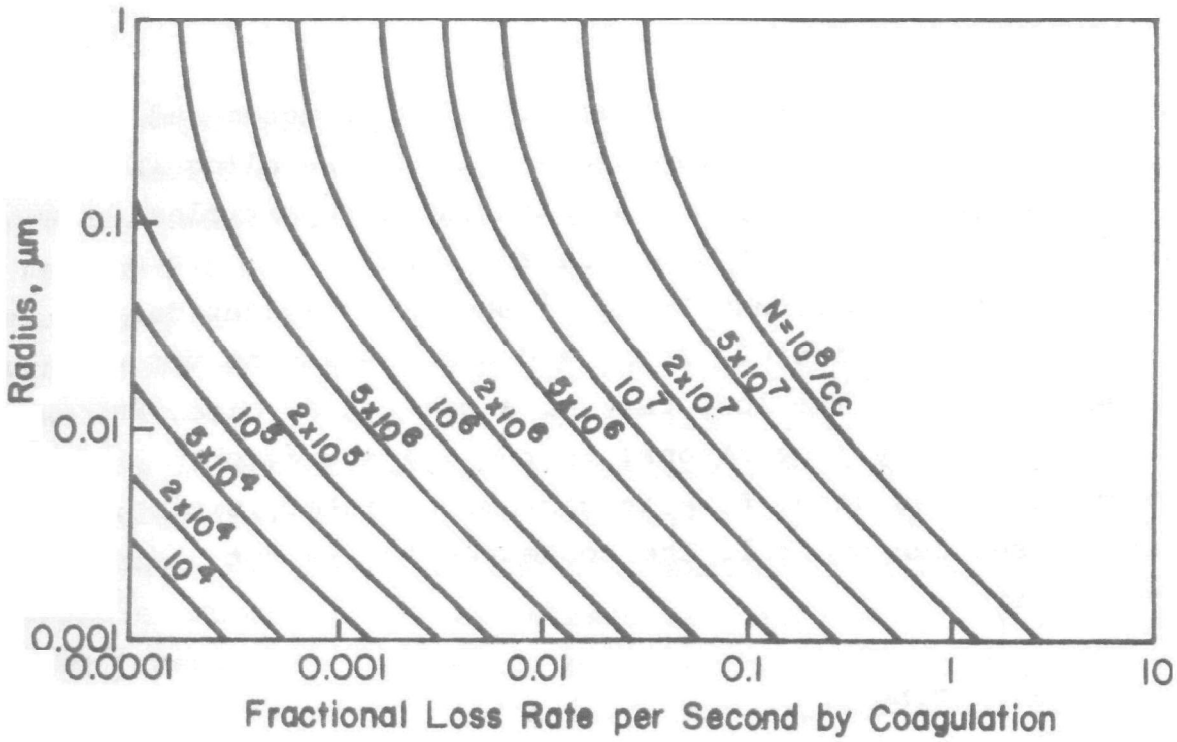

Figure 3. Fractional Loss Rate of Monodisperse Aerosols by Coagulation (after Haberl and Fusco[11]).

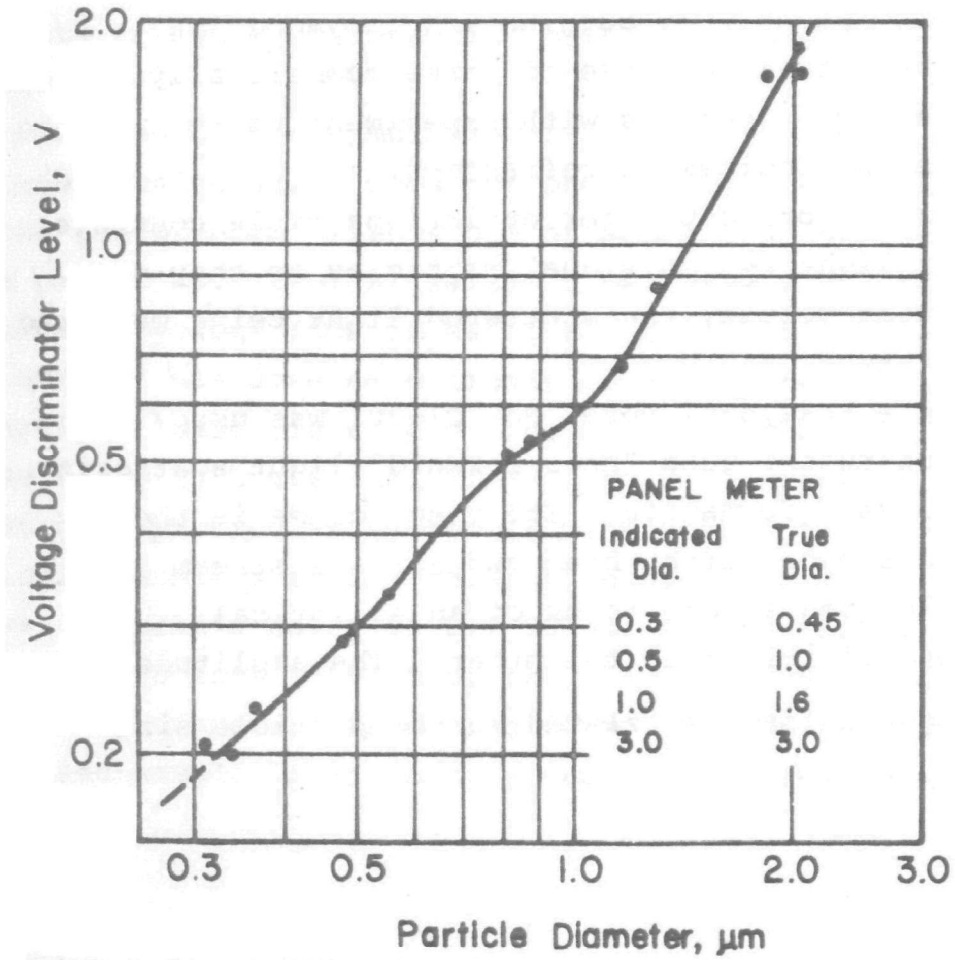

Figure 4. Calibration Curve for Climet Optical Particle Counter. Polystyrene latex (PSL) spheres were used as standards.

and the rate at which the pulses occur is related to the particle concentration. Thus, a counter of this type gives both size and number information. Operated in the configuration shown in Figure 2, with a cyclone precollector, the counter has an effective upper limit of about 1.5 μm for sizing. Also, the counter has an inherent lower limit of 0.3 μm. Thus, the counter responds to a limited size range, but gives information in an important regime, that where data from the diffusional and impactor measurements converge. The occurrence of more than one particle in the viewing volume is interpreted by the counter as a larger single particle. To avoid this effect, dilution to about 300 particles/cm^3 is necessary. This was done in the manner described in the previous section.

The intensity of the scattered light depends upon the viewing angle and upon the particle size, index of refraction, absorptivity, and shape. Some generalizations may be made from Hodkinson's review:[12]

When using white light as a source of illumination, the response to an assembly of randomly oriented, identical, nonspherical particles will be the same as that for the spherical particles of equal mean volume whose polydispersity resembles the "orientation polydispersity" of these particles. Since particles sizes are usually given in terms of some "diameter", the shape factor is relatively unimportant, but may result in more apparent polydispersity than actually exists.

If the scattered light is collected in some small angle about the forward direction, and white light is used, the dependence of the amplitude upon index of refraction can be minimized. For particles greater than 2 μm in diameter, the amplitude of the forward scattered light pulse is almost independent of the index of refraction and is proportional to the cross-sectional area of the particles. For particles less than

2 μm in diameter; however, there is no simple relationship between particle size and amplitude, and the index of refraction is more important. Berglund found that measurements deviated from theory by as much as a factor of two in the size range of 0.4 μm to 1 μm and, in some cases, the response was multivalued.

Figure 4 shows our laboratory calibration for polystyrene latex spheres having an index of refraction of 1.6. Because of the uncertainty in making a theoretical correction for index of refraction (n), the optical data was correlated with sedimentation data, a method which is independent of n. Referring again to Figure 1, if the diffusion batteries are laid on their sides, so that the long dimension of the slots is horizontal, the most important mechanism for the removal of large particles will be sedimentation, with rather high efficiencies being obtained for micron-sized particles. Concentrations of particles entering and exiting the sedimentation chambers can be measured with an optical particle counter. Sizes obtained in this way can be correlated with impactor or optical pulse height intensity data. Figure 5 shows data taken using the optical counter in conjunction with the sedimentation chambers while measuring the effluent from a coal-fired cyclone steam boiler. The particle size as indicated by the pulse height correlates very well with that calculated from sedimentation rates.

3. Diffusional Sizing

General - Diffusional sizing consists of passing an aerosol through a large number of small tubes in parallel, or between closely spaced parallel plates, and measuring the collection efficiency of the system (diffusion battery). Diffusional sizing is most useful in determining particle size distributions below 0.1 μm diameter.

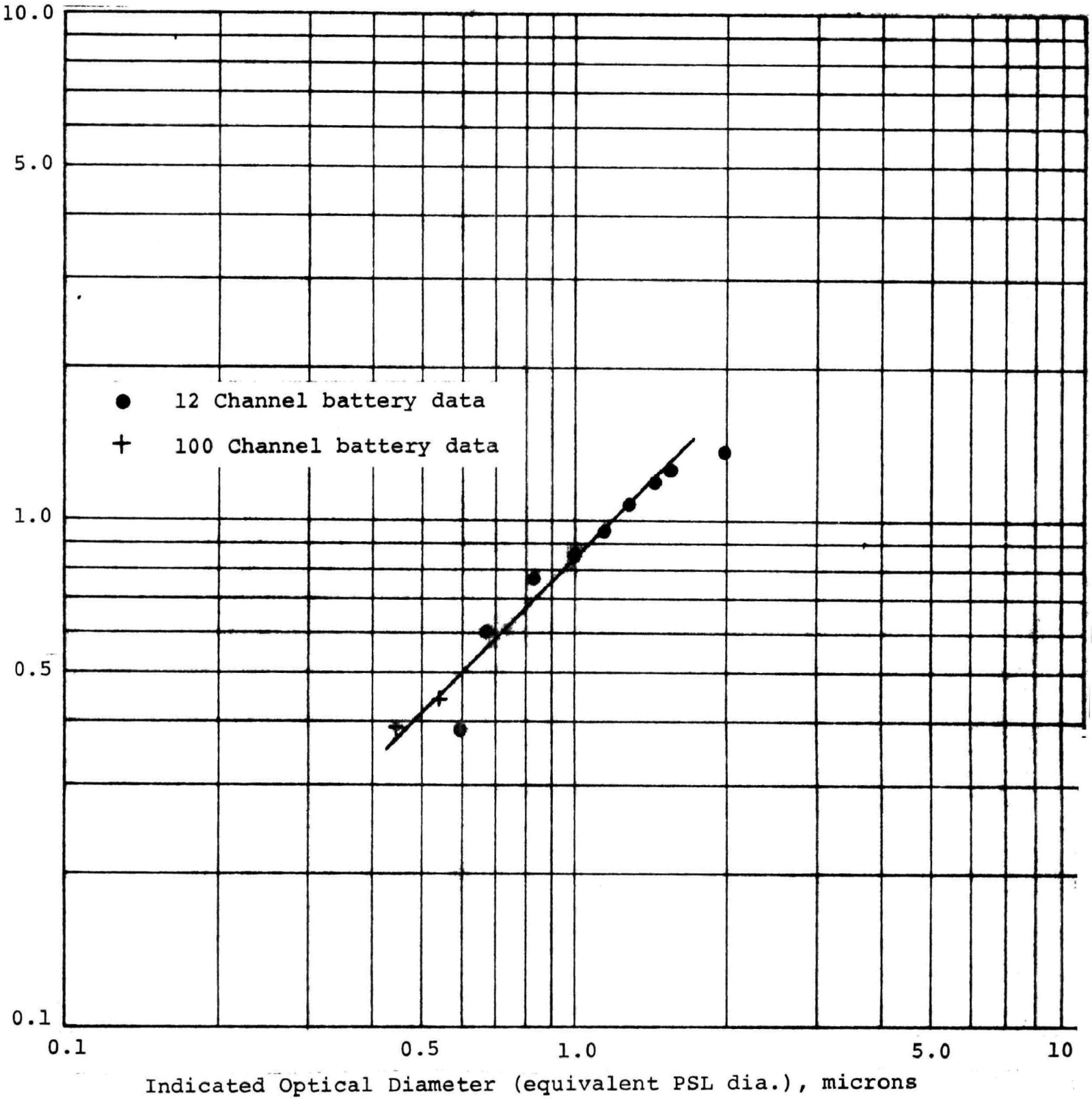

Figure 5. Correlation of Optical and Sedimentation Diameters. Data acquired using fly ash obtained from a coal-fired boiler.

Fuchs[14] has reviewed diffusion battery sizing work up to 1956, while Sinclair,[15] Breslin et al,[16] Twomey,[17] and Sansone and Weyel[18] have reported more recent work, both experimental and theoretical.

Diffusional measurements are less dependent upon the aerosol parameters than the other techniques discussed and perhaps are on a firmer basis theoretically. By changing the flow rate and diffusion battery geometry, a large number of data points can be established from which a particle size distribution may be calculated. Disadvantages are the bulk of the diffusion batteries, although advanced technology may eliminate this problem[15,16] and peculiar problems introduced by particular testing situations. For example, when testing emissions with a high SO_2 content, on one occasion, particles were actually "created" within the diffusion batteries by oxidation of SO_2 to SO_3 and subsequent formation of a sulfuric acid condensate. As in the case of optical sizing, dilution and drying of the sample air is necessary to prevent coagulation, growth of hygroscopic particles, and water condensation.

Theory - The geometry chosen for this experimental work was that of parallel plates, partly because of ease of fabrication and availability of suitable materials (Figure 1a), but also because sedimentation can be ignored if the slots are vertical, while additional information can be gained through settling, if the slots are horizontal. Sinclair[15] and Breslin et al[16] report success with more compact, tube-type arrangements in laboratory studies. The mathematical expression for the penetration (n/n_0) of a rectangular slot or parallel plate diffusion battery by a monodisperse aerosol was given in series form by Gormley.[19] The coefficients were calculated and tabulated

by Twomey[17] using a computer. The equation is:

$$n/n_0 = 0.91e^{-xmD} + 0.053e^{-11.37xmD} + 0.015e^{-33.06xmD} + 0.0068e^{-66.06xmD} + 0.0037e^{-110.4xmD} + \ldots\ldots$$

where

$x = 3.77\ bl/aQ$

b = height of each rectangular slot (cm),

l = length of each rectangular slot (cm),

$2a$ = width of each rectangular slot (cm),

Q = volumetric flow rate (cm^3/sec),

n = outlet concentration,

n_0 = inlet concentration,

D = diffusion coefficient of particles, (cm^2/sec) &

m = number of rectangular channels.

The classical diffusion coefficient is used, $D = KTb$, where the mobility "b" is size dependent.[14] If the Stokes Diameter is used to describe particle size, the penetration is virtually independent of physical properties of the individual aerosol particles.

Fuchs et al[20] presented a technique for calculating the particle-size distribution from raw data, assuming that the distribution is log normal. The technique used in this study was suggested by Sinclair[15] and does not include this restriction. A nomograph is prepared using the penetration for each diffusion battery geometry and flow rate and a large number of monodisperse particle sizes. Comparing this nomograph with experimental penetrations, one calculates the particle size distribution using a "graphical stripping" process.

Experimental - The diffusion batteries were constructed from 1 mm thick aluminum plates, with 1 mm spacing, sealed in a rectangular aluminum box. By using one to four large batteries in series, or the small battery, and several flow

rates for each configuration, a large number of data points can be obtained. The inlet and outlet concentrations may be measured with a single CN counter, or in cases where the concentrations fluctuate rapidly, the inlet and outlet concentrations can be monitored simultaneously using two CN counters. Flow pulsations caused by the cyclic processes in the CN counters were minimized by using anti-pulsation devices as described by Sinclair.[15]

Because of the time required to accomplish diffusion sizing, this technique is most useful where concentrations do not fluctuate rapidly. Diffusional sizing is independent of density, index of refraction, and to a large extent, shape. Further, if the response of the CN counter is linear, diffusional sizing is independent of errors in calibration of the CN counter. The calibrations of the instruments used in these studies were provided by the Environment One Corporation with the exception that concentrations were kept below 10^5 particles/cm^3 in accordance with the results of recent work by Liu.[21]

Figure 6 shows data taken at the inlet and outlet of a coal fired power boiler using all three techniques discussed above. The agreement among the methods in the overlap ranges is quite good.

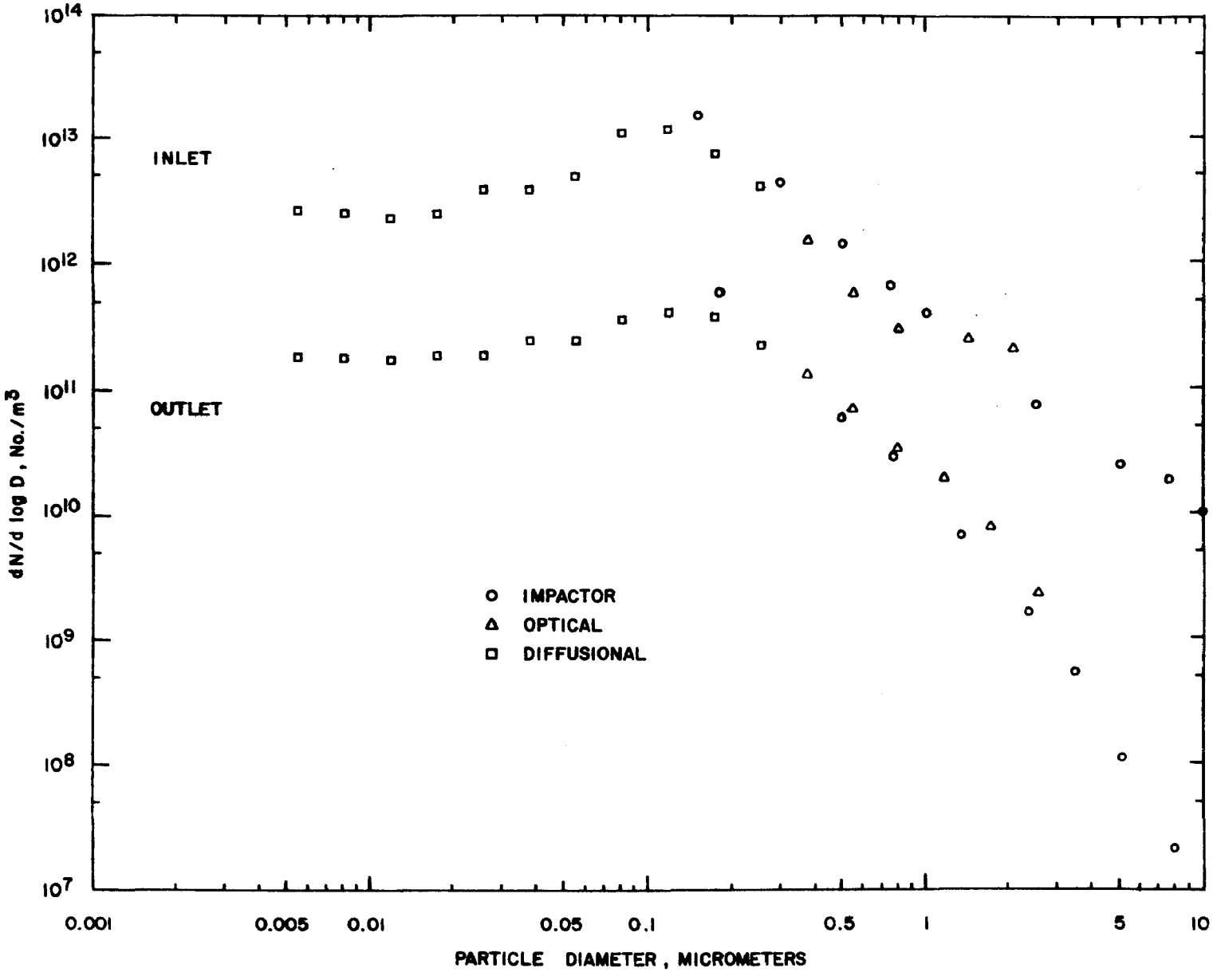

FIGURE 6. PARTICLE SIZE DISTRIBUTION AT INLET AND OUTLET OF ELECTROSTATIC PRECIPITATOR AT THE EFFLUENT OF A COAL FIRED POWER BOILER.

IV. FIELD AND LABORATORY EVALUATION OF VARIOUS INERTIAL PARTICLE SIZING DEVICES

A. Field Tests

Extensive field and laboratory studies have been conducted during this project to evaluate the performance of commercially available inertial particle sizing devices. Our early field test evaluations were reported in Progress Narrative Number 10 (NTIS Pub. No. PB-226-292/lwp). Since that time, we have performed several additional field tests and as a result, have gained additional insight into the proper use of these devices to yield valid particle size distributions. The following paragraphs are a summary of the knowledge gained through our field experience with cascade impactors.

- Of the inertial classifiers tested, no single device was found to be useful over the entire range of particle size and concentration needed for evaluation of a wide variety of particulate control device. In general, the inertial classifiers designed to operate at low sample flow rates are useful at the inlet of a control device where the particulate loading is high; the low flow rates permit reasonably long sampling times to be used. If these same low-flow-rate classifiers are used at the outlet of a control device, the sampling time may be impractically long, so that a high-flow-rate device is usually a better choice at the outlet.

- One possible solution to the problem of measuring fine particles in the presence of high concentrations of large particles is to use one or more small cyclones in front of the impactor. Modified Brink Impactors and the Andersen Model III were successfully used in this manner during our field tests. The Andersen cyclone was supplied by Andersen 2000 Inc.. The Brink Inline (C3) Cyclone and Brink External (C2) Cyclone were designed and built by Southern Research Institute.

- Most of the impactors have collection stages that are too heavy for obtaining accurate measurements of the weight of particles collected in a size fraction. It is helpful to cover the stage with a lightweight collection substrate made of aluminum foil, teflon, glass fiber filter material, or other suitable lightweight materials depending on the particular application. With such an arrangement, it is possible to make accurate weight determinations of collected samples that are small enough to prevent or at least minimize reentrainment. Weighing to a precision of at least 30 μg appears to be required for impactor size determination for submicron particles and 10 μg precision is desirable.

- When impactors are operated at flow rates higher than some critical value, particle bounce can lead to incorrect sizing with non-cohesive particulates. This is especially true in the lower (fine particulate) stages. In these lower stages, the high jet velocities cause scouring of the plates which are quite noticeable and is an almost certain indication of reentrainment. Experience with the University of Washington Mark III and the Brink Impactor indicate that the maximum jet velocities that can be used for impaction on ungreased substrates without severe reentrainment resulting from particle bounce is about 40 m/sec. Also, the physical properties of the particles can effect the maximum loading that can be safely obtained on an impaction stage. For example, with some emission sources, a small quantity of cohesive particulate materials will form a pile that will plug the stage orifice. For other types of emission sources with dry particulates, reentrainment and particle bounce problems can be severe, even with low flow rates. The use of a silicone grease that is stable at high stack temperatures is helpful for measuring dry particulates. It has been our experience that even with this grease, erosion and scouring can

occur on the lower stages with high jet velocities (velocities greater than 65 m/sec.)* The scouring and reentrainment can be reduced by reducing the flow rate in the impactor. For example, if the Brink sample flow is reduced from the recommended value of 2.8 l/min (0.1 cfm), to approximately 1.4 l/min (.05 cfm), the scouring effect can be eliminated. This change in flow rate increases the cut point of each size fraction and decreases the amount of information that can be obtained in the small particle size range. These comments are appropriate for the Andersen and other impactors as well as the Brink. However, the addition of a final stage to the impactor with the proper combination of velocity and jet diameter would make it possible to regain the information lost at the lower flow rate. This has been done on the Brink by adding a "6th" stage designed and built at Southern Research Institute.

- Glass fiber "back up" filters have generally been used after the final stage in our impactor tests. For some emission sources, the back-up filter frequently showed a weight loss instead of a weight gain. This result appears to be related to filter handling problems and poor design of filter retainers and seats. Care must be taken to avoid tightening of the Andersen Impactor too severely causing the steel o-rings to tear the filter substrates and leading to weight losses if pieces of the filter are lost or blown off.

- Particle size measurements have been made with the impactors mounted outside the stack. Sampling probes and lines

---

*Also, under some flue gas conditions, such as high SO_x content, we have experienced severe weight loss with the high vacuum grease. The reason for this weight loss is still unknown.

were used to transport the sample to the impactor. Based on simultaneous size determination with the instack and out-of-stack sampling arrangements, it seems almost certain that a significant quantity of particles are lost in the probe and sampling lines, particularly in sizes larger than 2 μm.

- A comparison of all of the fractional efficiency curves shows that measurements with the modified Brink Impactors, Brink with grease, Brink kit, Andersen Model II, and U. of W. Mark III all seem to result in about the same calculated efficiency.

B. Laboratory Tests

Laboratory evaluation of the particle sizing devices tested during this study involved the use of a vibrating orifice aerosol generator (VOAG) as a source of monodisperse aerosols. The VOAG used in this study was designed and built at Southern Research Institute, although similar devices have been reported by several authors previously.[22,23,24] Figure 7 is a schematic diagram showing the operating principle of the VOAG. A solution of known concentration (in our case, a solution of fluorescein in 0.1N NH_4OH) is forced through a small orifice (5, 10, 15, or 20 μm diameter). The orifice is attached to a piezoelectric ceramic which, under electrical stimulation, will vibrate at a known frequency. This vibration imposes periodic perturbations on the liquid jet causing it to break up into uniformly-sized droplets. Knowing the liquid flow rate and the perturbation frequency, the droplet size can be readily calculated. The solvent evaporates from the droplets leaving the nonvolatile solute as a spherical residue. The ultimate dry particle size is calculated from the droplet size through the known concentration of the liquid solution.

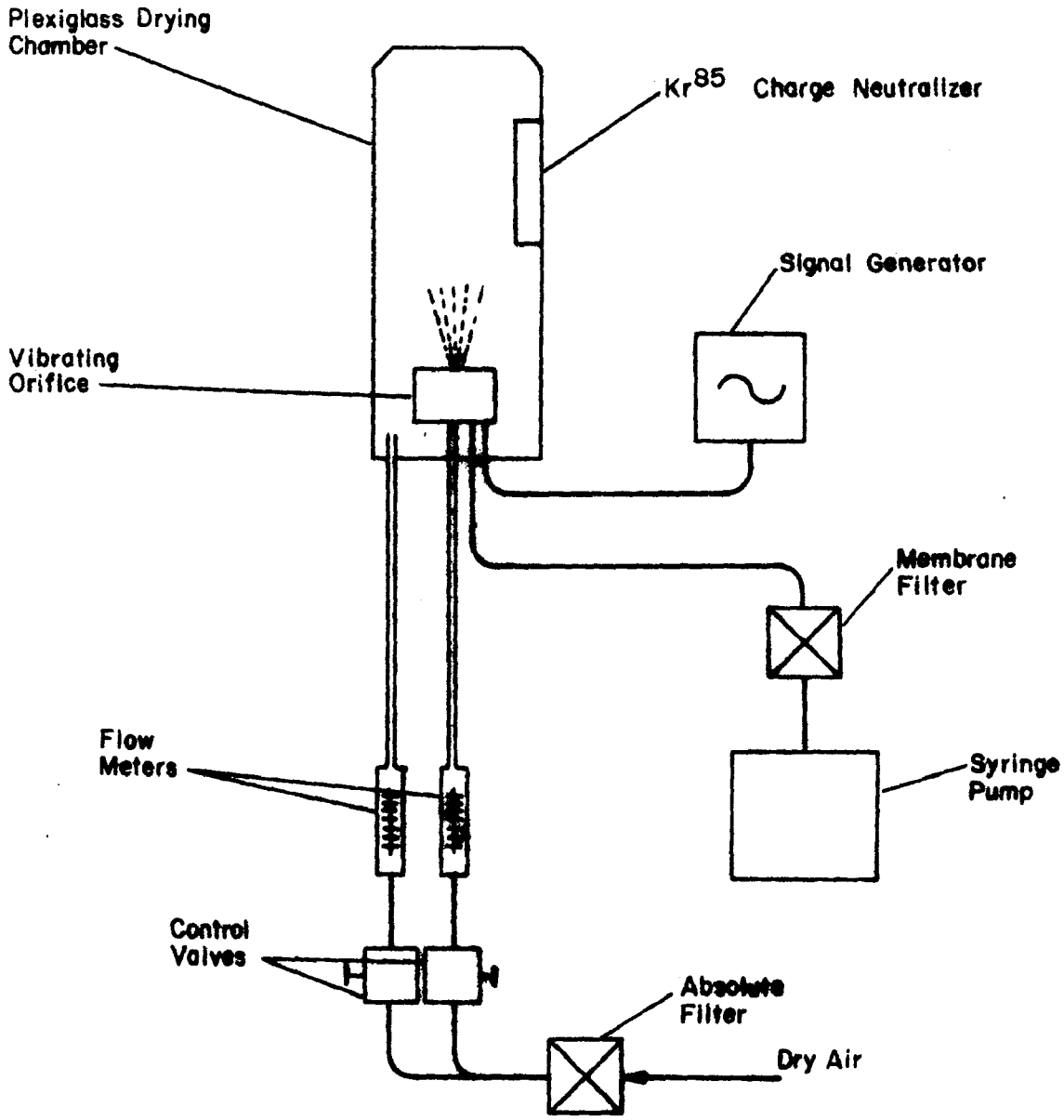

Figure 7. Schematic Representation of The Vibrating Orifice Aerosol Generator

To calculate the dry particle size, the expression

$$d_p = \left(\frac{6QC}{60\pi f} \right)^{1/3}$$ is used.

C is the solution concentration or $\frac{\text{volume of solute}}{\text{volume of solution}}$,

Q is the solution flow rate (cm^3/min.), and

f is the perturbation frequency (Hz).

By going to smaller orifices, one can obtain much higher operating frequencies. This yields higher particle number concentrations and allows shorter running times in the calibration studies. The running time must be sufficiently long to allow accurate determination of the stage collection efficiencies and wall losses. It was our experience that the 20 μm diameter orifice was consistently easier to use in particle generation, primarily because of clogging problems. The orifices were washed in detergent with ultrasonic agitation and then rinsed several times in distilled water, also with ultrasonic agitation. After the filter and liquid handling system was flushed several times with the aerosol solution to be used, the orifices were placed, still wet with distilled water, into the crystal holder and the syringe pump turned on. A jet of air was played over the orifice to keep the surface clear until enough pressure was built up behind the orifice to form a jet.

After a stream of particles was generated, a determination of monodispersity had to be made. There are two methods to do this. By using a small, well-defined air jet to deflect the stream of particles, it was possible to tell when the aerosol was mono- or polydisperse. Depending on particle size, the stream was deflected by the air at different angles. During polydispersity, several streams can be seen at one time. By varying the crystal oscillation frequency, the system could be

tuned to give only a single deflected particle stream, thus indicating monodispersity. On several occasions, the aerosol tended to drift from monodispersity. To protect against this occurrence, a filter sample was drawn to be viewed under an optical microscope. This was a good check on the quality of the aerosol because the final particles were investigated instead of the primary liquid droplet. This served as a check for proper drying, satellites, proper size, and multiplets. Kr^{85} beta sources were placed near the air stream as charge neutralizers to minimize the loss of particles due to electrostatic forces. A three-foot-high cylinder was placed on the generator and dispersion and dilution air turned on to disperse and loft the particles into a plenum with several sampling ports. It was found that drying columns had to be put in the dilution air line to adequately dry the particles before they enter the sizing devices. (This is not the case with alcohol as a solvent.) During each test, filter samples were drawn at intervals to insure continual monodispersity. Because of its nonhygroscopicity and physical[25] properties, ammonium fluorescein was used throughout these studies as our test aerosol, although in theory, any material that will dissolve readily in an evaporable solvent could be used. Figure 8 shows a 5.4 μm diameter test aerosol. In general, we found about 8% by mass of the particles were doublets.

The devices evaluated in this laboratory study were the Brink Cascade Impactor using bare plates, filter substrates, and greased plates; The Brink Precollector Cyclones (C2 externally mounted and the C3 inline cyclone); The Andersen Stack Sampler with filter substrates; The Andersen Precollector Cyclone; the University of Washington Source Test Cascade Impactor with greased plates; the ERC Tag Sampler with greased plates; and the McCrone Parallel Cyclone.

In all cases, a back-up filter was used to collect material

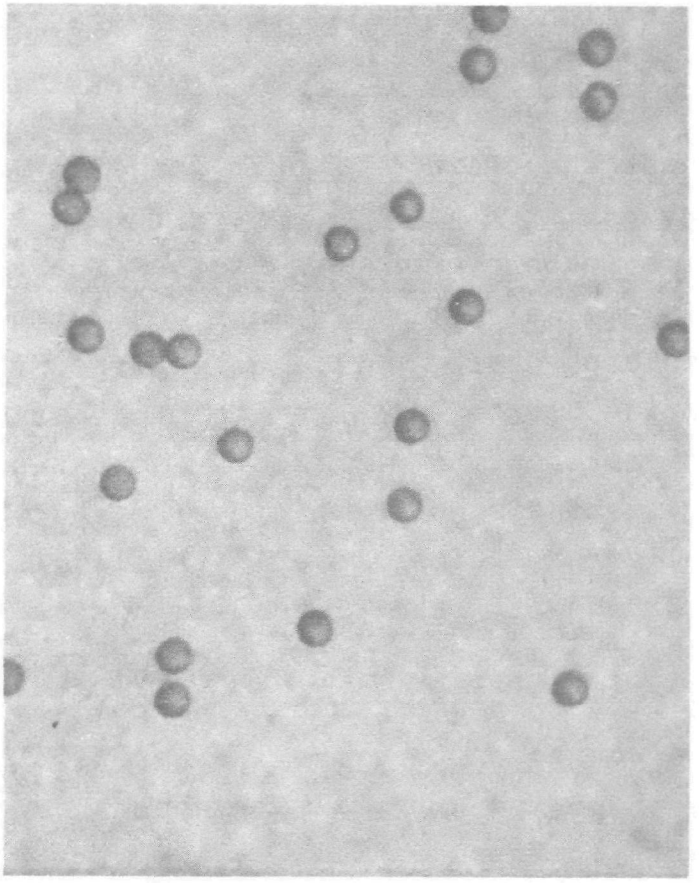

Figure 8. Ammonium Fluorescein Aerosol Particles Generated Using The Vibrating Orifice Generator. The Particle Diameters are 5.4 μm.

passing the last impaction stage. This insured our ability to calculate the collection efficiency of all stages tested.

After several trials using high vacuum silicone grease, agar, K-Y Jelly, and Vasoline, it was found that vasoline was the most convenient material to use as a greased substrate medium because it goes easily into solution in a small amount of benzene.

In the initial portion of this laboratory work, the larger aerosols were generated. During this period, only the upper impactor stages were prepared since all the aerosol should have been caught by at least the third or fourth stage in most cases. In all tests, a back-up filter was used after the last stage. For the McCrone device, each cyclone was tested separately with a back-up filter. As smaller particles were generated, more stages were tested in each device until the entire device was used. A pump and flow-metering device for each impactor insured repeatability in flow rate during each test. Most tests ran 30 minutes to 2 hours depending on particle size and the amount of material to be collected. After several trials, it was determined that the Brink with bare plates was not successful as a collection device due to severe bounce and reentrainment. Accordingly, testing of the Brink with bare plates was discontinued after sufficient data was taken to prove its unreliability as a sizing device. Only the Brink with filter substrates and greased plates were subsequently tested, as well as the C2 & C3 cylones.

At the conclusion of each test, each impactor was carefully disassembled and each internal surface cleaned using a solution of 0.1N NH_4OH. Using a known amount of solution, each plate and surface was washed to dissolve and rinse off the ammonium fluorescein particles. Where vasoline was used, a small amount of benzene was poured over the greased collection plate in a small dish which was then placed in an ultrasonic cleaner. A slight

amount of agitation caused the vasoline to dissolve and the ammonium fluorescein particles to become well mixed. Adding a known amount of 0.1N NH_4OH to the mixture with stirring caused the ammonium fluorescein to dissolve. After the benzene mixture floated on top of the NH_4OH, the ammonium fluorescein solution was pipetted off.

The mass of material on each surface was determined by fluorometric analysis. A Beckman Quartz Spectrophotometer, Model DU, calibrated with solutions of known concentration of ammonium fluorescein was used to measure the concentration of ammonium fluorescein in each wash. By knowing the amount of wash solution, the dilution factor, if any, and the absolute concentration, the mass of particles on each surface could be calculated. With the mass on each plate and surface known, the percent of total mass collected on each surface was then calculated. From this, the total wall losses and stage collection efficiencies could be calculated. Figures 9, 10, & 11 show the percent wall loss for the Andersen, Brink, and Pilat Impactors versus particle size. Regardless of size, 50% or more of the total wall loss was due to material in the nozzle and inlet cones of the impactor. By using the mass collected on each impaction plate, the collection efficiencies were calculated for each test. For many of the lower impactor stages, there is not yet enough data to accurately draw an efficiency curve because the smallest size particle that has been used to date has been 2.0 μm. It is instructive, however, to show examples of collection efficiency curves for some of the upper stages. Figures 12 and 13 show efficiency versus particle size for the first two Pilat stages. It can be seen that the initial Pilat stage in reality does not behave as the theory predicts. The D_{50} has shifted to about 14 μm from a calculated value of about 28 μm. Figures 14, 15, 16, & 17 show the collection

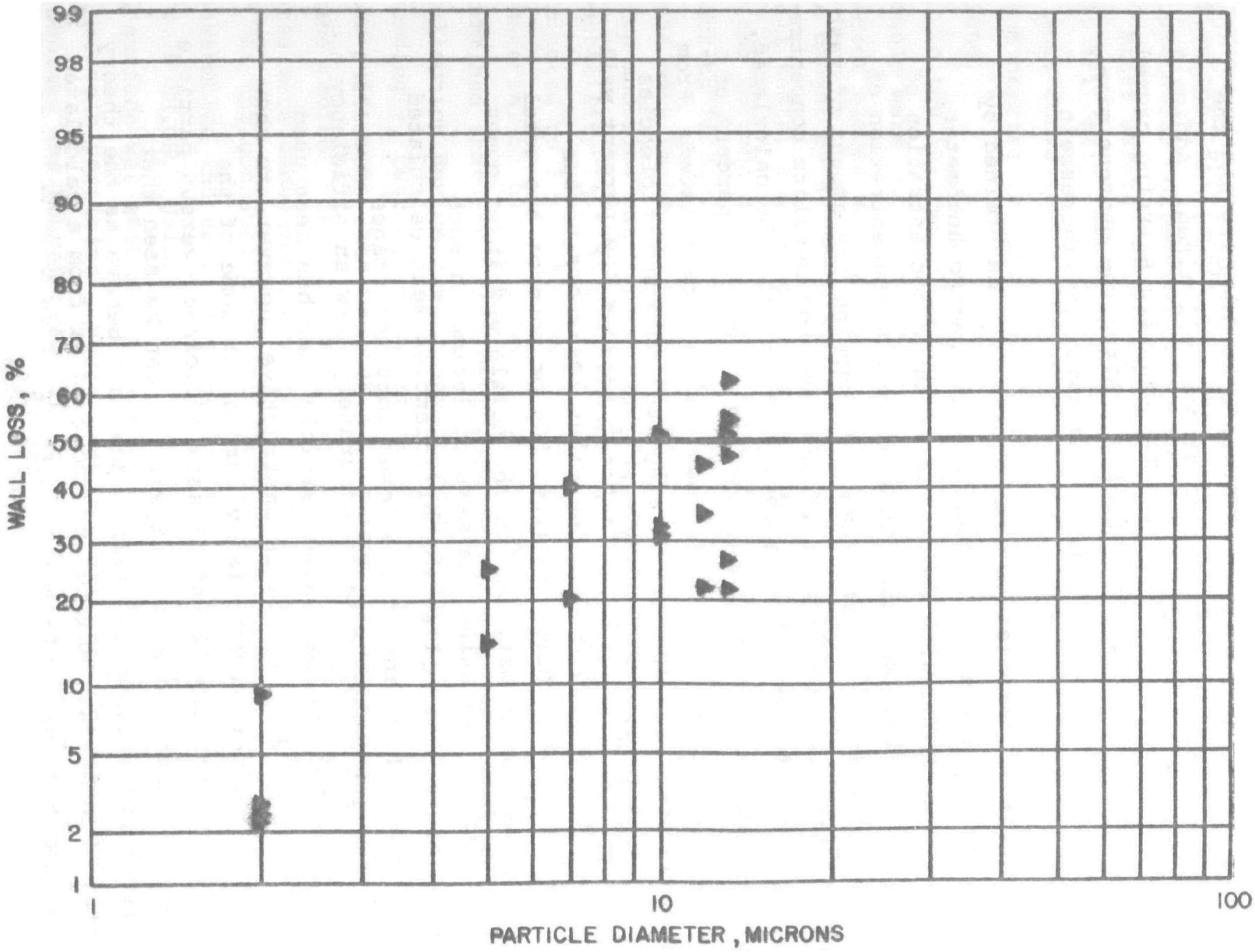

Figure 9. Percentage Wall Loss vs. Particle Size
Andersen Stack Sampler (0.5 acfm, 25°C, 29.60" Hg)

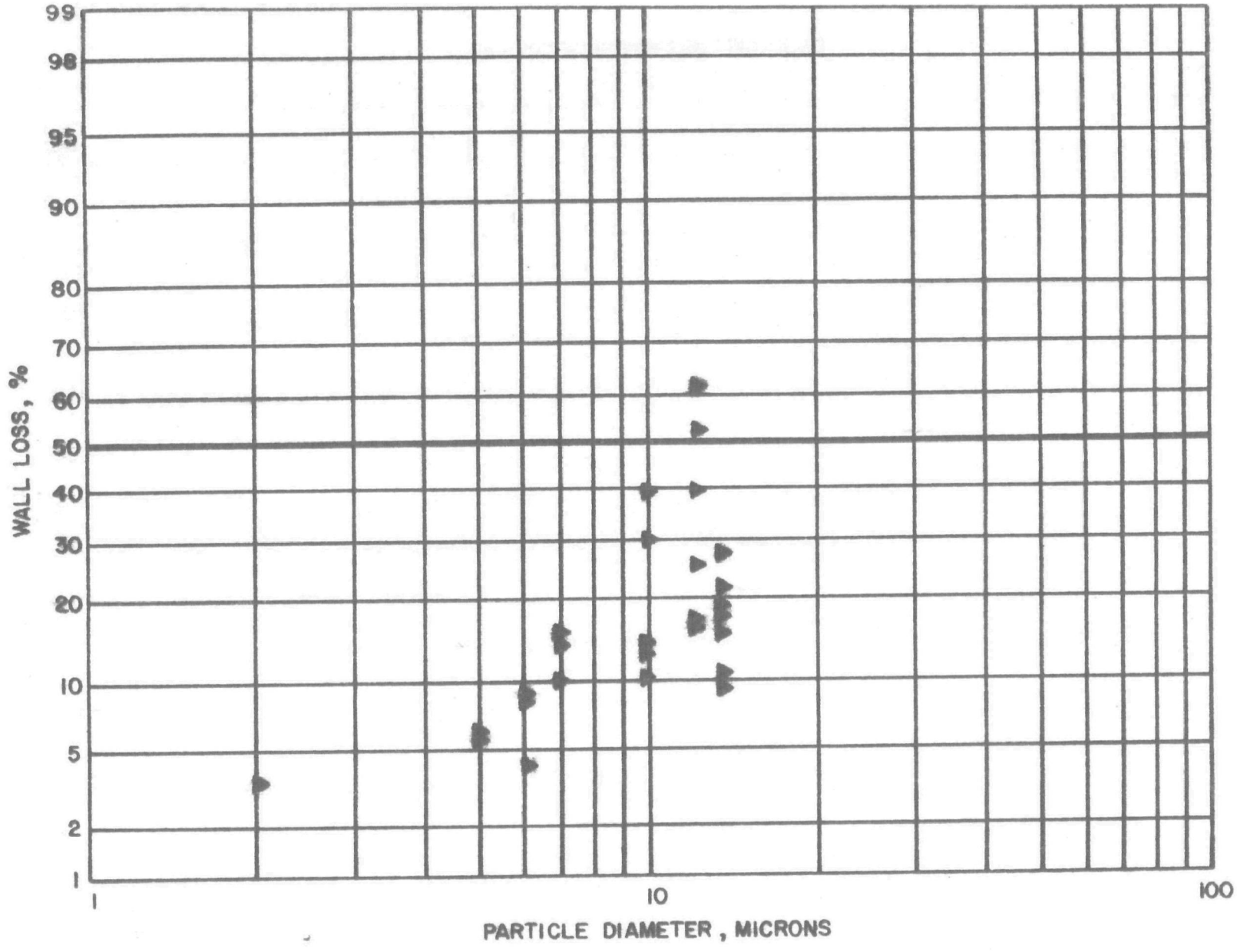

Figure 10. Percentage Wall Loss vs. Particle Size
Brink Cascade Impactor (0.03 acfm, 25°C, 29.60" Hg)

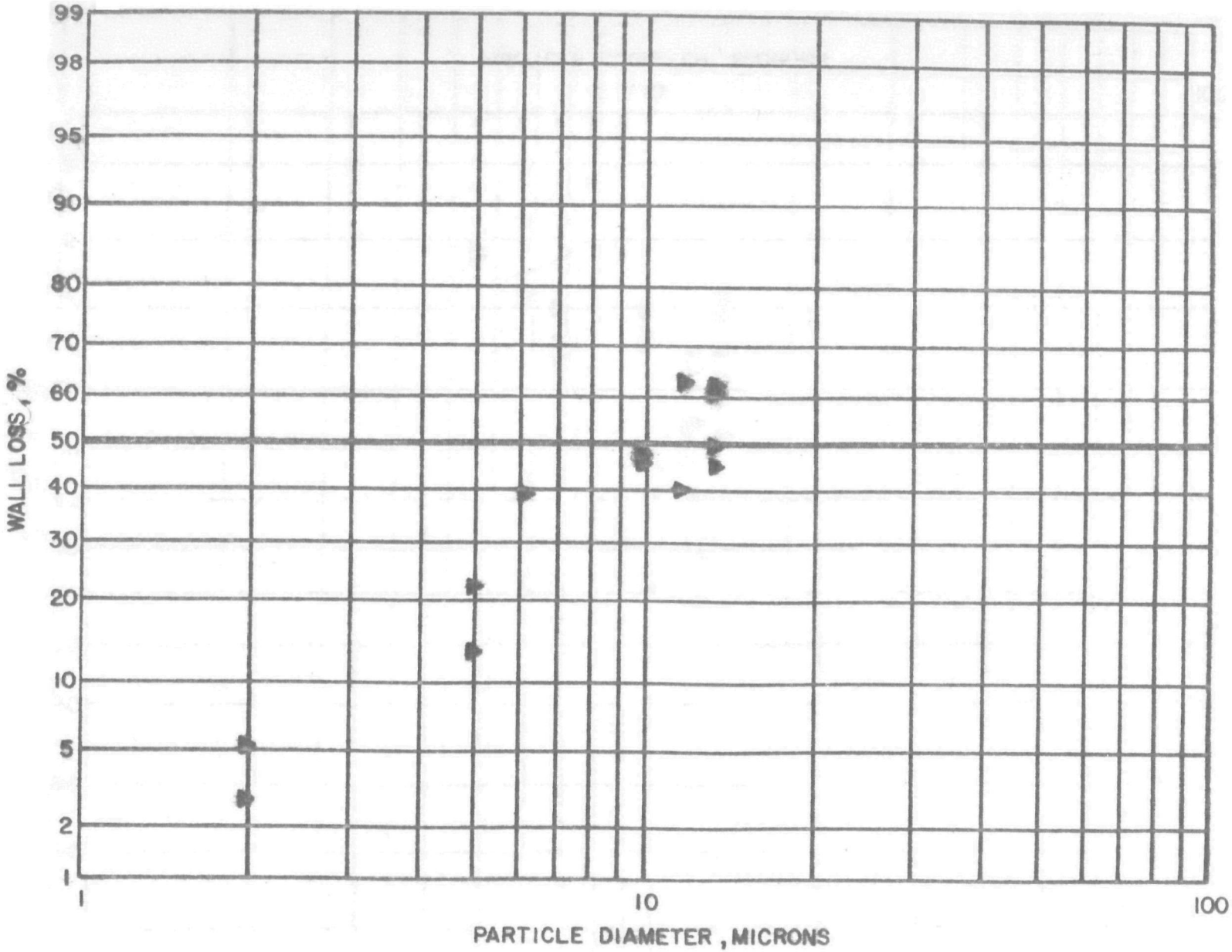

Figure 11. Percentage Wall Loss vs. Particle Size
University of Washington (Pilat) Impactor
(0.5 acfm, 25°C, 29.60" Hg)

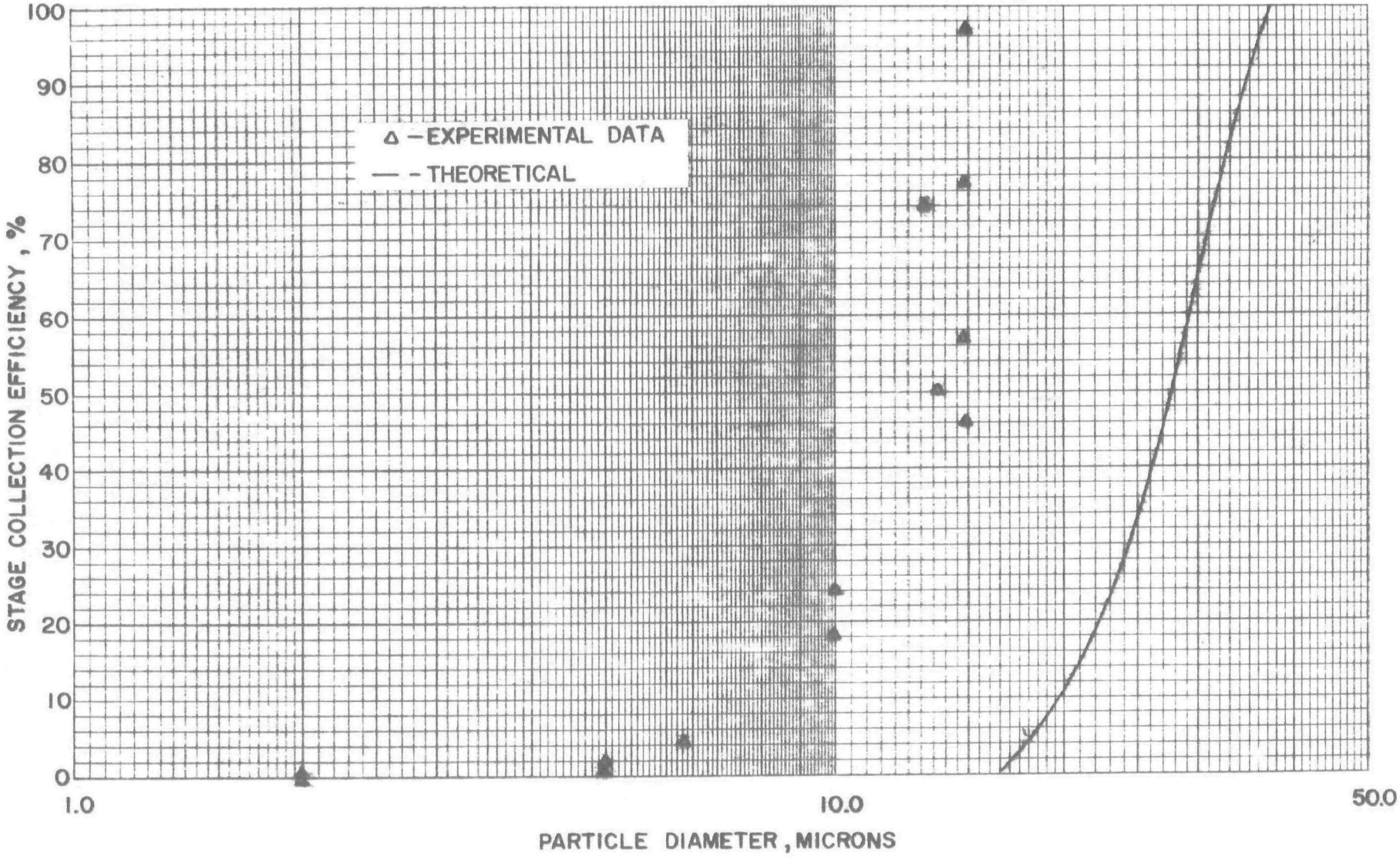

Figure 12. Stage Collection Efficiency vs. Particle Size
First Stage - University of Washington (Pilat) Impactor
(0.5 acfm, 25°C, 29.60" Hg)

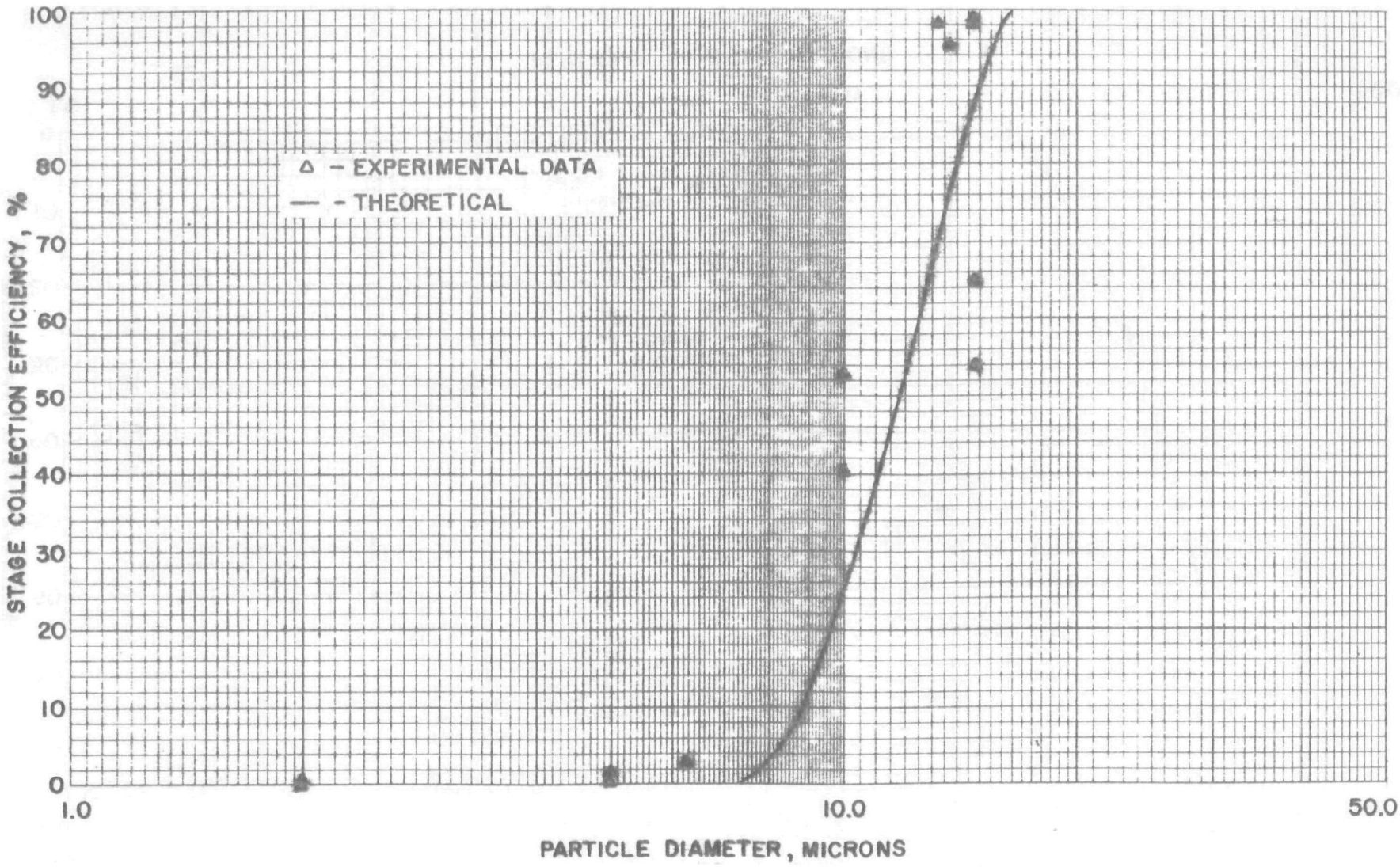

Figure 13. Stage Collection Efficiency vs. Particle Size
Second Stage - University of Washington (Pilat) Impactor
(0.5 acfm, 25°C, 29.60" Hg)

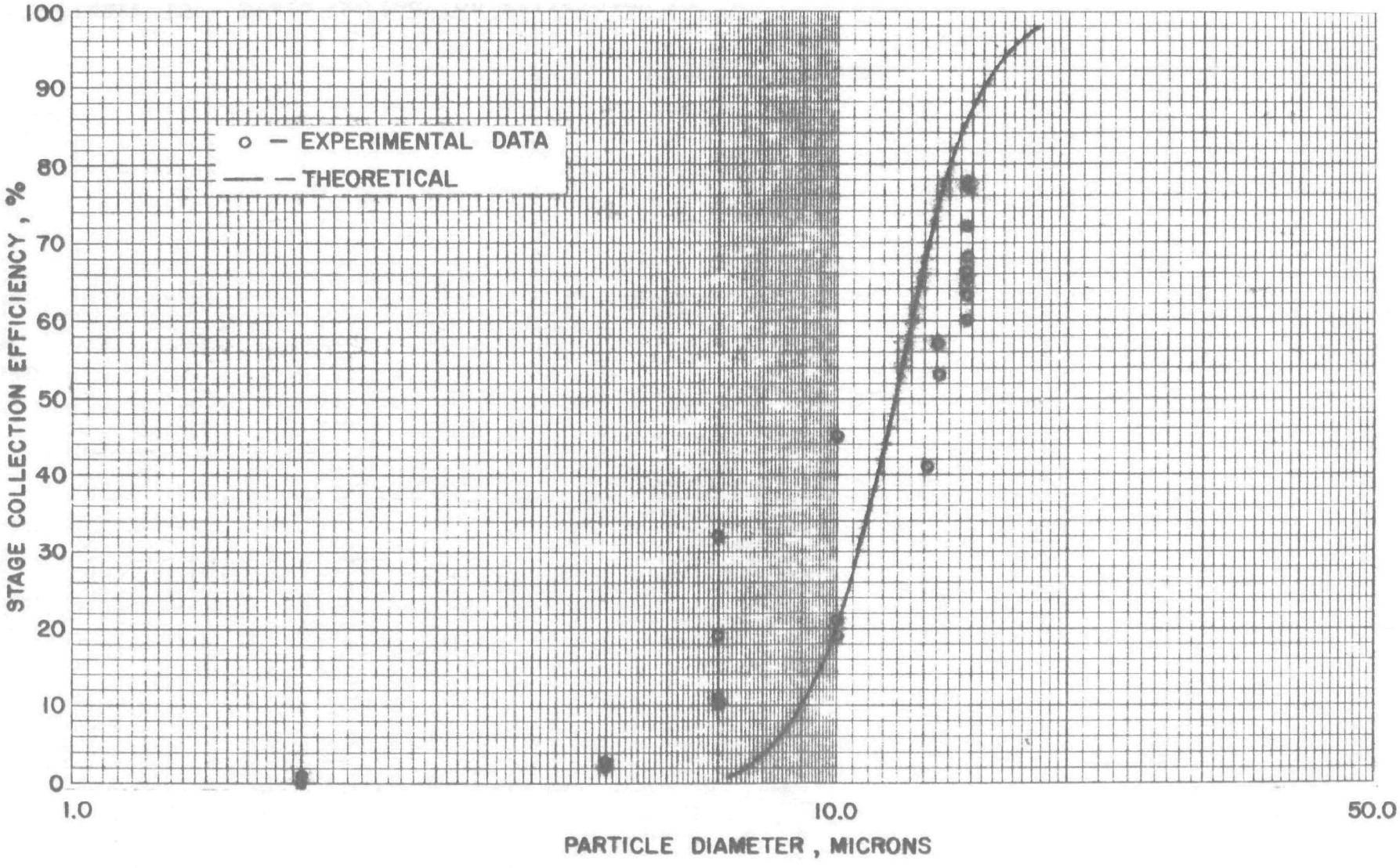

Figure 14. Stage Collection Efficiency vs. Particle Size
First Stage - Andersen Stack Sampler
(0.5 acfm, 25°C, 29.60" Hg)

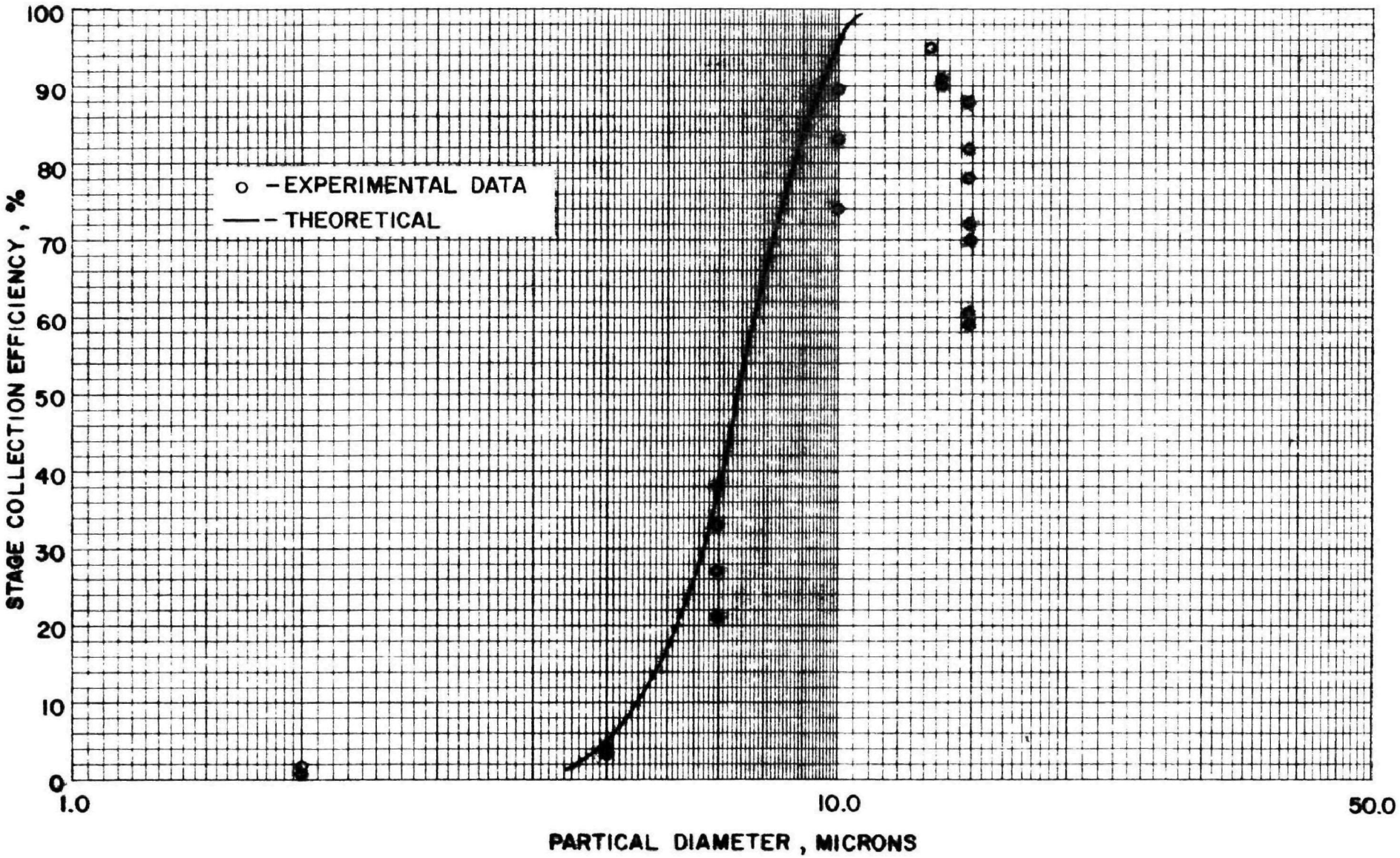

Figure 15. Stage Collection Efficiency vs. Particle Size
Second Stage - Andersen Stack Sampler
(0.5 acfm, 25°C, 29.60" Hg)

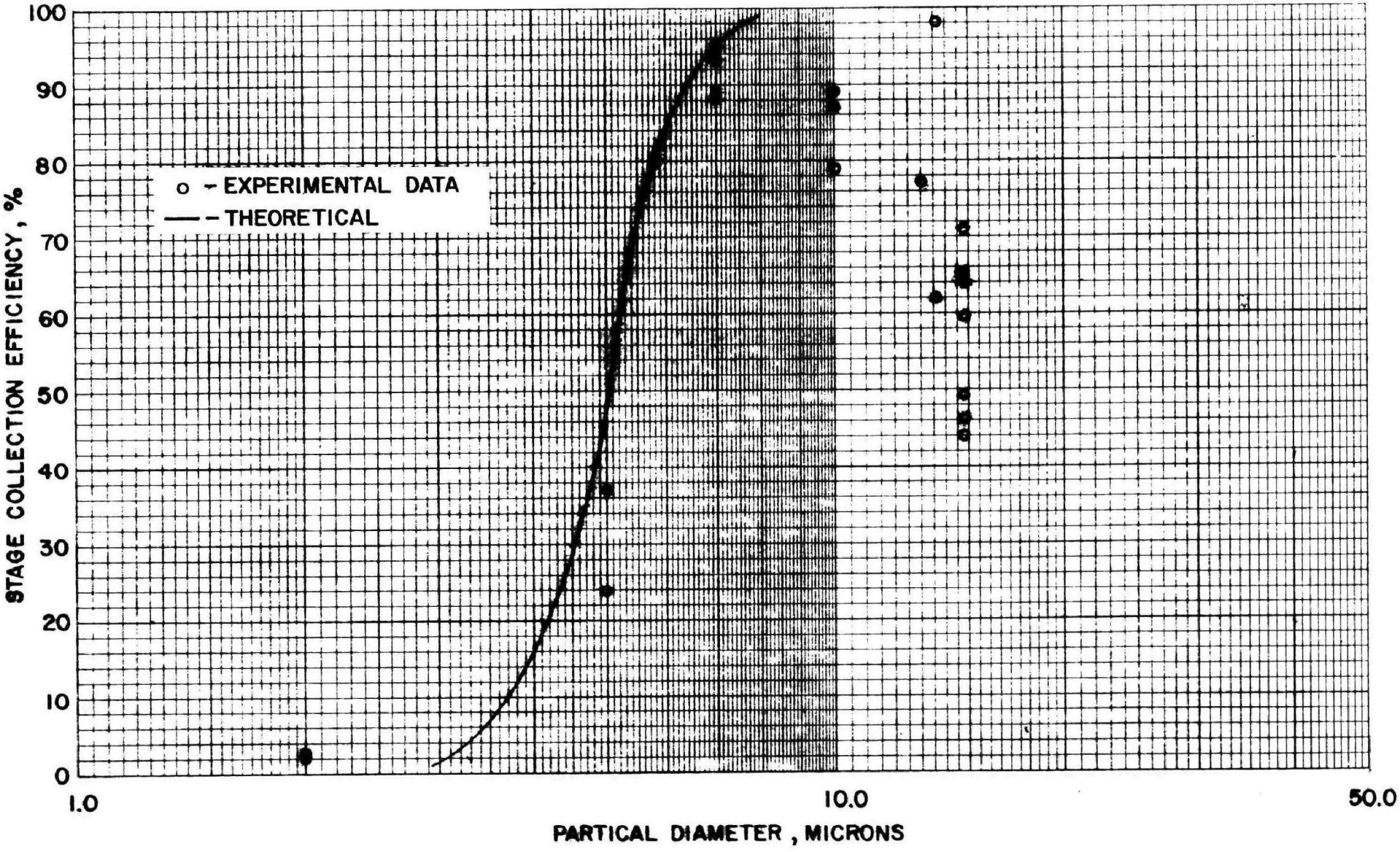

Figure 16. Stage Collection Efficiency vs. Particle Size
Third Stage - Andersen Stack Sampler
(0.5 acfm, 25°C, 29.60" Hg)

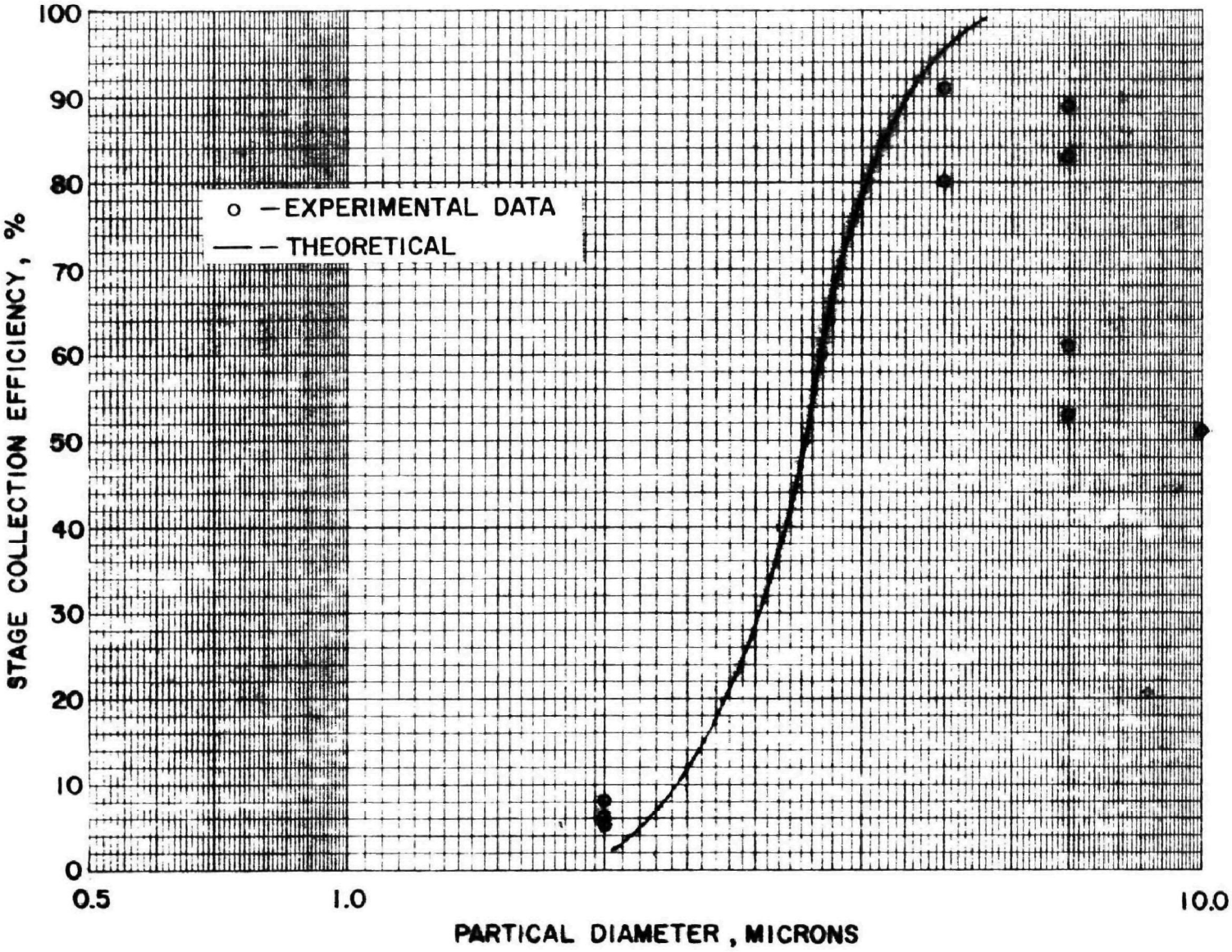

Figure 17. Stage Collection Efficiency vs. Particle Size
Fourth Stage - Andersen Stack Sampler
(0.5 acfm, 25°C, 29.60" Hg)

efficiency for the first four Andersen stages. Notice that the collection efficiency for stages 3 & 4 for large particles is well below 100%.

A more concise way of presenting all the data is to graph $\sqrt{\psi}$ vs. EFF as was done by Rantz and Wong.[4] In this way, the efficiency data on all stages can be presented on the same graph. The dimensionless parameter $\sqrt{\psi}$ is given by

$$\sqrt{\psi} = Dp \quad \frac{2}{\sqrt{18}\ \sqrt{\pi}\ \ 10^4} \left(\frac{\rho\ F\ 472\ POA\ C}{\mu\ (DC)^3\ X(I)\ PS} \right)^{\frac{1}{2}} \quad \text{where}$$

Dp = aerosol diameter (μm),
ρ = aerosol density (gm/cm³),
F = flow rate (cfm),
POA = air pressure at impactor inlet (atm),
C = Cunningham Correction Factor,
μ = air viscosity (poise),
DC = Jet diameter (cm),
X(I) = Number of holes per stage, &
PS = Air pressure at stage jet (atm)

It can be seen that for each stage, $\sqrt{\psi}$ is dependent only on Dp, the aerosol diameter, when all other parameters are held constant. Figures 18, 19, 20, 21, & 22 show $\sqrt{\psi}$ vs efficiency for the Andersen, Brink (bare plate), Brink (filter substrate), Brink (greased plate), and the Pilat Impactors. Separate symbols are employed to represent data for each stage. For each symbol, increasing $\sqrt{\psi}$ values indicate increasing aerosol size. Notice that the collection efficiency does not reach 100% for a large size and stay at that value for all larger sizes. In fact, if a single symbol is followed from left to right, it is apparent that the stage reaches a peak in efficiency and then falls off at larger sizes. This indicates that some large

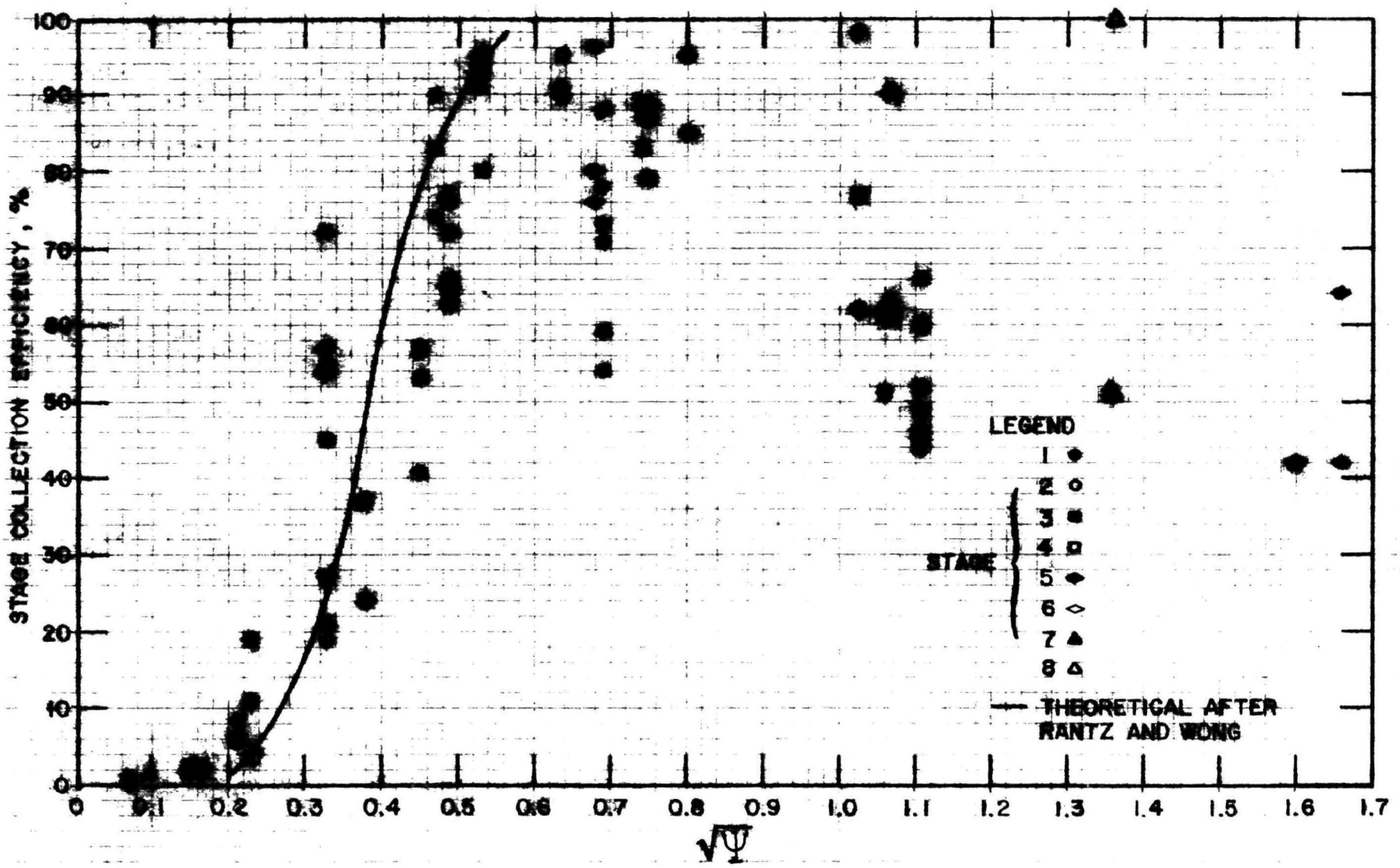

Figure 18. Stage Collection Efficiency vs. $\sqrt{\Psi}$
Andersen Stack Sampler - Glass Fiber Filter Substrates
(0.5 acfm, 25°C, 29.60" Hg)

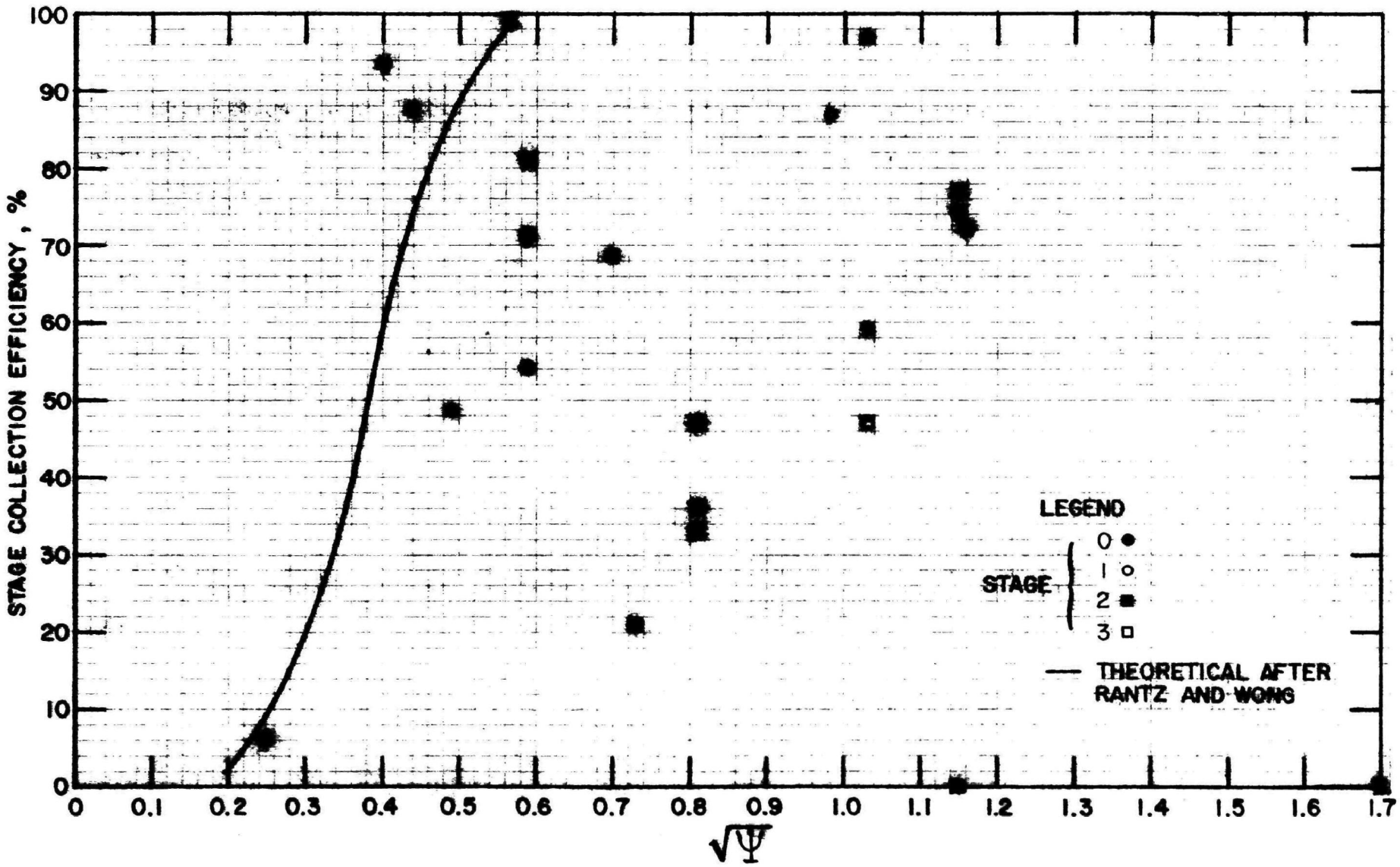

Figure 19. Stage Collection Efficiency vs. $\sqrt{\Psi}$
Brink Cascade Impactor - Bare Collection Plates
(0.03 acfm, 25°C, 29.60" Hg)

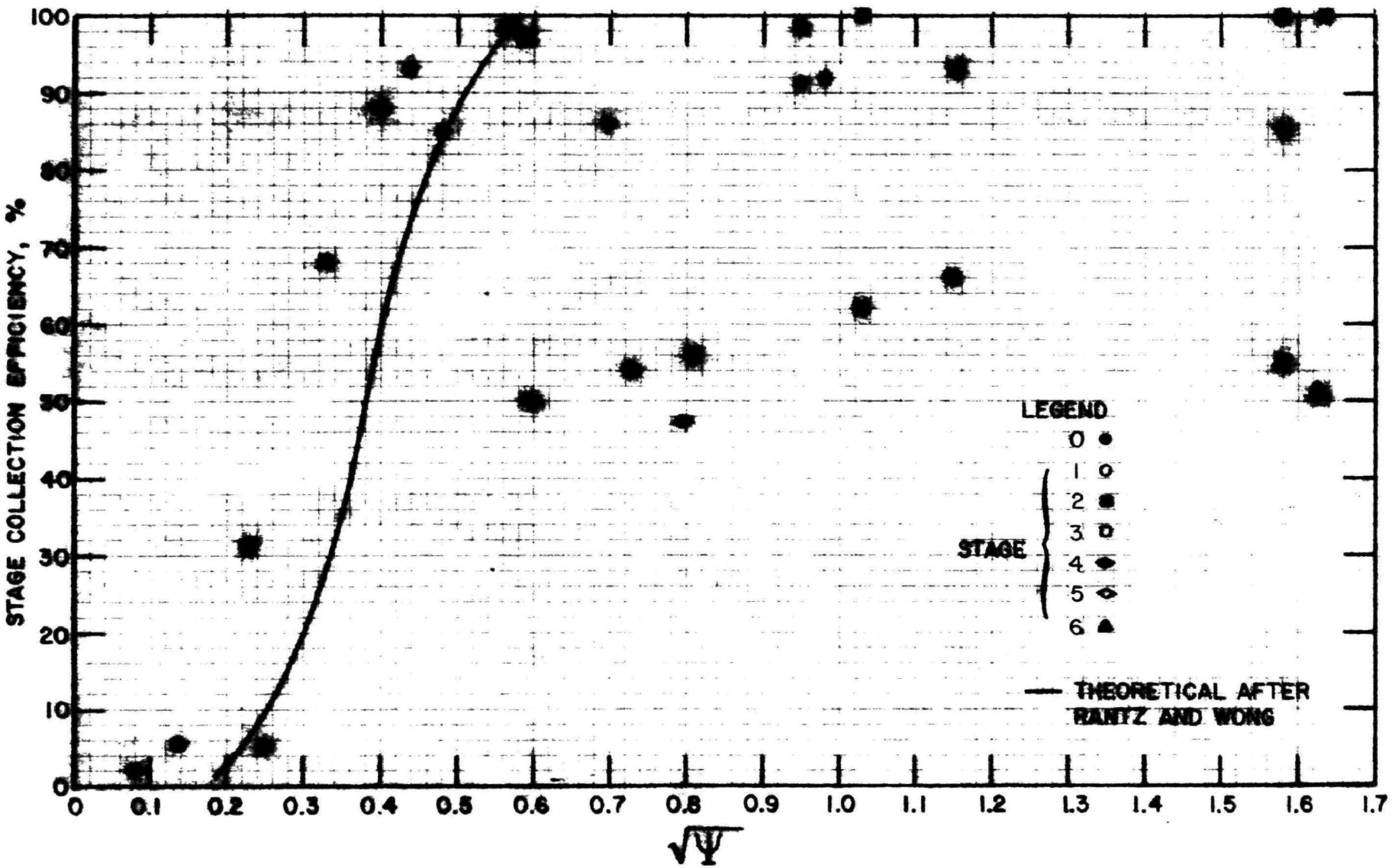

Figure 20. Stage Collection Efficiency vs. $\sqrt{\Psi}$
Brink Cascade Impactor - Glass Fiber Filter Substrates
(0.03 acfm, 25°C, 29.60" Hg)

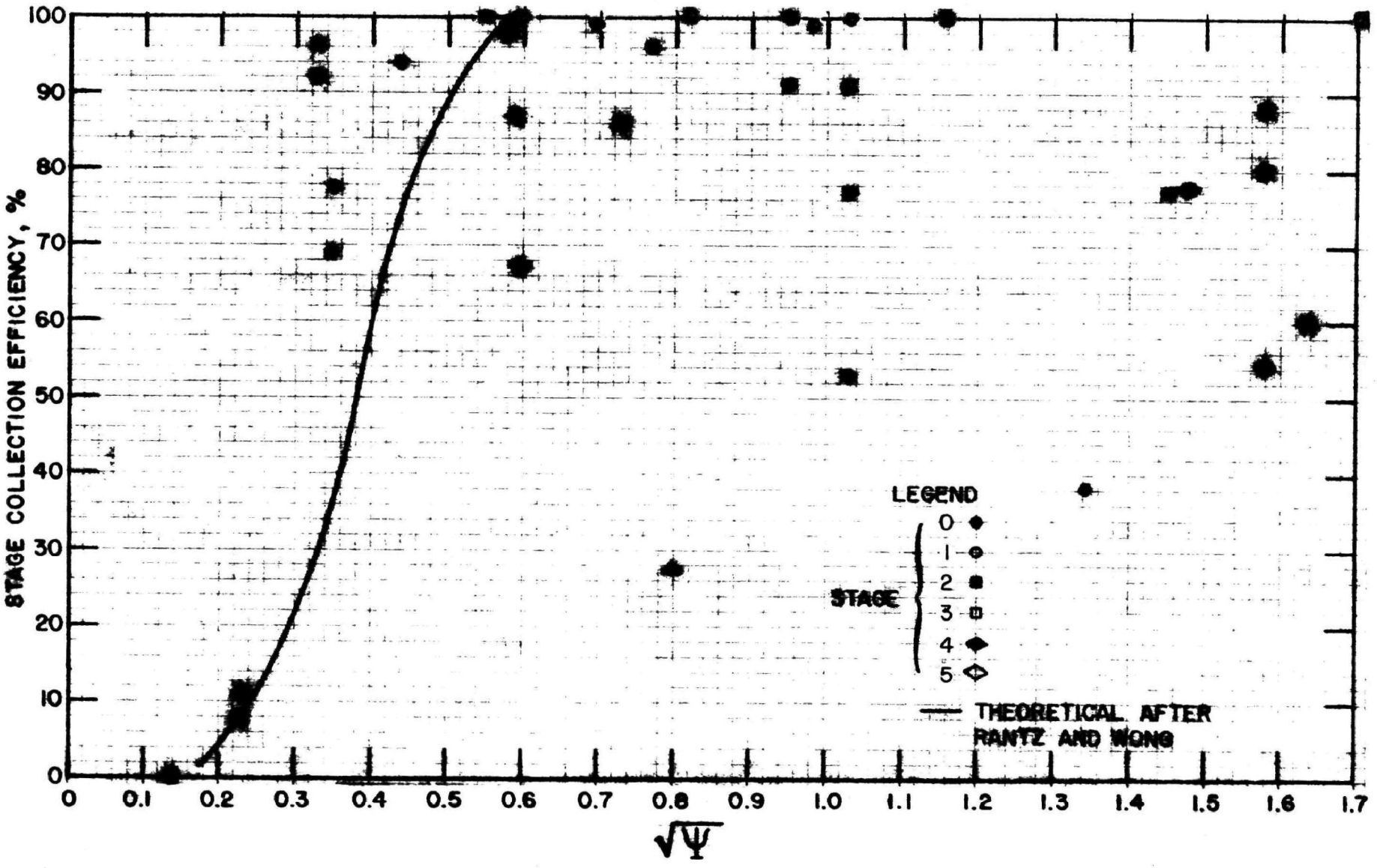

Figure 21. Stage Collection Efficiency vs. $\sqrt{\Psi}$
Brink Cascade Impactor - Greased Plates
90.03 acfm, 25°C, 29.60" Hg)

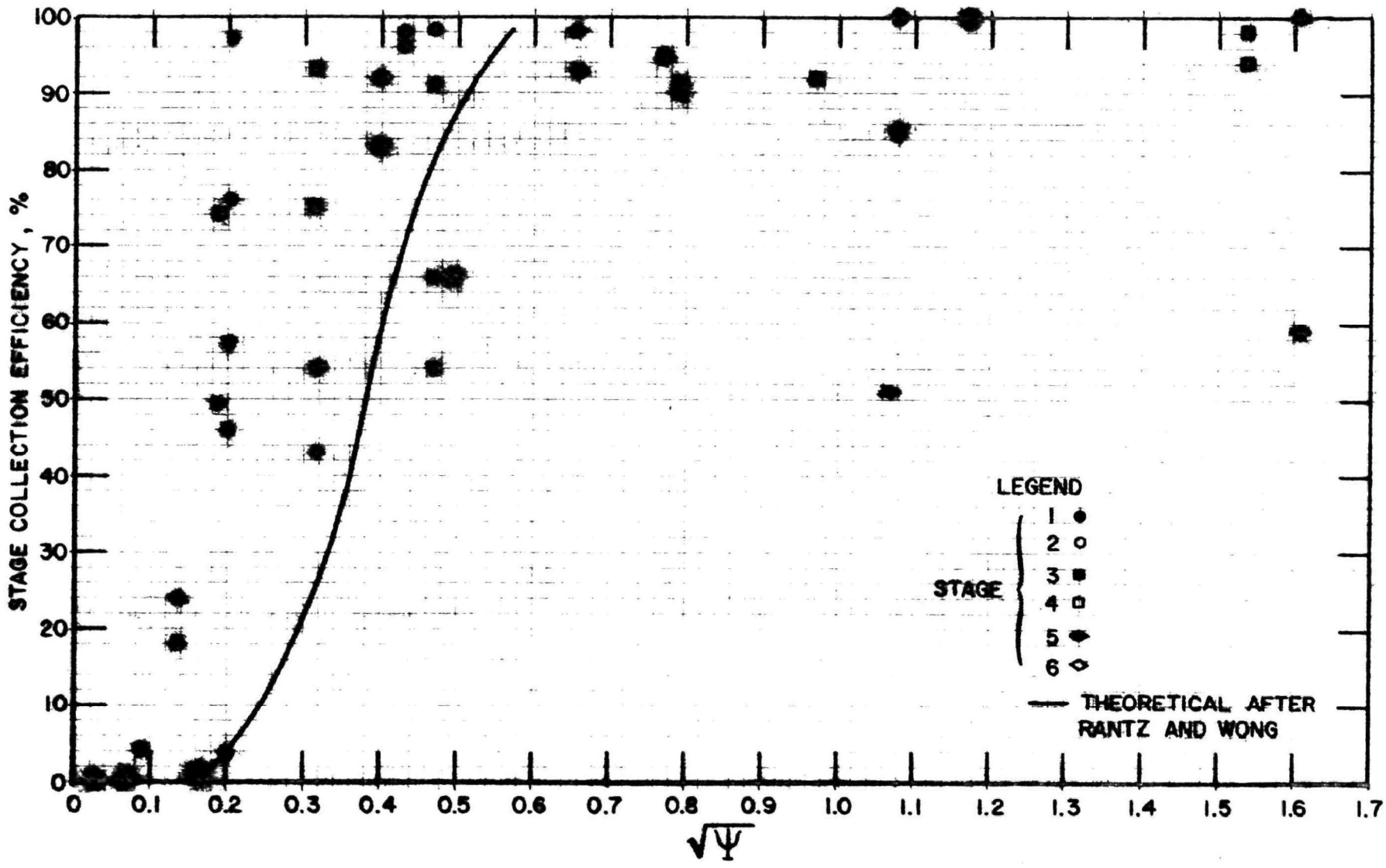

Figure 22. Stage Collection Efficiency vs. $\sqrt{\Psi}$
University of Washington (Pilat) Impactor
(0.5 acfm, 25°C, 29.60" Hg)

particles impact with enough momentum to bounce and be reentrained in the gas stream. Because of this, there may be difficulty in deciding where a particle will stop. If it is not caught by stage one or two, for example, there is a high probability that it will end up on a lower stage or back-up filter, thus decreasing the reliability of any size distribution calculated from the data. Figure 19 shows that the Brink Impactor with bare substrates did not perform well when compared to the same impactor with glass fiber as greased substrates. The poor performance of the initial Pilat stage as shown in Figure 22 is probably due to the failure of the inlet cone to define the diameter of the air jet. It is assumed in calculating the D_{50} for the inlet stage, that the gas stream expands to the full cone diameter. Apparently, this is not the case, and the effective jet diameter is somewhere between the nozzle inlet diameter and the cone exit diameter. This will probably not vary in a predictable fashion with flow rate and may necessitate redesign of the inlet cone.

Figures 23 and 24 show efficiency versus particle size for the C2 and C3 cyclone used with the Brink Impactor. Figure 25 presents the Andersen Cyclone data for efficiency. Data for the four McCrone Cyclones is presented in Figures 26, 27, 28, & 29. In some cases, there have not been enough small particles generated to indicate the trend of the efficiency at these sizes.

Because of the small number of tests performed on the E.R.C. TAG Sampler, collection efficiencies are presented in tabular form in Table II. Five tests are shown in this table. Each is indicated at the upper part of the sheet by the particle diameter and total percent wall loss. The columns marked I and II are for the percent by stage of the total collected mass and the stage collection efficiency, respectively. A column giving the theoretical stage D_{50}'s is presented to aid in understanding the stage collection efficiencies.

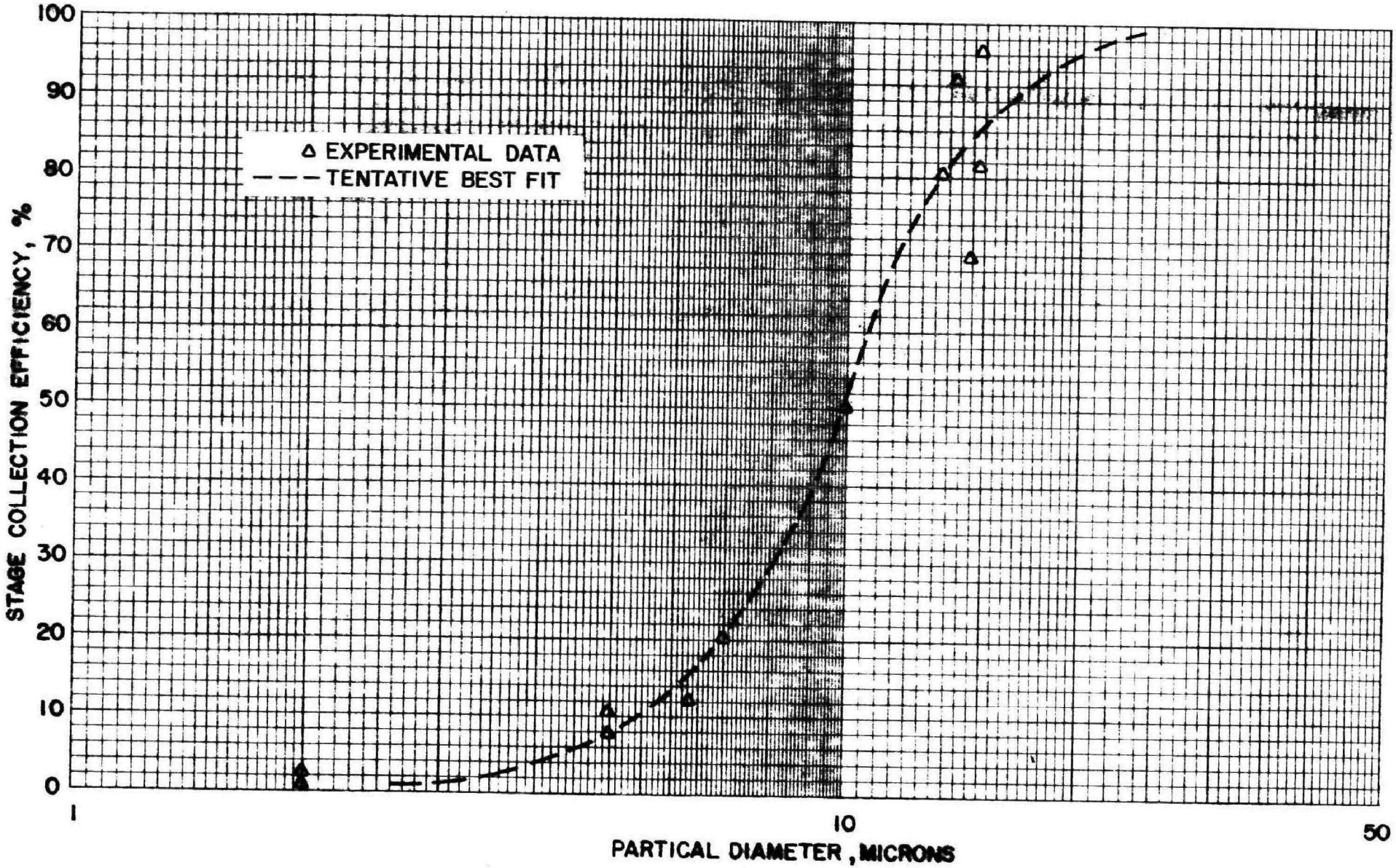

Figure 23. Stage Collection Efficiency vs. Particle Size
Brink C2 (Externally Mounted) Cyclone
(0.03 acfm, 25°C, 29.60" Hg)

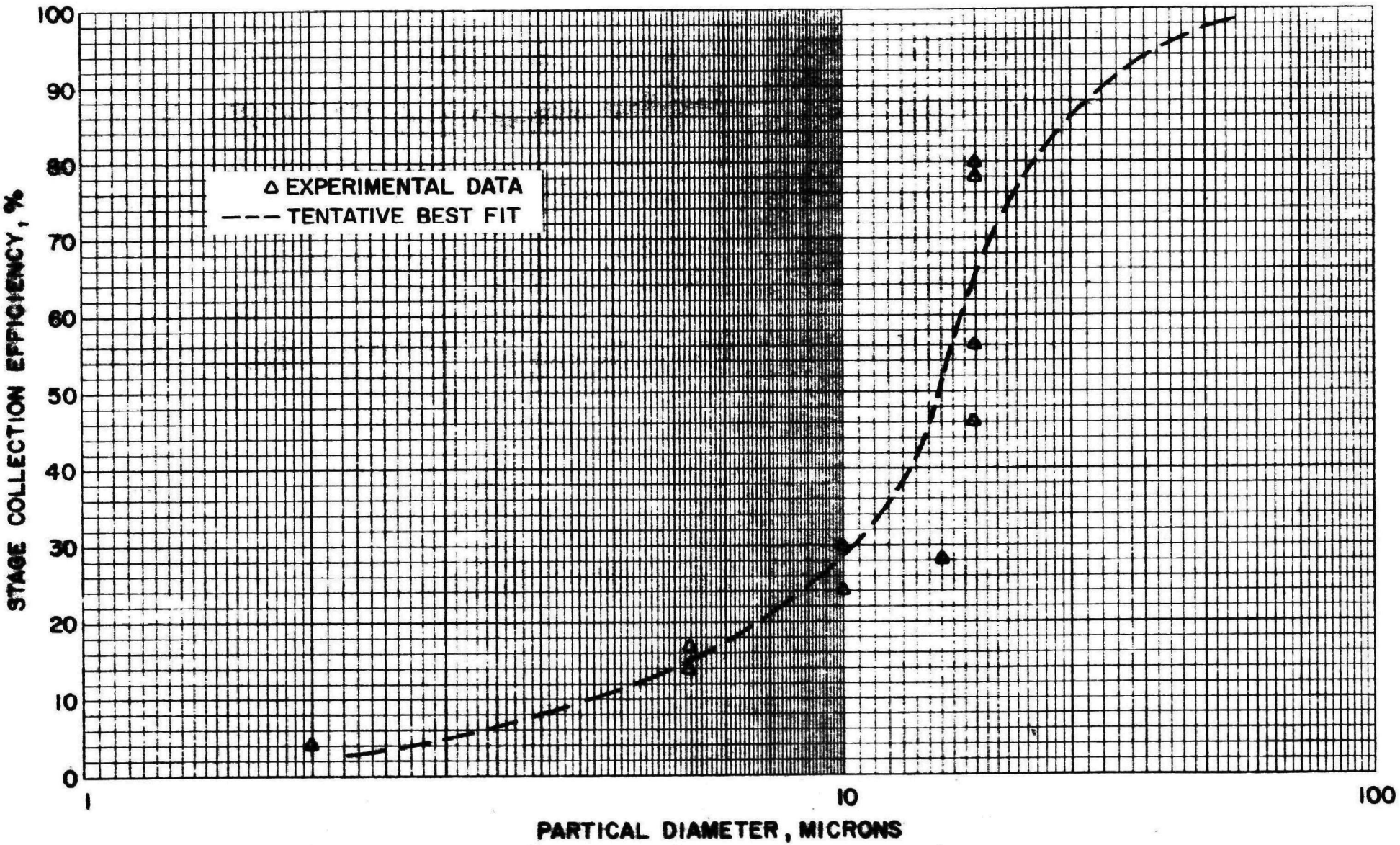

Figure 24. Stage Collection Efficiency vs. Particle Size
Brink C3 (Inline) Cyclone
(0.03 acfm, 25°C, 29.60" Hg)

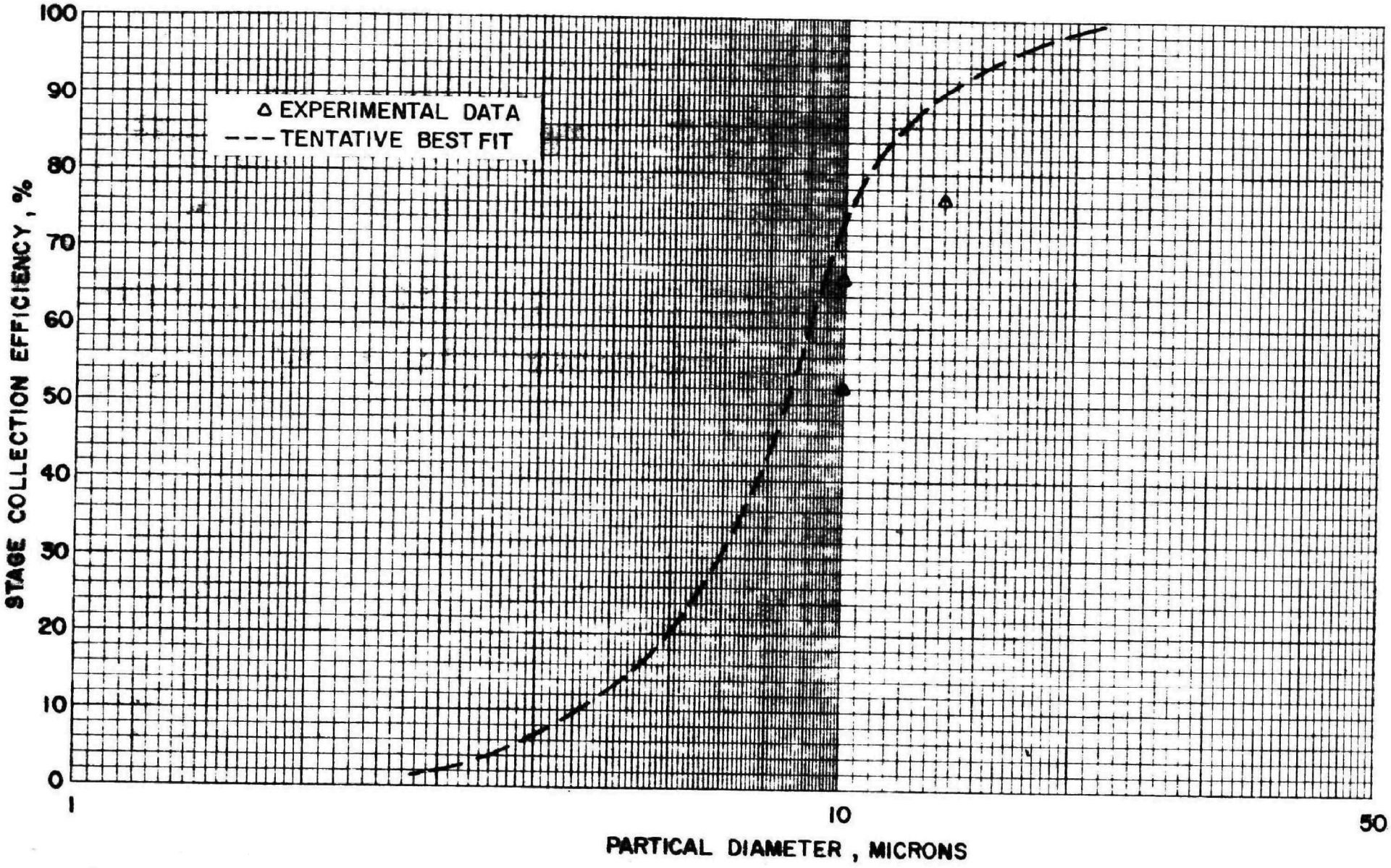

Figure 25. Stage Collection Efficiency vs. Particle Size
Andersen Cyclone Precollector
(0.5 acfm, 25°C, 29.60" Hg)

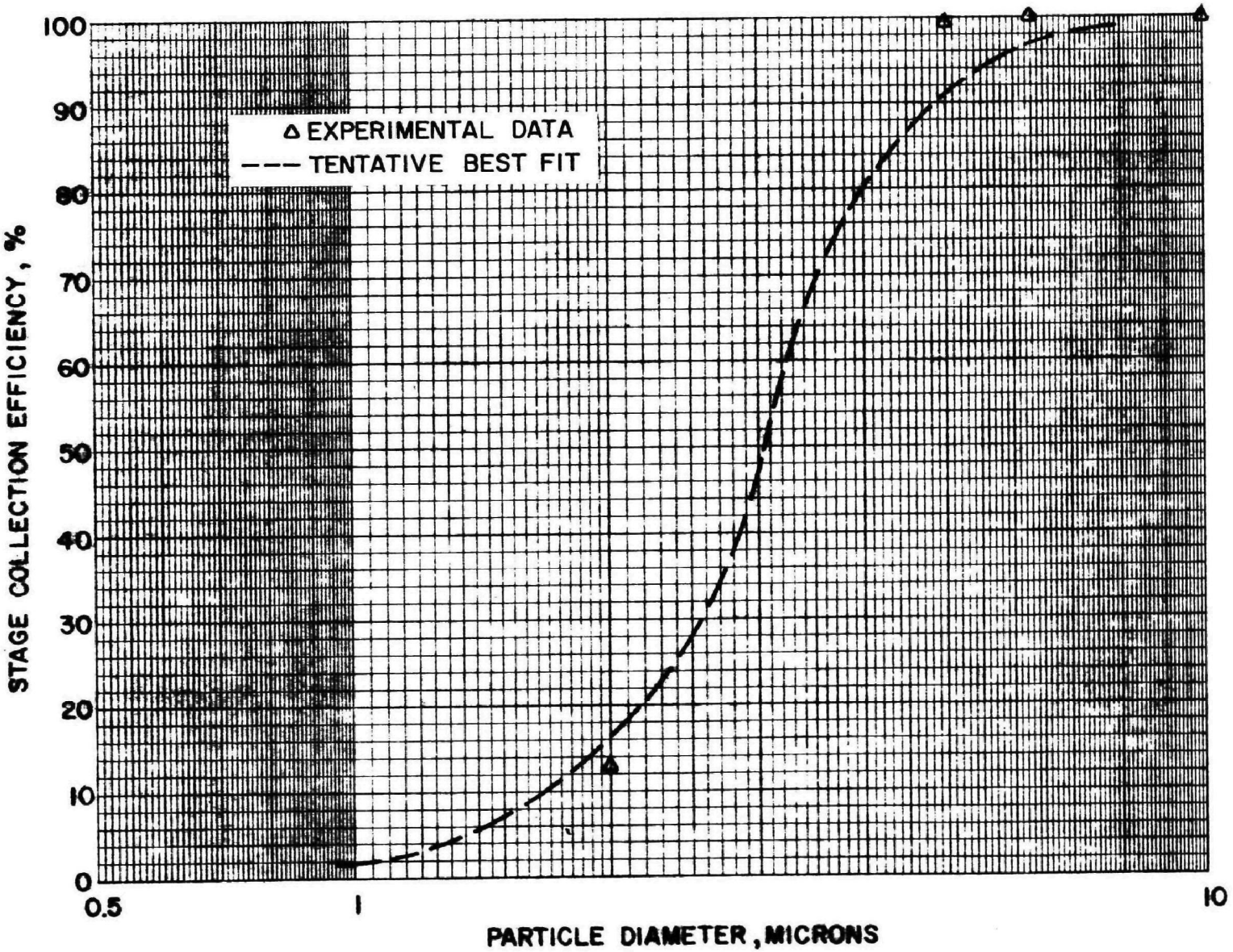

Figure 26. Stage Collection Efficiency vs. Particle Size McCrone Cyclone T2A - 0.13" H_2O

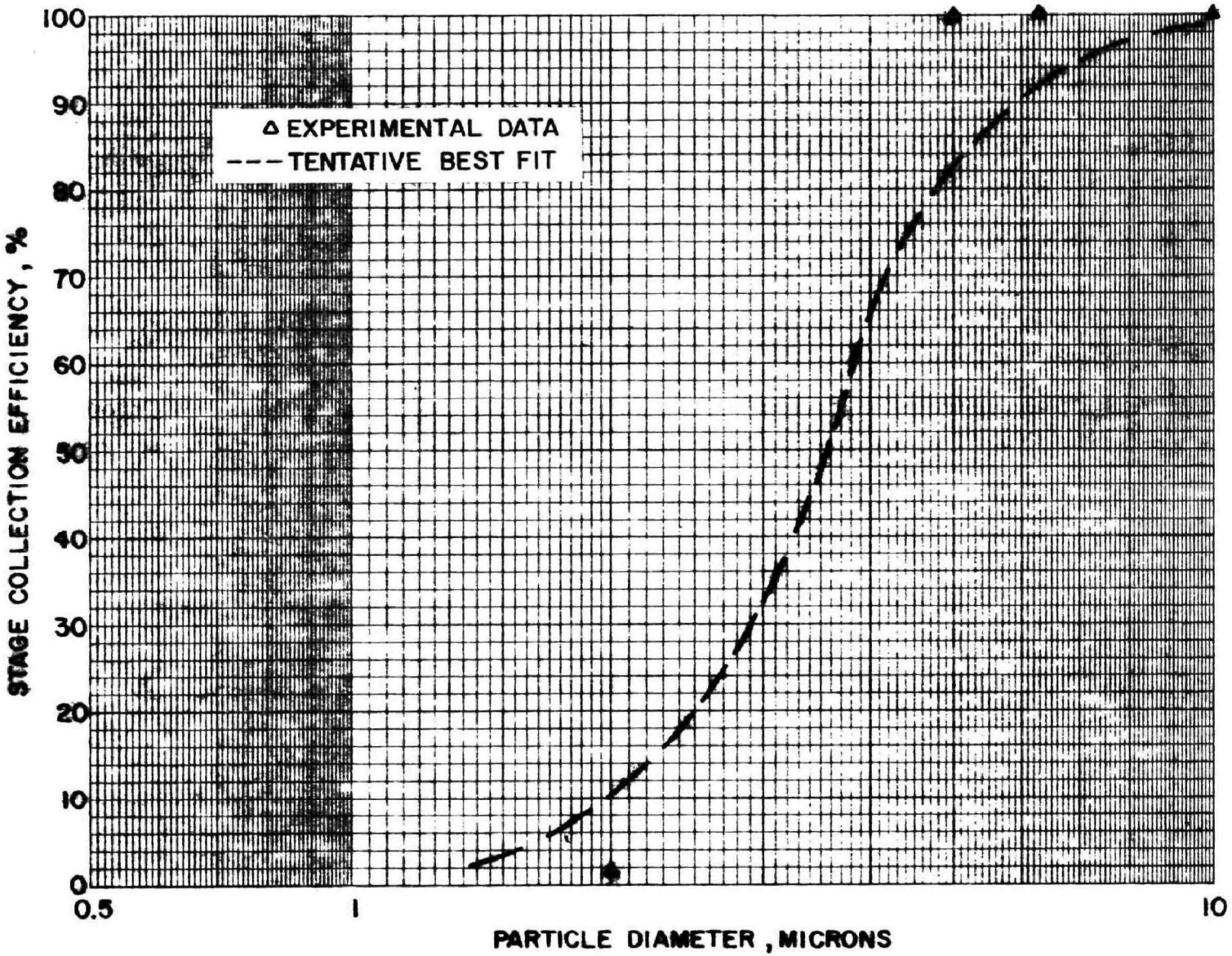

Figure 27. Stage Collection Efficiency vs. Particle Size McCrone Cyclone T2A - 1.00" H_2O

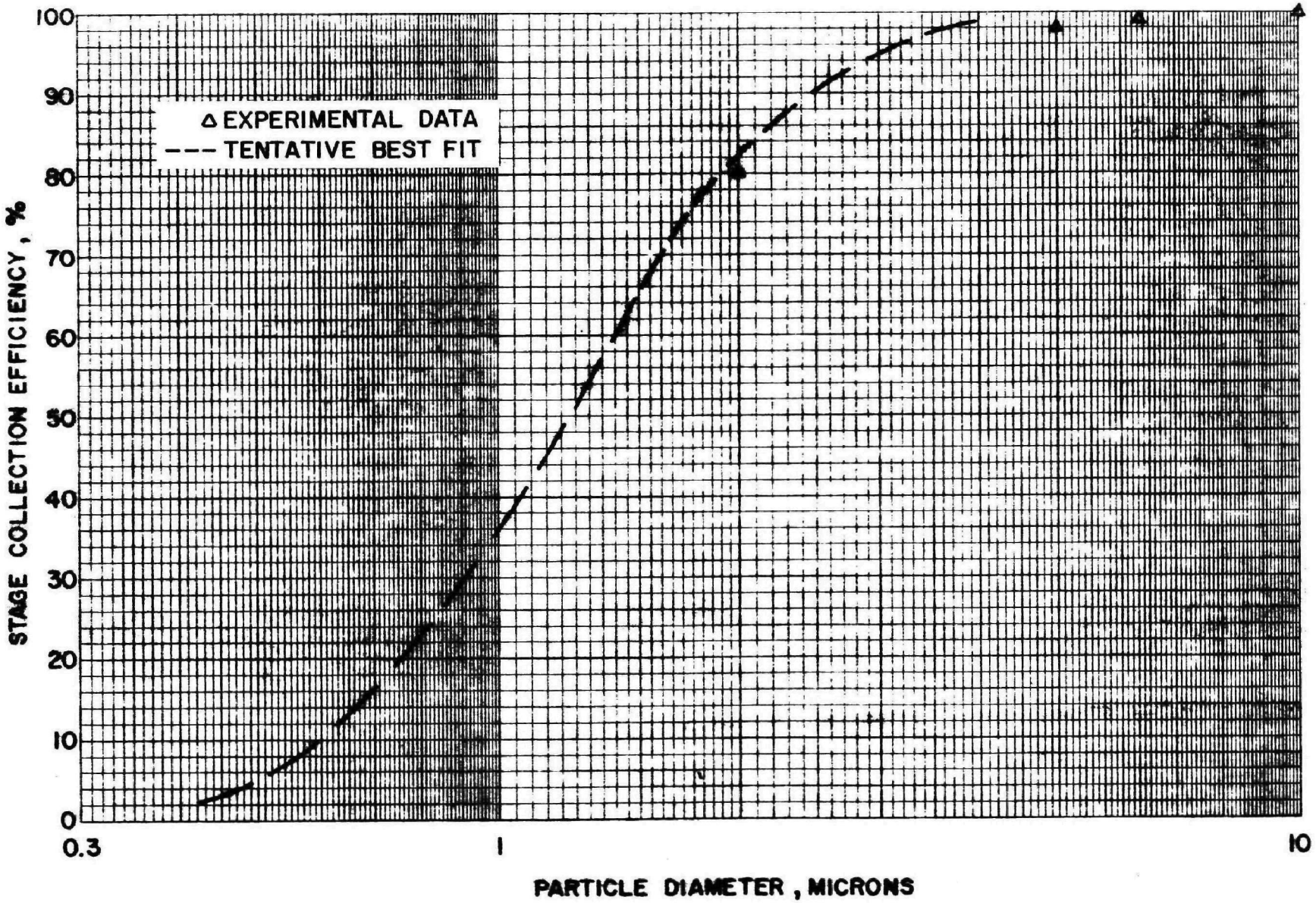

Figure 28. Stage Collection Efficiency vs. Particle Size
McCrone Cyclone T2B - 0.80" H_2O

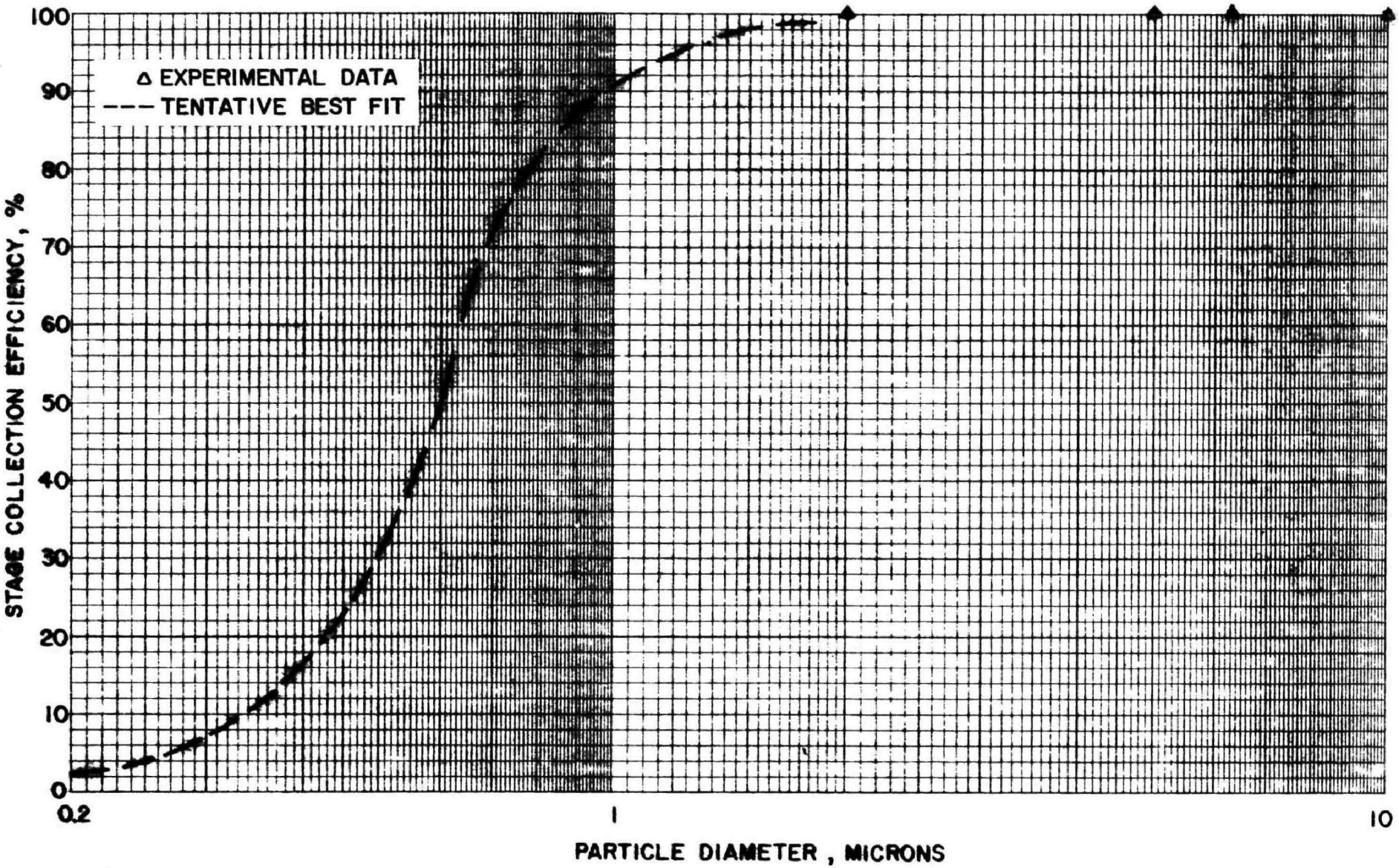

Figure 29. Stage Collection Efficiency vs. Particle Size McCrone T2B - 20.0" H_2O

TABLE II

ENVIRONMENTAL RESEARCH CORPORATION TAG SAMPLER (GREASED PLATES)

	Theoretical D_{50}'s (microns) (0.5 CFM)	I	II	I	II	I	II	I	II	I	II
Particle Size (microns)		6.3		5.0		5.0		2.0		2.0	
Percent Wall Loss		32.47		35.82		18.06		4.75		3.66	
Nozzle		26.74		32.58		9.65		0.50		0.64	
Inlet Cone		5.73		3.24		8.41		0.89		0.68	
O-Rings								3.36		2.34	
E-1		5.63	8.34	1.32	2.06	1.00	1.22	0.17	0.18	0.35	0.36
E-2	11.1	2.56	4.14	0.99	1.58	0.26	0.32	0.00	0.00	0.29	0.30
E-3	7.5	1.63	2.75	0.92	1.49	0.35	0.43	0.00	0.00	0.20	0.21
E-4	5.5	28.13	48.75	1.58	2.59	2.19	2.73	0.00	0.00	0.25	0.26
E-5	4.0	15.28	51.67	5.96	10.04	11.24	14.39	0.65	0.68	0.40	0.42
E-6	2.8	10.08	70.54	47.54	89.03	56.83	84.96	85.26	90.29	72.13	76.05
E-7	2.0	3.41	80.99	5.38	91.81	7.34	72.96	8.34	90.95	20.13	89.39
E-8	1.3	0.51	63.75	0.36	75.00	0.75	27.57	0.71	85.54	1.52	63.07
E-9	0.9	0.23	79.31	0.00	---	0.90	45.68	0.12	100.0	0.29	32.58
E-10	0.63	0.02	33.33	0.00	---	0.45	42.06	0.00	---	0.05	8.33
Filter		0.04	100.00	0.12	---	0.62	100.00	0.00	---	0.55	100.0

C. Cascade Impactor Data Reduction

Throughout this work on the use of cascade impactors, an effort has been continually made to improve the accuracy and convenience of our data reduction schemes. Two methods are mentioned below. The "D_{50}" method is used at this time for the majority of cascade impactor work, but it is an oversimplification which can lead to a loss of information. Picknett[26] has introduced a more sophisticated method, yielding maximum information from the experimental data. This technique, however, is more difficult to apply and requires the use of a computer.

● COMPARISON OF THE D_{50} AND PICKNETT DATA REDUCTION TECHNIQUES USING REAL AND SIMULATED STAGE LOADINGS

In investigating data reduction techniques, it is difficult to separate inaccuracies in the theory and errors introduced by reentrainment, bounce, scouring, and poor calibration of the impactors. This problem can be eliminated by simulating the capture of a fictitious aerosol using the efficiency curves shown in Figure 30. Once the stage loadings are calculated, this data is used to recalculate a particle-size distribution, using either the D_{50} or Picknett method, which should ideally be identical to the fictitious input distribution.

Figure 31 is a test of both the D_{50} and Picknett techniques using a fictitious aerosol. The fictitious, or "true", aerosol consisted of 20% - 1 μm, 20% - 2 μm, 20% - 4 μm, 20% - 8 μm, and 20% - 12 μm diameter by mass. The zero through fifth stages were used, and cyclone C_3, as shown in Figure 30.

It can be seen that both methods give very nearly correct values for the mass median diameter, although neither scheme can resolve the step functions in the distribution. The Picknett method is much better at the large particle end, because the D_{50}

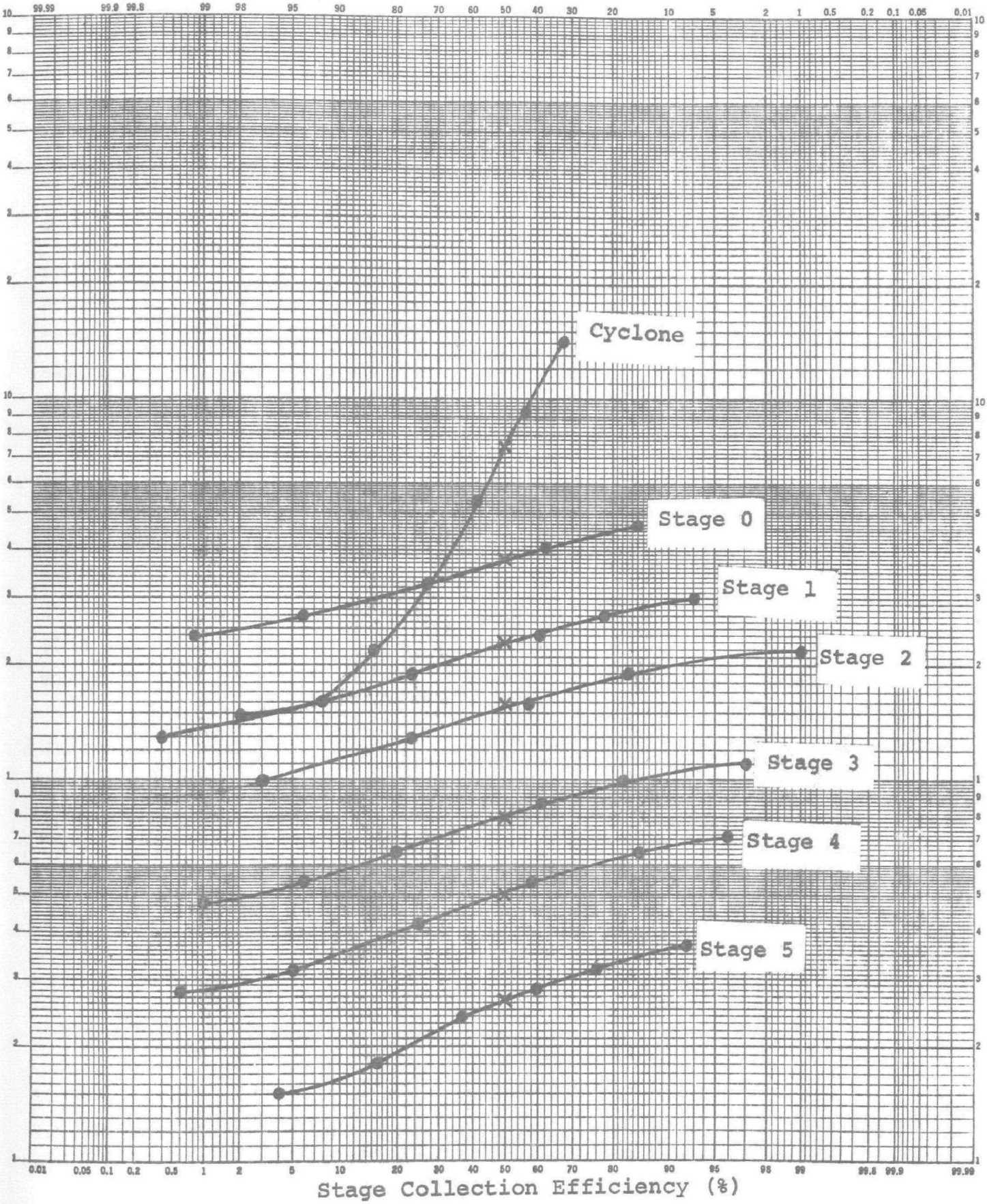

Figure 30. Stage Collection Efficiency for a Brink Cascade Impactor with a Pre-collector Cyclone.

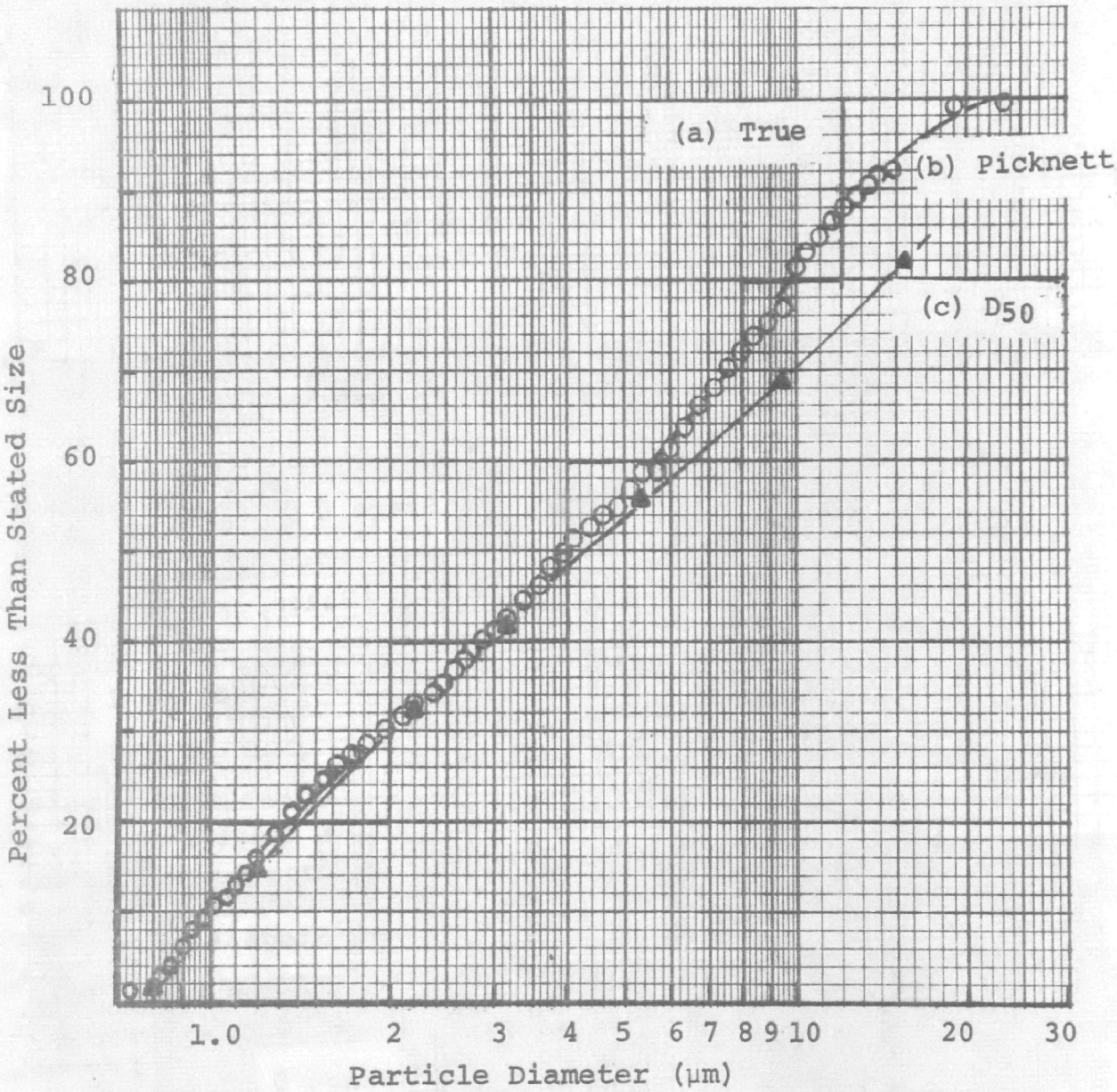

Figure 31. Simulated Impactor Tests: a) Input "true" distribution, b) Calculated distribution (Picknett method), c) Calculated distribution (D_{50} method).

method does not account for the fact that the cyclone collects some particles which would otherwise reach the upper stages. The Picknett method does take this overlap in collection efficiencies into effect, and gives a good "average" of the distribution, smoothing out the abrupt steps.

Figure 32 is another simulation for which the input, or "true", distribution, the sum of two log normal distributions is bimodal and continuous. It can be seen that the Picknett scheme gives an excellent representation of the true distribution. Once again the D_{50} method distorts the distribution at the larger sizes.

Figure 33 shows true and calculated particle size distributions using actual experimental stage loadings. An 8.3 μm diameter ammonium fluorescein aerosol was generated using the vibrating orifice aerosol generator. About 4% of the particles were found to be doublets (8% of mass). This time, we see that neither method approximates the real distribution accurately, although the Picknett method does give a good mass median diameter. At this point, it is impossible to isolate the cause of the discrepancy, but there was visual evidence of reentrainment.

At the present time, the D_{50} method is still used for our data reduction (See Appendix A). Work is continuing to improve our computer program based on the Picknett method. We believe that this method will ultimately be more valuable because it extracts the maximum amount of particle size information from the experimental data.

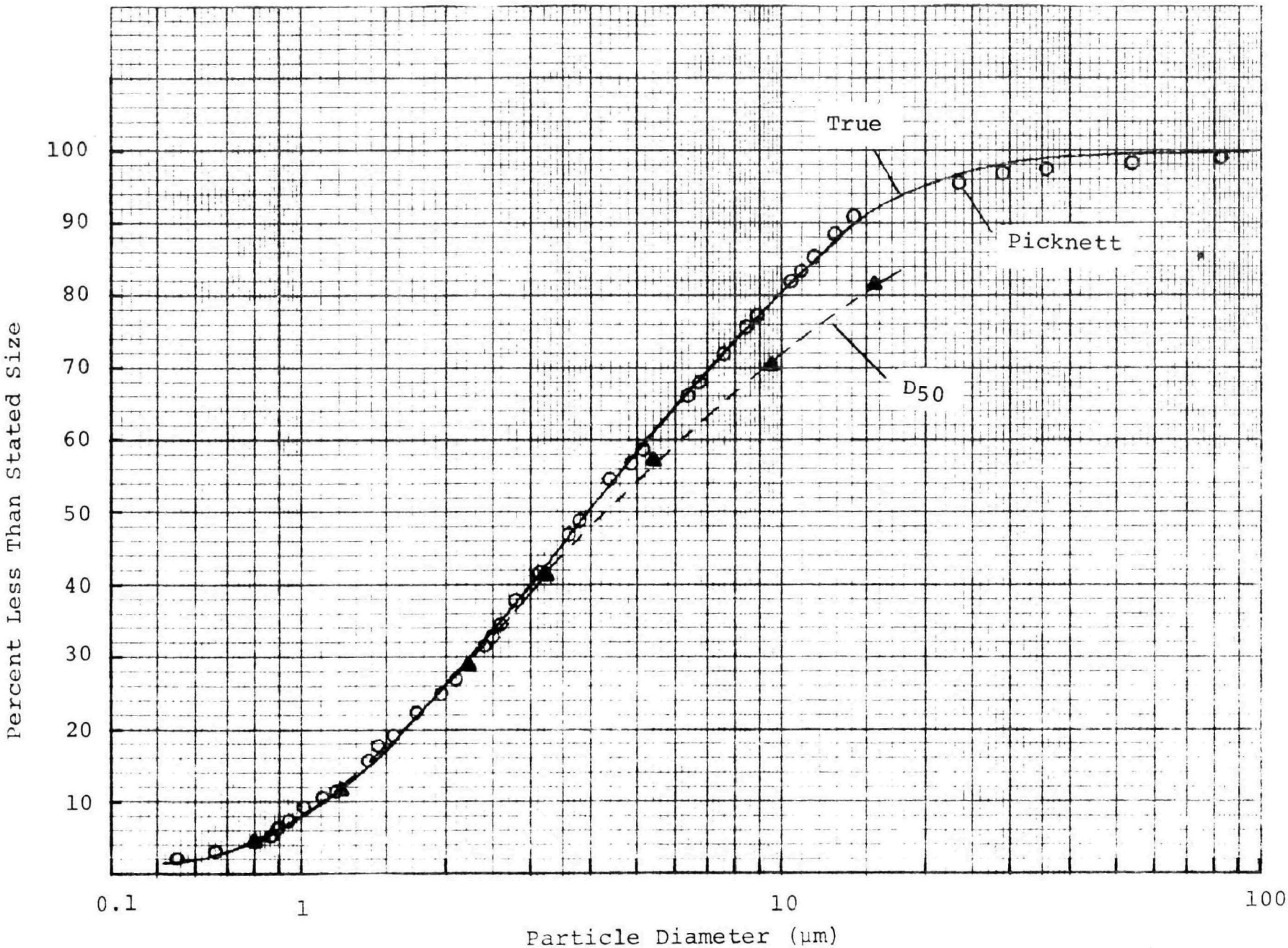

Figure 32. Simulation of a Continuous Particle Size Distribution

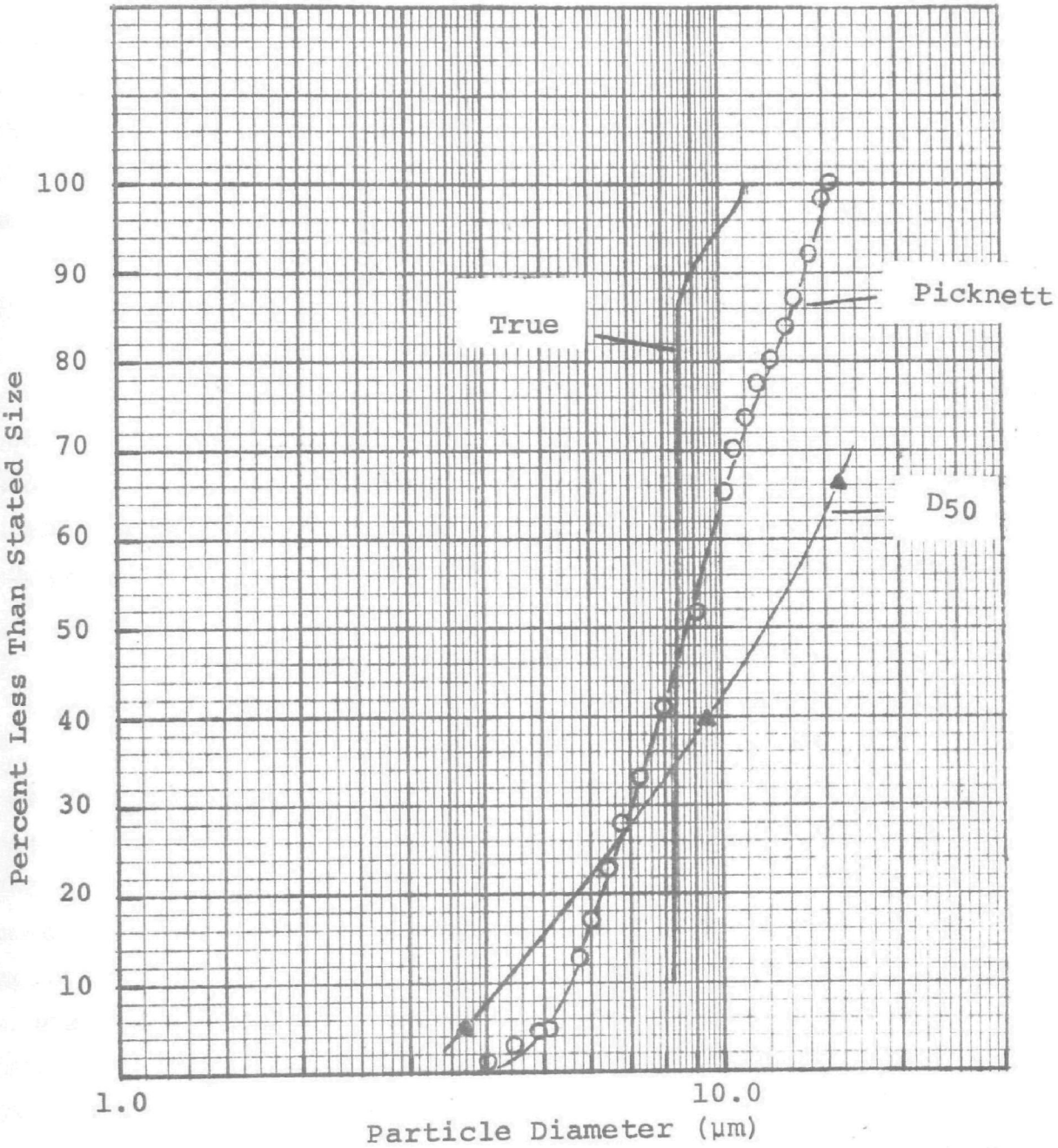

Figure 33. Impactor Tests Using a Known Particle Size Distribution

APPENDIX A - IMPACTOR OPERATING TECHNIQUES

A. Impactor Selection

In deciding which cascade impactor is the appropriate device for a sampling program, the main criteria is the mass loading and its effect on sampling time. In high grain loading situations such as the inlet to control devices, a low flow rate impactor (less than 0.1 acfm) is preferable because it permits reasonably long process averaging times, although in some cases, even with low flow rates the sampling time may be limited to only a few minutes. The use of a high flow rate impactor in these cases, would be unwise because impractically short sampling times would be required in order to avoid impactor overloading. On the other hand, low dust concentrations would result in excessively long sampling times with the low flow units. Impactors operating at flow rates near 0.5 acfm are normally used under these conditions to keep sampling times reasonably short. Even high flow rate impactors frequently require sampling times in excess of two hours to collect weighable stage loadings, especially at the outlet of high efficiency collectors.

The Brink Impactor is an example of a low flow rate impactor which is useful under heavy dust loading conditions, while the Andersen or Pilat (University of Washington) impactors are the high flow rate units which were used most often at control device outlets.

In many instances, the percentage (by weight) of material with sizes larger than the first impaction stage cut point can be quite high. In such cases, precollector cyclones are necessary to prevent the upper impactor stages from overloading. The Andersen cyclones are available from the manufacturer. The Brink cyclones used in this study were designed and fabricated by Southern Research Institute personnel.

To insure a valid size distribution from impactor measurements, it is imperative that isokinetic sampling be used, if at all possible. Figure A1 depicts the relationship between flue gas velocity and impactor flow rate for various nozzle sizes. This graph is used as a convenient means of selecting nozzle sizes to insure isokinetic sampling when the gas velocity is known and the appropriate impactor flow rate has been chosen. Also indicated on the graph are heavy horizontal lines giving the upper flow rate limits for various impactors to insure that severe reentrainment does not occur.

B. Sampling Time

The length of the sampling time is dictated by mass loading and size distribution. An estimate for initial tests can be made from Figure A2. Tests subsequent to the first should have sampling times adjusted such that no single stage, excluding a cyclone, if one is used, contains more than 10 mg. of mass.

C. Collection Substrates and Adhesives

Due to the necessity for high weighing accuracy and the restriction of low tare capacity in the case of most field useable precision balances, foil or glass fiber collection substrates are used with all impactors. The Brink is generally used with aluminum foil or glass fiber substrates, the Andersen utilizes special glass fiber inserts, and the Pilat is used with aluminum or stainless steel foil substrates. Depending on the temperature in the sampling duct, silicone vacuum grease or other high viscosity grease may be used on the foil substrates to aid in the retention of the impacting particles. It has been found that a thick (20%) solution or suspension of benzene and grease

NOTE
HEAVY HORIZONTAL LINES INDICATE MAXIMUM FLOW RATES WITHOUT REENTRAINMENT FOR VARIOUS IMPACTORS.

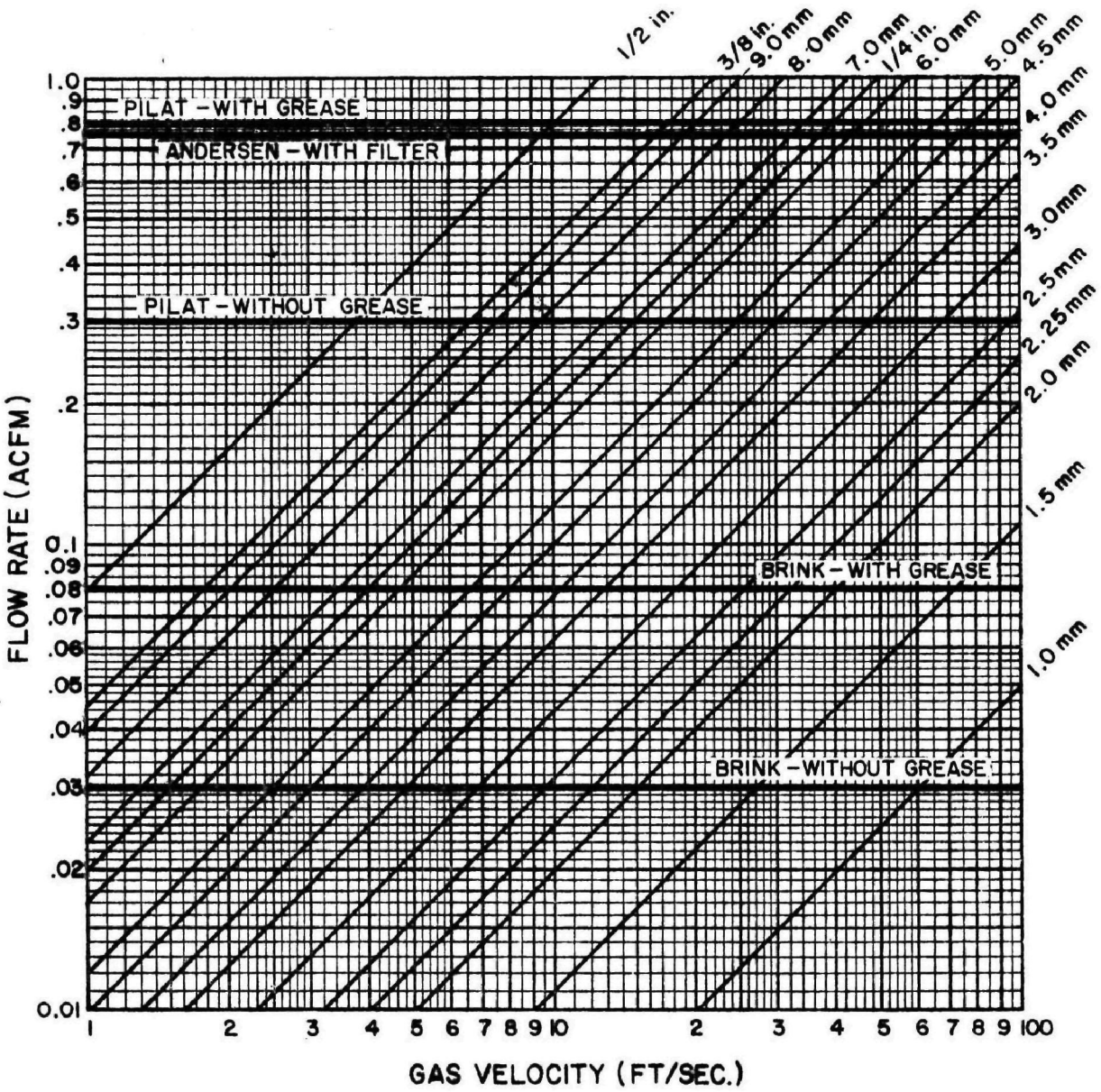

Figure A1. Nomograph For Selecting Nozzles For Isokinetic Sampling.

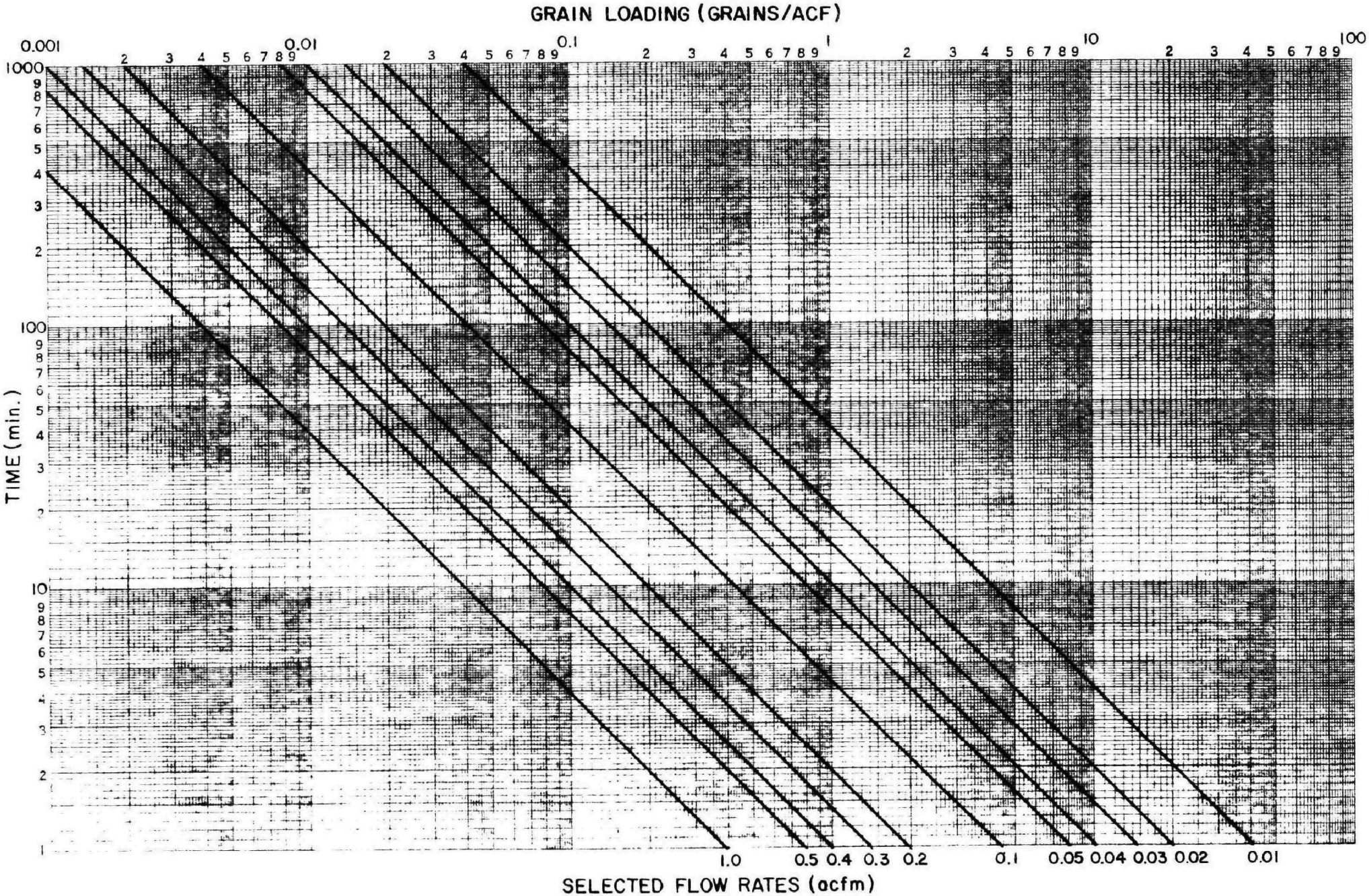

Figure A2. Sampling Time Determination For Total Mass Collection of 25 Milligrams.

serves this purpose well and is fairly easy to apply. If duct temperatures are 400°F or lower, this grease-benzene mixture will hold up satisfactorily under most sampling conditions. Horizontal operation of the impactors with greased substrates is not recommended due to possible flow of the grease. The Brink and Pilat foil substrates are fitted to the shape of the collection plates. After being shaped, an eye dropper is used to place the benzene and high vacuum grease solution on the foils. Four to five drops are placed on the upper stage Brink foils leaving a residue of about 20 mg. after evaporation of the benzene, and a single drop is placed in the center of the last two Brink stage foils. Enough solution is placed on the Pilat substrates to adequately cover the area under the jets (∿30 mg. of grease). These greased substrates are then baked at 400°F for 1 to 2 hours. If stage loadings are low, smaller amounts of grease can be used. When a new batch of grease is used, checks should be made for weight loss by the grease subsequent to the initial bakeout. After removal from the oven, the substrates are conditioned in a desiccator for 12 to 24 hours prior to weighing.

The use of grease with Brink and Pilat Impactors is necessary because of problems with reentrainment and particle bounce, which is especially severe at jet velocities over 35 to 40 m/sec and occurs in some instances at even lower velocities. High impactor flow rates result in high jet velocities in the lower stages. The use of grease allows higher flow rates than would be useable without grease by improving the particle retention of the impaction surface, but care must also be taken to insure that grease is not blown off the substrates. Grease blow off can occur at jet velocities greater than 65 m/sec.. Therefore, for each impactor there is a maximum permissible flow rate, the value of which depends on the type of impaction substrate that is being used.

The Andersen Impactor uses pre-formed glass fiber

filter substrates provided by the manufacturer. Handling of the Andersen substrates is simplified by cutting aluminum foil squares slightly larger than the substrates into which the substrates are folded twice before desiccation and weighing. After sampling, the substrates are returned to the same foil wrappers for conditioning and final weighing.

Back-up filters are used on all impactors to collect the material that passes the last impaction stage. Binderless glass fiber filter material such as Gelman Type A Glass Fiber Filter Web is used for this purpose. For the Brink, 1" diameter circular discs are placed under the last spring in the outlet stage of the impactor. The filter is protected by a teflon washer and a second filter disc placed behind the actual filter, which acts as a support. The Andersen uses 2½" diameter filter discs placed above the final "F" stage. The Pilat Impactor uses 47 mm filter discs in an integral filter holder.

D. Multipoint Sampling

Although it is desirable to sample at several points across a duct to insure that the sample collected is representative of the flue gas, the impactors should be operated isokinetically at a constant flow rate for each point sample. To accomplish a traverse, the impactor is operated at several discrete points across the duct, with properly selected nozzles and flow rates for isokinetic sampling, and the results averaged to give an "average" dust loading.

E. Impactor Orientation

Whenever possible, the impactors are oriented vertically to minimize gravitational effects such as flow of grease or falloff of collected particles. Horizontal placement is necessary at

times and extra care must be taken on such to not bump the impactor against the port during removal operations.

F. Heating Impactor

All condensible vapors must be in a gaseous state until they exit from the impactor unless a condensate is the prime aerosol being measured. In streams above 350°F, auxiliary heating is not usually required. Below 350°F, the exit temperature of the impactor is maintained at least 20°F above the process temperature. A thermocouple is normally used to monitor the temperature of the exit gas from the impactor.

Whether the impactor is being heated in the duct or externally, with heater tape, etc., an allowance of 30 minutes warm-up time is allowed as a minimum to insure that the impactor has been heated to duct or operating temperature.

G. Probes

Sampling probes to an impactor outside the duct are used only if there is no other way. Probes are kept to a minimum length and contain the fewest possible bends. A precollector cyclone is mounted at the end of the probe to remove the large particles and thus reduce line losses.

H. Balance Requirements

For accurate weighing of collected material, a balance with a sensitivity of at least 0.01 milligrams is required. This is especially true for the lower stages of the Brink Impactor where collection of 0.3 mg. or less is not uncommon. The balance must also be insensitive to vibration if it is to be

used in the field. During this study, a Cahn Model G-2 Electrobalance was used and found satisfactory.

I. Sampling Configurations

Several sampling train arrangements are available depending on the impactor used, flow, sampling time, etc.. The original Brink design called for a system similar to that shown in Figure A3. The flow rate is determined by the pressure drop across the impactor. When low flow rates are required, it is very difficult to accurately measure the pressure drop across the Brink. The low flow rates also make a dry gas meter useless. In performing most of our tests, we have used an in-stack system which incorporates a calibrated orifice as shown in Figure A4.

To insure proper measurement by the orifices and dry gas meter and to protect the vacuum pumps from damage resulting from condensable vapors, it is necessary to cool and dry the sampled gases immediately after they leave the impactor. For long sampling times or in cases where there is high water content, a series of condensers in an ice bath is useful in removing the water. A drying column is normally used after the condensers for further protection of the gas meter. Different size orifices such as 0.03, 0.06, 0.09 inches allow for a wide range of flow rates with reasonable pressure drops using a water manometer. Normally a Hg manometer is placed upstream of the orifice to determine the pressure at the inlet to the orifice.

The use of a calibrated orifice to monitor the impactor flow rate involves the following equation giving the pressure drop across the orifice water manometer.

$$\Delta P = \Delta P_o \left(\frac{QI}{QC}\right)^2 (1-F_{H_2O})^2 \frac{P_s^2}{P_o P_c} \frac{T_o T_c}{T_s^2} \left(\frac{MM}{MA}\right) \qquad \text{(A1)}$$

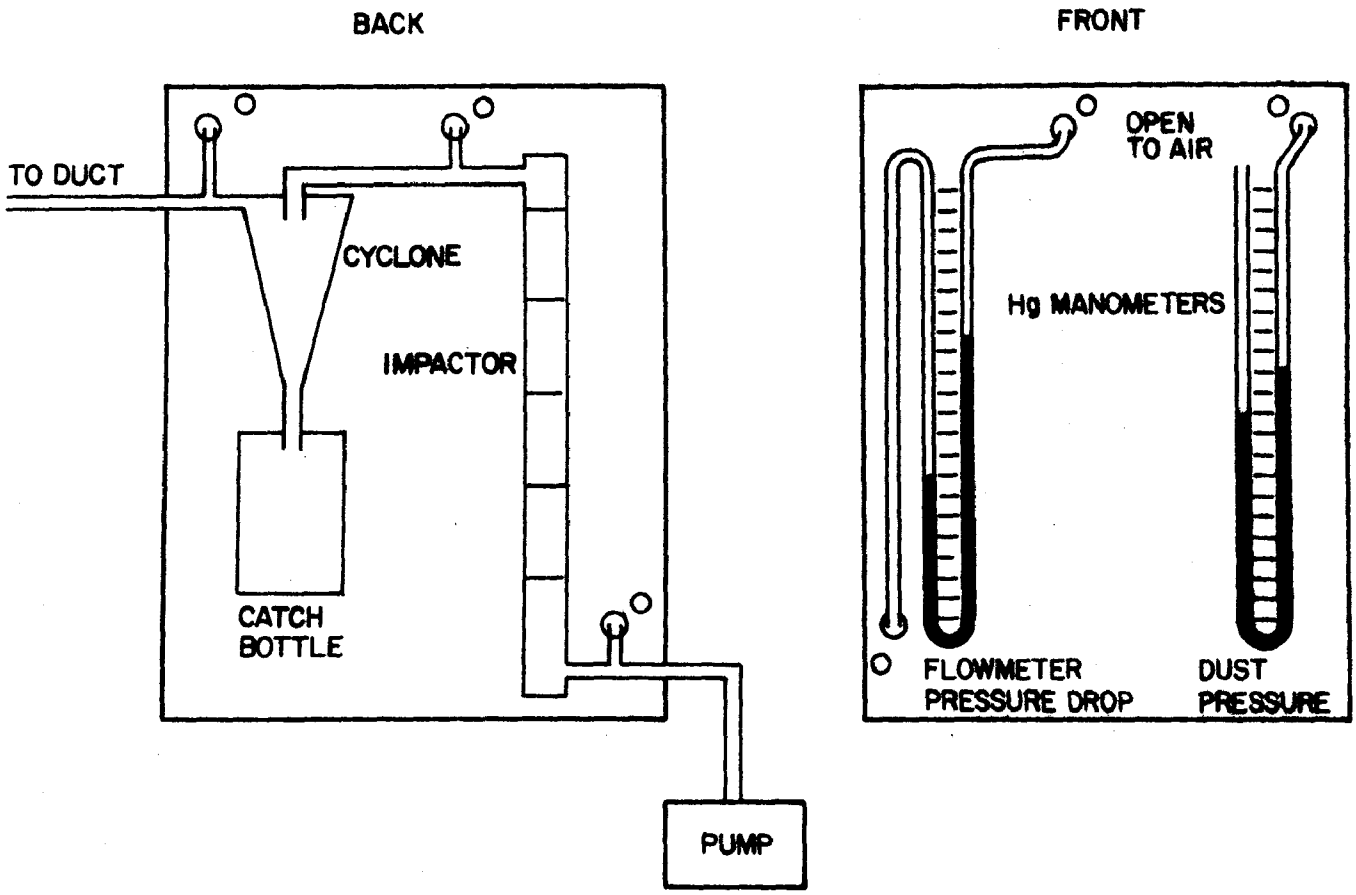

Figure A3. The Original Brink Impactor System,
BMS-11,
Set-up for out of stack sampling.

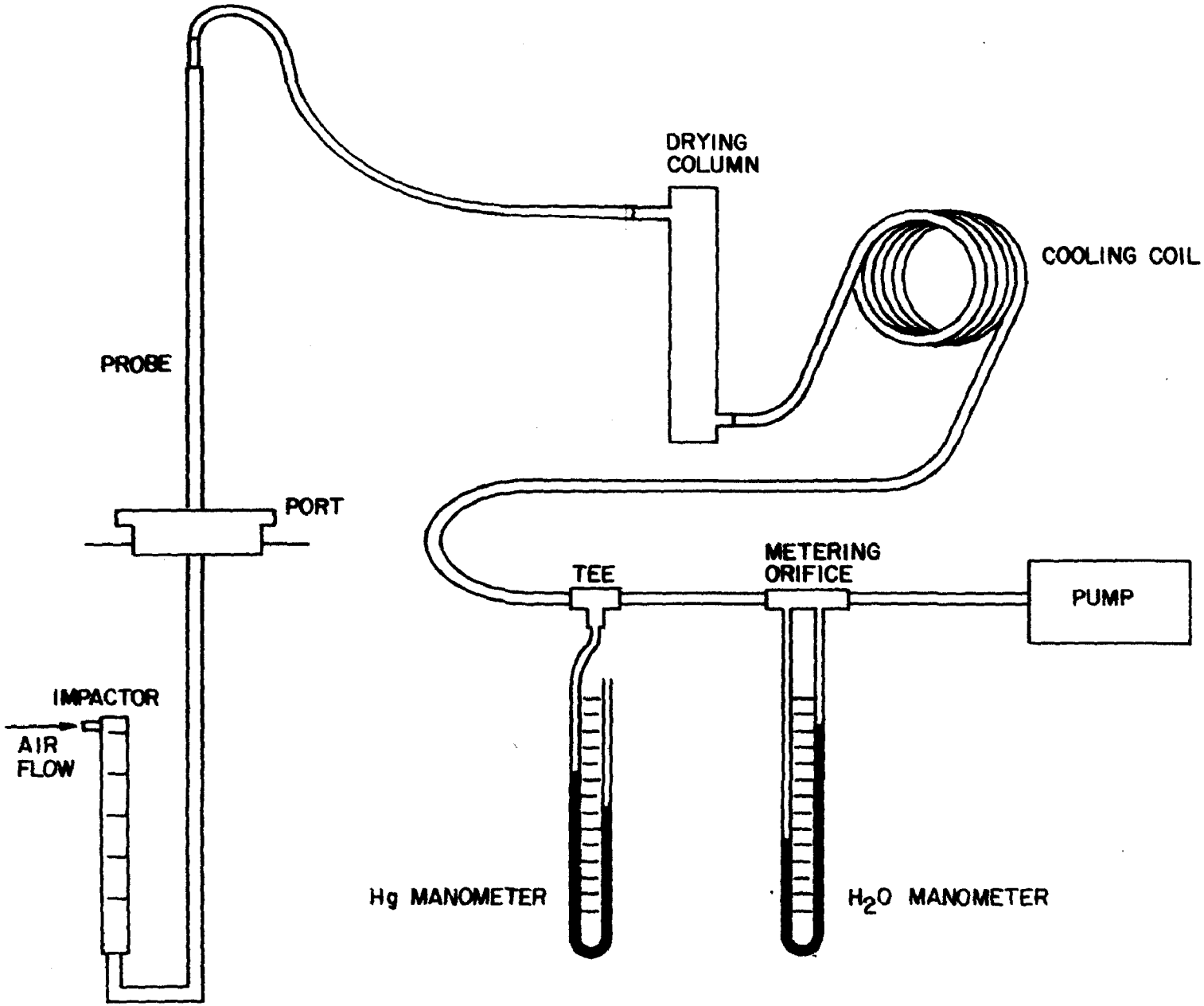

Figure A4. An Improved Method of Flow Control for the Brink Impactor using a calibrated orifice flowmeter.

MM = Mean Molecular Weight of Flue Gas

MA = Mean Molecular Weight of Air

ΔP = Calibrated orifice pressure drop "H_2O

ΔP_o = Pressure drop at which orifice calibrated "H_2O

QI = Impactor flow rate chosen for isokinetic sampling ACFM

Q_c = Calibration flow rate for orifice ACFM

F_{H_2O} = Volume fraction of water in the flue gas

P_s = Ambient stack pressure $P_s = P_a + \Delta P_s$ "Hg

P_o = Pressure upstream of orifice referred to ambient "Hg

P_c = Ambient pressure when orifice calibrated "Hg

T_o = Temperature of the orifice ^oR

T_c = Temperature of the orifice when calibrated ^oR

T_s = Stack temperature ^oR

To monitor impactor flow rate with a dry gas meter, either individually or in conjunction with a calibrated orifice, the following equation pertains:

$$Q_m = Q_s \frac{T_a}{T_s} \frac{P_s}{P_a} (1 - F_{H_2O})$$

Q_m = Flow rate indicated by the dry gas meter ACFM

T_a = Temperature of metered air ^oR

T_s = Flue gas temperature ^oR

P_a = Ambient pressure upstream of the meter "Hg

P_s = Ambient stack pressure "Hg

F_{H_2O} = Volume fraction of water in flue gas

In-stack sampling is recommended in all cases where practical; however, in certain cases, out-of-stack sampling is the only solution.

To apply equation A1, monitoring of the orifice or meter inlet pressures is necessary. We have found that the total

volume of gas sampled, as measured by the calibrated orifice and by the dry gas meter, agree within a fraction of one percent. Thus, the gas meter may be left out of the system if it is inconvenient or difficult to use at a particular location. For most cases, with the Andersen and Pilat Impactors, where large gas volumes are to be sampled, the system shown in Figure A5 can be used depending primarily on the ability of the gas meter to withstand the large pressure differentials in the system. A sufficiently long piece of pipe is attached to the impactor to insure proper positioning and traverse capabilities in the duct and to insure that the impactor is not cooled by heat transfer along the probe if external heating of the impactor is not used.

Negative duct pressures can cause problems resulting from backflow through the impactor causing material to be blown off the collection substrates onto the underside of the jet plate after conclusion of sampling. Thus, care was taken to insure that no gas flow through the impactor takes place except when sampling.

J. Preparing the Impactors

The impactor is carefully loaded with the preweighed stage substrates. The Andersen requires that extra attention be paid to the alignment of the substrate to the stage and stage to stage insuring that the jets are not blocked by the substrate and the jets of one stage are above the collection surface of the next stage. After all stages are loaded, the entrance cap is placed on the Brink and the shells are placed on the Andersen and Pilat. The Brink is tightened with wrenches to make certain the asbestos gaskets are seated. Handtightening is sufficient for the Andersen or Pilat Impactors. Over tightening will cause the stainless seals to cut into the Andersen substrates. After assembly, the appropriate nozzle is added. (See Figure A1.)

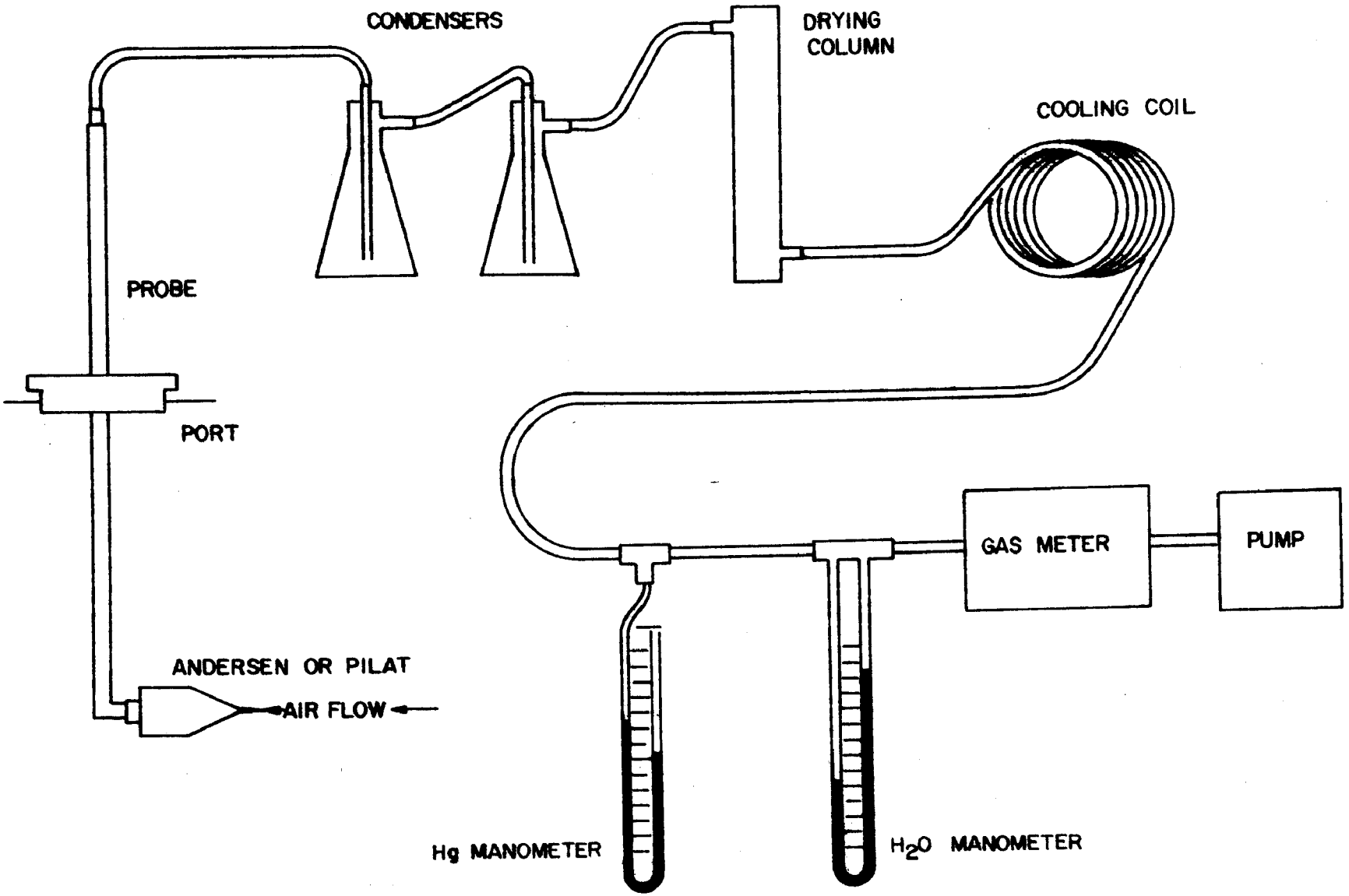

Figure A5. The typical Andersen or Pilat setup using calibrated orifice and dry gas meter.

If supplemental heating is required, the heating tapes, insulation and temperature monitors need to be added. A thermocouple mounted in the gas flow immediately after the impactor is best for controlling heating. This also yields the temperature needed for calculating impactor cut points. A heating tape of sufficient heating capacity is wrapped around the impactor. Fiber glass tape is used for holding the heating tape. Insulation such as asbestos tape is then wound around the impactor. Fiber glass tape is again added to hold the asbestos in place as insulation. An easily removed wrapping of aluminum foil is sometimes used to keep the impactor clean while in the duct.

The impactor is then mounted on the appropriate probe, taken to the sampling position and installed in the sampling system.

K. Taking the Sample

The impactor should be preheated for at least 30 minutes before sampling. If supplemental heat is being used, the impactor should be brought up to temperature outside the duct and then allowed some time to equilibrate after insertion. The nozzle should not point upstream into the gas flow during this phase.

The flow rate must be maintained at the predetermined level during testing to assure stable cut points. Any attempt to modulate flow to provide isokinetic sampling could destroy the validity of the data. The correct flow rate should be established quickly, especially for the short sampling times typically found at inlets.

L. Disassembling the Impactor

The post test procedure is very important in obtaining useful results. The crucial part is to make sure the collected material stays where it originally impacted. After the test, the impactor should be carefully removed from the duct without jarring, removed from the probe, and allowed to cool. Disassembly is quite tricky in some cases. It is good to have a pair of fine tweezers and a balance brush. Careful disassembly of a Brink is a necessity for obtaining good stage weights. If a precollector cyclone has been used, all material from nozzle to the outlet of the cyclone is included with the cyclone catch. All of this material is brushed onto a small tared 1" x 1" aluminum foil square to be saved for weighing. Cleaning the nozzle well is also important, especially if it is a small bore nozzle. All material between the cyclone outlet and second stage nozzle is generally included with material collected on the first collection substrate. All appropriate walls are brushed off as well as around the underside of the nozzle where a halo frequently occurs on the upper Brink stages. All material between the second stage nozzle and third stage nozzle is generally included with that on the second collection substrate. This process should be continued down to the last collection substrate. Care is necessary in taking out the filter. A good pair of sharp fine tweezers is essential in removing the foil substrates from the plates without losing grease and collected material.

Cleaning an Andersen is a demanding chore. A foil to hold the Stage 1 substrate is laid out. Next, the nozzle and entrance cone are brushed out and onto the foil. Then the material on Stage 0 is brushed off. Next, any material on the top o-ring and bottom of Stage 0 is brushed onto the foil. Finally, the

Stage 1 filter substrate material is placed on the foil and last, the top of the Stage 1 plate o-ring and cross piece is brushed off. Depending on how tight the impactor was screwed shut, some filter material may stick to the stainless steel edge contacting the substrate. This is carefully brushed onto the appropriate foil. This process is continued through the lower stages. Finally, the filter is carefully removed. Again, all material is desiccated 12 to 24 hours before final weighing.

Pilat clean up is similar to the Brink. Some problems have been noted with o-rings sticking and care must be exercised not to dislodge the sample while trying to separate the stages.

M. Data Logging

Records should be kept in notebooks for all phases of the sampling program. It was generally found convenient to keep three notebooks, one for recording weight, which remains in the lab with the balance and one each for recording the details on inlet and outlet sampling runs. A form similar to that shown in Figure A6 was used for recording the necessary information while sampling.

N. Cascade Impactor Data Reduction

After an impactor runs, it is necessary to obtain a particle size distribution from the mass loadings on each stage. The conditions at which the impactor was run determine the stage D_{50} cut points. These can be calculated by an iterative solution of the following two equations:

$$D_{50} = 1.43 \times 10^4 \left[\frac{\mu D^3 {}_c P_s \; X(I)}{\rho_p Q_I \; P_o \; C \; 472.0} \right]^{1/2}$$

IMPACTOR IDENT.		RUN CODE NO.
OPERATOR	DATE	SAMPLING LOCATION
PORT NO.	PROBE DEPTH	STACK PRES.
AMB. PRES.	STACK TEMP.	IMPACTOR TEMP.
IN STACK/OUT-OF-STACK		SCALPING CYCLONE(S)
PITOT DELTA P	GAS VELOCITY	IMP. FLOW RATE
NOZZLE DIA.	IMPACTOR DELTA P.	START TIME
GAS METER END		TOTAL SAMPLING TIME
GAS METER START		METERING ORIFICE ΔP
METERING ORIFICE TEMP.		PRESS. AT METERING ORIFICE

REMARKS:

Figure A6. Form used for logging field test data.

$$C = 1 + \frac{2L}{D_{50} \times 10^{-4}} \left[1.23 + 0.41 \text{ EXP} \left[(-0.44\ D_{50})/L \times 10^{-4} \right] \right]$$

where

D_{50} is the stage cut point (μm),
μ = gas viscosity (poise),
D_c = stage jet diameter (cm),
P_s = local pressure at stage jet (atm),
ρ_p = particle density (gm/cm^3),
Q_I = impactor flow rate (cfm),
P_o = ambient pressure at impactor inlet (atm),
C = Cunningham Correction Factor,
L = Gas mean free path (cm), and
X(I) = Number of holes per stage.

The most feasible way to calculate these cut points is to write a computer program. Otherwise, it is a slow and tedious process. The size parameter reported can be either aerodynamic diameter, that is, diameter based on the behavior of unit density particles, or approximate physical diameter, based on the estimate of the true particle density. In either case, the particles are assumed to be spherical.

After calculation of the stage D_{50}'s, there are two possible methods of presenting the data. The "D_{50}" method is used at this time for the majority of cascade impactor work, but it is an oversimplification which can cause loss of information. Picknett[26] has developed a method which takes into account the non-ideal nature of cascade impactor collection efficiencies, specifically, the fact that a single particle can be collected by two or more stages is incorporated into the theory. In the Picknett method, discrete particle sizes are arbitrarily chosen using the D_{50} as an initial set, and their concentration calculated

such that the measured stage loadings would be obtained if the real particle size distribution had consisted of these chosen sizes. A large number of particle sizes may be chosen, giving a very good representation of the real distribution.

The particle size distribution may be presented on a differential or cumulative basis.

- Differential Particle Size Distributions - It is assumed for the purpose of analysis that all of the mass caught upon an impaction stage consists of material having aerodynamic diameters equal to, or greater than the D_{50} for that stage, and less than the D_{50} for the next higher stage. For the first stage (or cyclone), it is assumed that all the material caught has aerodynamic diameters greater than, or equal to, the D_{50} for that stage (or cyclone), but less than some arbitrarily large value, say 100 μm.

If the true particle size distribution constituted a continuum, the amount of material having diameters between D and D+dD could be represented by $\frac{dM}{dD}$. Then the integral

$$\int_{D_1}^{D_2} \frac{dM}{dD} \cdot dD$$

would yield the total mass having diameters between D_1 and D_2.

Because the intervals between the stage D_{50}'s are logarithmically related, and to minimize scaling problems, the differential particle size distributions are plotted on log-log or semi-log paper with

$$\frac{dM}{d\ (\log D)}$$

as the ordinate and Log D_{geo} as the abscissa. (D_{geo} is the geometric mean of D_1 and D_2.) The mass on stage "n" is designated by dM_n.

The d(log D) associated with dM_n is $\log (D_{50})_{n+1} - \log (D_{50})_n$. The total mass having diameters between $(D_{50})_m$ and $(D_{50})_n$ is equal to the area under the curve

$$\text{Mass} = \sum_{t=m}^{n} \frac{dM_t}{\log (D_{50})_{t+1} - \log (D_{50})_t} \cdot \left[\log (D_{50})_{t+1} - \log (D_{50})_t\right]$$

or

$$\text{Mass} = \int_{D_m}^{D_n} \frac{dM}{d\ (\log D)} \cdot d\ (\log D)$$

for a near continuum.

The procedure outlined above describes the construction of a histogram. In practice, a smooth curve is drawn through the points, yielding an approximation to the real particle size distribution. Such a curve is needed to calculate fraction efficiencies of control devices if the D_{50}'s differ between inlet and outlet measurements. The accuracy of the approximation is limited by the number of points, and by the basic inaccuracy of neglecting the non-ideal behavior of the impactors, especially overlapping collection efficiencies for adjacent stages.

● Cumulative Particle Size Distributions - The data may be presented on a cumulative basis by summing the mass on all the collection stages and back-up filter, and plotting the fraction of the mass below a given size, versus size. This is frequently done on special log-probability paper. This paper is especially convenient for log normal distributions, but semi-log paper may be preferable for interpretation, especially if the distribution is not log normal. In general, cumulative distributions are more difficult to interpret than differential plots. The abscissa is the logarithm of the particle diameter, and the ordinate is the percentage smaller than this size. The value of the ordinate

at a given $(D_{50})_n$ would be

$$\text{Percent less than stated size} = \frac{\sum_{t=o}^{t=n} dM_t}{\sum_{t=o}^{N} dM_t} \times 100\%$$

where

t = o corresponds to the filter, and

t = N corresponds to the coarsest jet or cyclone.

Alternately, an analytical curve might be fitted to the cumulative distribution obtained above, and values of dM/d (log D) obtained by differentiation of the analytical expression.

The curve fitting approach is especially useful when using the Picknett method because the method results in the development of a "best fit" cumulative distribution providing a large number of discrete points on the cumulative distribution curve.

On the following pages is our computer program for impactor data reduction based on the D_{50} scheme. The program presented is especially for the Brink Cascade Impactor. It can be adapted for the Andersen or Pilat by altering the number of stages, the number of holes per stage, the jet diameter, the jet to plate spacing, the initial D_{50} estimate, and the fraction of the pressure drop at each stage.

```
C
C       MODIFIED BRINK CASCADE IMPACTOR
C
C       THIS IS A FORTRAN IV PROGRAM FOR CALCULATING STAGE CUT POINTS
C       (D50'S) AND THE PARTICLE SIZE DISTRIBUTION OF MATERIAL COL-
C       LECTED BY A MODIFIED BRINK CASCADE IMPACTOR .  COMMENT CARDS
C       DESCRIBE THE INPUT AND OUTPUT DATA AND THE IMPORTANT CALCULA-
C       TIONS.
C
C
      INTEGER X(7)
      REAL MASS(9),JSPA(7),MM,MU,L(7)
      REAL IMASS(9),ICUMM(9)
      DIMENSION PRCU(9)
      COMMON MASS,JSPA,MM,MU,L,X,POA,DPA,TTK,RHO,DUR,RA,F,CCUMM,MC,MCC
      COMMON MO,MM1,H,DMAX,DELP(7),FG(5),DC(7),SUB(7),PERCU(9),CUMM(9)
      COMMON GRNA,GRNS,GRNAM,GRNSM,CYC2,CYC3,DPC(7),REYN1(7),REYN2(7)
      COMMON FD(7),PS(7),AMASS(9)
      COMMON IMASS,MC2,MC3,MOO,MS
C
C       IF E=0, READ A NEW SET OF DATA.  IF E=1, STOP.
C
   12 READ(2,99) E
      IF(E) 11,11,93
C
C       PO -- GAS PRESSURE AT IMPACTOR INLET.  INCHES OF MERCURY.
C       DP -- PRESSURE DROP ACROSS THE IMPACTOR.  INCHES OF MERCURY.
C       T -- TEMPERATURE OF IMPACTOR.  DEGREES FAHRENHIET.
C       RHO -- PARTICLE DENSITY.  GRAMS/CUBIC CENTIMETER.
C       DUR -- DURATION OF IMPACTOR SAMPLING.  MINUTES.
C       DMAX -- MAXIMUM DIAMETER OF MATERIAL COLLECTED.  MICRONS.
C      IF C2 USED,  MC2=1; OTHERWISE, MC2=0.
C      IF C3 USED, MC3=1; OTHERWISE, MC3=0.
C      IF S0 USED, MOO=1; OTHERWISE, MOO=0.
C      IF LAST STAGE IS S5(S6), MS=5(6).
C      IF BACK-UP FILTER USED, MF=1; OTHERWISE, MF=0.
C       G -- IF G=1, WRITE REYNOLD'S NUMBERS AND JET VELOCITIES.
C       IF G=0, DO NOT WRITE THEM
C
   11 READ(2,300) PO,DP,T,RHO,DUR,DMAX,MC2,MC3,MOO,MS,MF,G
C
C       READ IN GAS COMPOSITION IN THIS ORDER--CO2(DRY)  CO(DRY)
C       N2(DRY)  O2(DRY)  H2O
C
      READ(2,102) (FG(I),I=1,5)
C
C       READ IN STAGE COLLECTIONS IN MILLIGRAMS IN THIS ORDER:
C       FILTER  STAGES(6,5,4,3,2,1,0)  C3 OR C2
C
      READ(2,106)  (MASS(I),I=1,9)
      DO 299 I=1,9
      MASS(I)=MASS(I)/1000.0
  299 CONTINUE
C
C       READ IN IMPACTOR SAMPLING FLOW RATE IN ACFM.
C
      READ(2,310) F
C
C       READ IN TEST INFORMATION(DATE,TIME,ETC.) BETWEEN COLUMNS
```

```
C        2 TO 51.  PUT A 1 IN COLUMN 1.
C
   13 READ(2,200)
C
C        CHANGE DRY GAS COMPOSITION TO WET.
C
      DO 251 I=1,4
      FG(I)=FG(I)*(1.0-FG(5))
  251 CONTINUE
C
C        DELP(I) IS THE FRACTION OF IMPACTOR PRESSURE DROP AT EACH STAGE.
C
      DELP(1)=0.00
      DELP(2)=0.004
      DELP(3)=0.008
      DELP(4)=0.014
      DELP(5)=0.045
      DELP(6)=0.143
      DELP(7)=1.000
C
C        DC(I) IS THE JET DIAMETER AT EACH STAGE IN CENTIMETERS.
C
      DC(1)=0.361
      DC(2)=0.249
      DC(3)=0.1775
      DC(4)=0.1396
      DC(5)=0.0946
      DC(6)=0.0731
      DC(7)=0.056
C
C        SUB(I) IS AN INITIAL ESTIMATE OF D50'S USED IN CALCULATING FINAL
C        VALUES OF SAME.  MICRONS.
C
      SUB(1)=6.00
      SUB(2)=3.15
      SUB(3)=1.69
      SUB(4)=1.10
      SUB(5)=0.57
      SUB(6)=0.33
      SUB(7)=0.20
C
C        X(I) IS THE NUMBER OF HOLES PER STAGE.
C
      X(1)=1
      X(2)=1
      X(3)=1
      X(4)=1
      X(5)=1
      X(6)=1
      X(7)=1
C
C        JSPA(I) IS THE JET TO PLATE SPACING IN CENTIMETERS.
C
      JSPA(1)=1.016
      JSPA(2)=0.747
      JSPA(3)=0.533
      JSPA(4)=0.419
      JSPA(5)=0.282
      JSPA(6)=0.220
      JSPA(7)=0.190
```

```
C
C       CHANGE PO TO ATMOSPHERES.
C
      POA=PO/29.92
C
C       CHANGE DP TO ATMOSPHERES.
C
      DPA=DP/29.92
C
C       RA IS THE AVERAGE MOLECULAR WEIGHT OF AIR.
C
      RA=28.97
C
C       MM IS THE AVERAGE MOLECULAR WEIGHT OF THE FLUE GAS.
C
      MM=44.10*FG(1)+28.01*FG(2)+28.02*FG(3)+32.00*FG(4)+18.02*FG(5)
C
C       CHANGE THE TEMPERATURE TO DEGREES CENTIGRADE.
C
      TT=5.0*(T-32.0)/9.0
C
C       CHANGE THE TEMPERATURE TO DEGREES KELVIN.
C
      TTK=273.0+(5.0*(T-32.0)/9.0)
C
C       THIS SUBROUTINE CALCULATES THE LOCAL PRESSURE AT EACH STAGE.
C
      CALL STAGEB
C
C       THIS SUBROUTINE CALCULATES THE GAS VISCOSITY.
C
      CALL VISB
C
C       THIS SUBROUTINE CALCULATES THE MOLECULAR MEAN FREE PATH.
C
      CALL MEANB
C
C       THIS SUBROUTINE CALCULATES THE D50 OF EACH STAGE.
C
      CALL CUTB
C
C       THIS SUBROUTINE CALCULATES THE CUMMULATIVE MASS AND CUMMULATIVE
C       PERCENT DISTRIBUTION.
C
      CALL CUMB
C
C       THIS SUBROUTINE CALCULATES THE REYNOLDS NUMBERS AT EACH STAGE ANI
C       AND THE LINEAR VELOCITY THROUGH THE STAGE JETS.
C
      CALL REYNNB
C
C       THIS LOOP CHANGES THE FLUE GAS COMPOSITION TO PERCENT.
C
      DO 10 I=1,5
      FG(I)=FG(I)*100.0
 10   CONTINUE
C
C       THIS LOOP ROUNDS OFF AND INVERTS THE ORDER OF THE MASS, CUMMULA
C       TIVE MASS, AND CUMMULATIVE PERCENT.
C
```

```
      DO 30 I=1,9
      K=IABS(I-10)
      IMASS(K)=MASS(I)
      ICUMM(K)=CUMM(I)+0.000005
      PRCU(K)=PERCU(I)+0.005
   30 CONTINUE
C
C       THIS STATEMENT WRITES THE TEST INFORMATION.
C
      WRITE(3,200)
C
C       THIS STATEMENT WRITES THE FLOW RATE, THE TEMPERATURE, AND THE
C       SAMPLING DURATION.
C
      WRITE(3,201) F,T,DUR
C
C       THIS STATEMENT WRITES THE PARTICLE DENSITY AND THE AMBIENT
C       PRESSURE.
C
      WRITE(3,202) RHO,PO
C
C       THIS STATEMENT WRITES THE FLUE GAS COMPOSITION.
C
      WRITE(3,203) FG(1),FG(2),FG(3),FG(4),FG(5)
C
C       THIS STATEMENT WRITES THE GRAINS PER ACTUAL CUBIC FOOT, THE
C       GRAINS PER STANDARD DRY CUBIC FOOT, AND THE IMPACTOR PRESSURE
C       DROP.
C
      WRITE(3,204) GRNA,GRNS,DP
C
C       THIS STATEMENT WRITES THE MILLIGRAMS PER ACTUAL CUBIC METER,
C       THE MILLIGRAMS PER STANDARD DRY CUBIC METER.
C
      WRITE(3,214) GRNAM,GRNSM
C
C       THIS STATEMENT WRITES A HEADING.
C
      WRITE(3,205)
C
C       THIS LOOP WRITES THE STAGE D50'S, THE STAGE COLLECTED MASS,
C       THE CUMMULATIVE MASS, AND THE CUMMULATIVE PERCENT.
C
      IF(MC2) 40,40,50
   50 WRITE(3,206) CYC2,IMASS(1),ICUMM(1),PRCU(2)
   40 IF(MC3) 60,60,70
   70 WRITE(3,207) CYC3,IMASS(1),ICUMM(1),PRCU(2)
   60 IF(MOO) 80,80,90
   90 WRITE(3,208) DPC(1),IMASS(2),ICUMM(2),PRCU(3)
   80 DO 100 I=1,MS
      WRITE(3,209) I,DPC(I+1),IMASS(I+2),ICUMM(I+2),PRCU(I+3)
  100 CONTINUE
      IF(MF) 110,110,120
  120 WRITE(3,210) IMASS(9),ICUMM(9)
  110 CONTINUE
C
C       IF G=1 THIS GROUP WRITES THE REYNOLD'S NUMBERS AND THE LINEAR
C       VELOCITY AT EACH STAGE.
C
   97 IF(G) 95,95,94
```

```
   94 WRITE(3,211)
      WRITE(3,212)
      DO 303 I=1,7
      WRITE(3,213) REYN1(I),REYN2(I),FD(I)
  303 CONTINUE
   95 CONTINUE
C
C       THIS SUBROUTINE CALCULATES THE SIZE DISTRIBUTION ON A MASS BASIS
C
      CALL DMDLDB
   98 GO TO 12
   93 STOP
   99 FORMAT(I1)
  300 FORMAT(F5.2,F6.3,F6.1,F4.2,F5.1,F5.1,I1,I1,I1,I1,I1,I1)
  102 FORMAT(5F6.4)
  106 FORMAT(9F6.5)
  310 FORMAT(F7.4)
  111 FORMAT(9F6.2)
  112 FORMAT(F6.2,4I1,F6.2)
  200 FORMAT(1H1,'                                                        ')
  201 FORMAT(1H0,2X,'FLOW RATE = ',F6.3,' ACFM',9X,'TEMPERATURE = ',F6.
     1,' F',5X,'SAMPLING DURATION = ',F5.2,' MIN')
  202 FORMAT(1H0,2X,'ASSUMED PARTICLE DENSITY = ',F4.2,' GM/CC',11X,'BA
     1OMETRIC PRESSURE = ',F6.2,' HG')
  203 FORMAT(1H0,2X,'CO2 = ',F5.2,7X,'CO = ',F5.2,6X,'N2 = ',F5.2,7X,'O
     1 = ',F5.2,7X,'H2O = ',F5.2)
  204 FORMAT(1H0,2X,'CALC. GRAIN LOADING = ',F10.5,' GR/ACF',6X,F10.5,'
     1GR/SDCF',10X,'DELTA P = ',F6.3,' HG')
  205 FORMAT(1H0,10X,'LOWER SIZE LIMIT',8X,'MASS',8X,'CUM MASS',8X,
     1'PER CENT CUM')
  206 FORMAT(1H0,4X,'C2',10X,F5.2,11X,F7.5,10X,F7.5,13X,F6.2)
  207 FORMAT(1H0,4X,'C3',10X,F5.2,11X,F7.5,10X,F7.5,13X,F6.2)
  208 FORMAT(1H0,4X,'S0',10X,F5.2,11X,F7.5,10X,F7.5,13X,F6.2)
  209 FORMAT(1H0,4X,'S',I1,10X,F5.2,11X,F7.5,10X,F7.5,13X,F6.2)
  210 FORMAT(1H0,2X,'FILTER',8X,'-----',11X,F7.5,10X,F7.5)
  211 FORMAT(1H1,'REYNOLDS NUMBERS AND LINEAR VELOCITY AT EACH STAGE')
  212 FORMAT(1H0,5X,'REYN-DC',10X,'REYN-JSPA',10X,'LIN-VEL')
  213 FORMAT(1H0,4X,F8.2,9X,F8.2,10X,F9.2)
  214 FORMAT(1H0,2X,'CALC. GRAIN LOADING = ',F9.4,' MGM/ACM',6X,F9.4,
     1' MGM/SDCM')
      END
```

```
      SUBROUTINE STAGEB
C
C
C       THIS SUBROUTINE CALCULATES THE PRESSURE AT EACH STAGE.
C
C
      INTEGER X(7)
      REAL MASS(9),JSPA(7),MM,MU,L(7)
      COMMON MASS,JSPA,MM,MU,L,X,POA,DPA,TTK,RHO,DUR,RA,F,CCUMM,MC,MCC
      COMMON MO,MM1,H,DMAX,DELP(7),FG(5),DC(7),SUB(7),PERCU(9),CUMM(9)
      COMMON GRNA,GRNS,GRNAM,GRNSM,CYC2,CYC3,DPC(7),REYN1(7),REYN2(7)
      COMMON FD(7),PS(7),AMASS(9)
      DO 10 I=1,7
      PS(I)=POA-DELP(I)*DPA
   10 CONTINUE
      RETURN
      END
```

```
      SUBROUTINE VISB
C
C
C       THIS SUBROUTINE CALCULATES THE VISCOSITY OF THE GAS USING
C       A METHOD PRESENTED BY C. R. WILKE IN A PAPER ENTITLED
C       "A VISCOSITY EQUATION FOR GAS MIXTURES" IN THE JOURNAL OF
C       CHEMICAL PHYSICS  VOLUME 8, NUMBER 4, APRIL 1950, PAGE 517.
C
C
      INTEGER X(7)
      REAL MASS(9),JSPA(7),MM,MU,L(7)
      DIMENSION WT(5),VS(5)
      COMMON MASS,JSPA,MM,MU,L,X,POA,DPA,TTK,RHO,DUR,RA,F,CCUMM,MC,MCC
      COMMON M0,MM1,H,DMAX,DELP(7),FG(5),DC(7),SUB(7),PERCU(9),CUMM(9)
      COMMON GRNA,GRNS,GRNAM,GRNSM,CYC2,CYC3,DPC(7),REYN1(7),REYN2(7)
      COMMON FD(7),PS(7),AMASS(9)
      TT=TTK-273.0
C
C       VS(I) ARE THE PURE GAS VISCOSITIES OF CO2,CO,N2,O2,H2O.
C
      VS(1)=138.494+0.499*TT-0.267E-02*TT*TT+0.972E-05*TT*TT*TT
      VS(2)=165.763+0.442*TT-0.213E-03*TT*TT
      VS(3)=167.086+0.417*TT-0.316E-03*TT*TT
      VS(4)=190.187+0.558*TT-0.336E-03*TT*TT+0.139E-06*TT*TT*TT
      VS(5)=87.800+0.374*TT+0.238E-04*TT*TT
C
C       WT(I) ARE THE MOLECULAR WEIGHTS OF CO2,CO,N2,O2,H2O.
C
      WT(1)=44.10
      WT(2)=28.01
      WT(3)=28.02
      WT(4)=32.00
      WT(5)=18.02
      MU=0.0
      DO 200 I=1,5
      IF(FG(I)-0.0) 200,199,200
  199 FG(I)=1.0E-20
  200 CONTINUE
      DO 300 I=1,5
      XPHEE1=0.0
      XPHEE=0.0
      PHEE=0.0
      DO 400 J=1,5
      XPHEE=((1.0+(SQRT(VS(I)/VS(J)))*((WT(J)/WT(I))**0.25))**2.0)/((4.
     1/1.414)*(SQRT(1.0+(WT(I)/WT(J)))))
      XPHEE1=FG(J)*XPHEE
      IF(J-I) 399,400,399
  399 PHEE=PHEE+XPHEE1
  400 CONTINUE
      PHEE=PHEE/FG(I)+1.0
      MU=MU+VS(I)/PHEE
  300 CONTINUE
C
C       THE FINAL VISCOSITY MU IS IN POISE.
C
      MU=MU*1.0E-06
      RETURN
      END
```

```
001          SUBROUTINE MEANB
002    C
003    C
004    C       THIS SUBROUTINE CALCULATES THE MOLECULAR MEAN FREE PATH AT EACH
005    C       STAGE JET IN CENTIMETERS.
006    C
007    C
008          INTEGER X(7)
009          REAL K
010          REAL MASS(9),JSPA(7),MM,MU,L(7)
011          COMMON MASS,JSPA,MM,MU,L,X,POA,DPA,TTK,RHO,DUR,RA,F,CCUMM,MC,MCC
012          COMMON MO,MM1,H,DMAX,DELP(7),FG(5),DC(7),SUB(7),PERCU(9),CUMM(9)
013          COMMON GRNA,GRNS,GRNAM,GRNSM,CYC2,CYC3,DPC(7),REYN1(7),REYN2(7)
014          COMMON FD(7),PS(7),AMASS(9)
015          K=1.38E-16
016          DO 30 I=1,7
017          L(I)=(2.0*MU/(PS(I)*1.01325E06))*(SQRT((K*TTK*602.3E21)/(3*MM)))
018       30 CONTINUE
019           RETURN
020          END
```

```
      SUBROUTINE CUTB
C
C
C       THIS SUBROUTINE CALCULATES THE STAGE CUT POINTS OR D50'S BASED
C       ON EQUATIONS DEVELOPED BY RANZ AND WONG GIVEN IN "IMPACTION
C       OF DUST AND SMOKE PARTICLES ON SURFACE AND BODY COLLECTORS",
C       INDUSTRIAL AND ENGINEERING CHEMISTRY, 1952.
C
C
      INTEGER X(7)
      REAL MASS(9),JSPA(7),MM,MU,L(7)
      COMMON MASS,JSPA,MM,MU,L,X,POA,DPA,TTK,RHO,DUR,RA,F,CCUMM,MC,MCC
      COMMON MO,MM1,H,DMAX,DELP(7),FG(5),DC(7),SUB(7),PERCU(9),CUMM(9)
      COMMON GRNA,GRNS,GRNAM,GRNSM,CYC2,CYC3,DPC(7),REYN1(7),REYN2(7)
      COMMON FD(7),PS(7),AMASS(9)
C
C       THIS ITERATIVE LOOP CONTINUES UNTIL CONVERGENCE WITHIN 0.1%.
C
      DO 30 I=1,7
      C=0.0
      DPC(I)=SUB(I)
    4 DPCI=DPC(I)
    5 C=1.0+(2.0*L(I)/(DPC(I)*1.E-4))*(1.23+0.41*EXP(-.44*DPC(I)*1.E-4
     1/L(I)))
      DPC(I)=1.43E04*(SQRT(MU*X(I)*(DC(I)**3)*PS(I)/(RHO*F*472.0*POA*C))
     1)
      IF(ABS(1.0-(DPC(I)/DPCI))-0.001) 30,30,4
   30 CONTINUE
      CYC2=155.6*SQRT(MU/(RHO*F))
      CYC3=232.2*SQRT(MU/(RHO*F))
      RETURN
      END
```

```
      SUBROUTINE CUMB
C
C
C       THIS SUBROUTINE CALCULATES THE CUMMULATIVE MASS AND CUMMULATIVE
C       PERCENT DISTRIBUTION AT EACH STAGE.
C
C
      INTEGER X(7)
      REAL MASS(9),JSPA(7),MM,MU,L(7)
      COMMON MASS,JSPA,MM,MU,L,X,POA,DPA,TTK,RHO,DUR,RA,F,CCUMM,MC,MCC
      COMMON MO,MM1,H,DMAX,DELP(7),FG(5),DC(7),SUB(7),PERCU(9),CUMM(9)
      COMMON GRNA,GRNS,GRNAM,GRNSM,CYC2,CYC3,DPC(7),REYN1(7),REYN2(7)
      COMMON FD(7),PS(7),AMASS(9)
      SUM=0.0
      DO 50 I=1,9
      SUM=SUM+MASS(I)
      CUMM(I)=SUM
   50 CONTINUE
      DO 60 I=1,9
      PERCU(I)=(CUMM(I)/SUM)*100.0
   60 CONTINUE
C
C       GRNA IS THE GRAINS PER ACTUAL CUBIC FOOT.
C
      GRNA=(SUM*15.4324)/(F*DUR)
C
C       GRNS IS THE GRAINS PER STANDARD DRY CUBIC FOOT.
C
      GRNS=((SUM*15.4324)/((F*DUR*298.0*POA)/(TTK*1.0)))/(1.0-FG(5))
C
C       GRNAM IS THE MILLIGRAMS PER ACTUAL CUBIC METER.
C
      GRNAM=GRNA*2288.34
C
C       GRNSM IS THE MILLIGRAMS PER STANDARD DRY CUBIC METER.
C
      GRNSM=GRNS*2288.34
      RETURN
      END
```

```
      SUBROUTINE REYNNB
C
C
C       THIS SUBROUTINE CALCULATES THE LINEAR VELOCITY OF THE GAS AT
C       EACH STAGE JET IN CM/SEC, AND THE REYNOLD'S NUMBERS BASED ON
C       JET TO PLATE SPACING AND JET DIAMETER.
C
C
      INTEGER X(7)
      REAL MASS(9),JSPA(7),MM,MU,L(7)
      DIMENSION PP(10),RHOD(10)
      COMMON MASS,JSPA,MM,MU,L,X,POA,DPA,TTK,RHO,DUR,RA,F,CCUMM,MC,MCC
      COMMON M0,MM1,H,DMAX,DELP(7),FG(5),DC(7),SUB(7),PERCU(9),CUMM(9)
      COMMON GRNA,GRNS,GRNAM,GRNSM,CYC2,CYC3,DPC(7),REYN1(7),REYN2(7)
      COMMON FD(7),PS(7),AMASS(9)
      DO 101 I=1,7
      PP(I)=(POA-DPA*DELP(I))*29.92
  101 CONTINUE
      DO 110 I=1,7
      FD(I)=(F*4.0*29.92/(X(I)*DC(I)*DC(I)*PP(I)*3.14159))*472.0
  110 CONTINUE
      DO 120 I=1,7
      RHOD(I)=0.001185*((MM*298.0*PP(I))/(RA*TTK*29.92))
  120 CONTINUE
      DO 130 I=1,7
      REYN1(I)=RHOD(I)*FD(I)*DC(I)/MU
      REYN2(I)=RHOD(I)*FD(I)*JSPA(I)/MU
  130 CONTINUE
      RETURN
      END
```

```
      SUBROUTINE DMDLDB
C
C
C      THIS SUBROUTINE CALCULATES THE SIZE DISTRIBUTION ON A MASS BASIS.
C
C
      INTEGER X(7)
      REAL IMASS(9)
      REAL MASS(9),JSPA(7),MM,MU,L(7)
      DIMENSION GGRNS(9),DIFF(9),DMDLD(9),GEOMD(9)
      COMMON MASS,JSPA,MM,MU,L,X,POA,DPA,TTK,RHO,DUR,RA,F,CCUMM,MC,MCC
      COMMON MO,MM1,H,DMAX,DELP(7),FG(5),DC(7),SUB(7),PERCU(9),CUMM(9)
      COMMON GRNA,GRNS,GRNAM,GRNSM,CYC2,CYC3,DPC(7),REYN1(7),REYN2(7)
      COMMON FD(7),PS(7),AMASS(9)
      COMMON IMASS,MC2,MC3,M00,MS
C
C        THIS LOOP CALCULATES THE GRAINS PER STANDARD DRY CUBIC FOOT PER
C        STAGE.
C
      DO 505 I=1,9
      GGRNS(I)=((IMASS(I)*15.4324)/((F*DUR*298.0*POA)/(TTK*1.0)))/((100.
     10-FG(5))/100.0)
  505 CONTINUE
      WRITE(3,) (GGRNS(I),I=1,9)
      WRITE(3,507)
  507 FORMAT(1H0,5X,'GRAINS/SDCF/STAGE',10X,'DM/DLOGD',10X,'GEO. MEAN DI
     1A.')
  506 FORMAT(1H ,9X,F10.5,13X,F10.5,10X,F10.5)
      IF(MC2) 10,10,20
   20 IF(MS-5) 30,30,40
   30 CONTINUE
C
C        DIFF(I) IS THE DIFFERENCE IN THE COMMON LOGS OF THE STAGE D50'S.
C
      DIFF(1)=0.434294*(ALOG(DMAX)-ALOG(CYC2))
      DIFF(2)=0.434294*(ALOG(CYC2)-ALOG(DPC(2)))
      DIFF(3)=0.434294*(ALOG(DPC(2))-ALOG(DPC(3)))
      DIFF(4)=0.434294*(ALOG(DPC(3))-ALOG(DPC(4)))
      DIFF(5)=0.434294*(ALOG(DPC(4))-ALOG(DPC(5)))
      DIFF(6)=0.434294*(ALOG(DPC(5))-ALOG(DPC(6)))
      DIFF(7)=0.434294*(ALOG(DPC(6))-ALOG(0.08))
C
C        DMDLD IS A DIFFERENTIAL SIZE DISTRIBUTION ON A MASS BASIS.
C
      DMDLD(1)=GGRNS(1)/DIFF(1)
      DMDLD(2)=GGRNS(3)/DIFF(2)
      DMDLD(3)=GGRNS(4)/DIFF(3)
      DMDLD(4)=GGRNS(5)/DIFF(4)
      DMDLD(5)=GGRNS(6)/DIFF(5)
      DMDLD(6)=GGRNS(7)/DIFF(6)
      DMDLD(7)=GGRNS(9)/DIFF(7)
C
C        GEOMD(I) IS THE GEOMETRIC MEAN OF THE STAGE D50'S.
C
      GEOMD(1)=EXP(2.302585*(0.434294*ALOG(CYC2)+0.5*DIFF(1)))
      GEOMD(2)=EXP(2.302585*(0.434294*ALOG(DPC(2))+0.5*DIFF(2)))
      GEOMD(3)=EXP(2.302585*(0.434294*ALOG(DPC(3))+0.5*DIFF(3)))
      GEOMD(4)=EXP(2.302585*(0.434294*ALOG(DPC(4))+0.5*DIFF(4)))
      GEOMD(5)=EXP(2.302585*(0.434294*ALOG(DPC(5))+0.5*DIFF(5)))
```

```
      GEOMD(6)=EXP(2.302585*(0.434294*ALOG(DPC(6))+0.5*DIFF(6)))
      GEOMD(7)=EXP(2.302585*(0.434294*ALOG(0.08)+0.5*DIFF(7)))
      WRITE(3,506) GGRNS(1),DMDLD(1),GEOMD(1)
      WRITE(3,506) GGRNS(3),DMDLD(2),GEOMD(2)
      WRITE(3,506) GGRNS(4),DMDLD(3),GEOMD(3)
      WRITE(3,506) GGRNS(5),DMDLD(4),GEOMD(4)
      WRITE(3,506) GGRNS(6),DMDLD(5),GEOMD(5)
      WRITE(3,506) GGRNS(7),DMDLD(6),GEOMD(6)
      WRITE(3,506) GGRNS(9),DMDLD(7),GEOMD(7)
      GO TO 150
   40 CONTINUE
      DIFF(1)=0.434294*(ALOG(DMAX)-ALOG(CYC2))
      DIFF(2)=0.434294*(ALOG(CYC2)-ALOG(DPC(2)))
      DIFF(3)=0.434294*(ALOG(DPC(2))-ALOG(DPC(3)))
      DIFF(4)=0.434294*(ALOG(DPC(3))-ALOG(DPC(4)))
      DIFF(5)=0.434294*(ALOG(DPC(4))-ALOG(DPC(5)))
      DIFF(6)=0.434294*(ALOG(DPC(5))-ALOG(DPC(6)))
      DIFF(7)=0.434294*(ALOG(DPC(6))-ALOG(DPC(7)))
      DIFF(8)=0.434294*(ALOG(DPC(7))-ALOG(0.08))
      DMDLD(1)=GGRNS(1)/DIFF(1)
      DMDLD(2)=GGRNS(3)/DIFF(2)
      DMDLD(3)=GGRNS(4)/DIFF(3)
      DMDLD(4)=GGRNS(5)/DIFF(4)
      DMDLD(5)=GGRNS(6)/DIFF(5)
      DMDLD(6)=GGRNS(7)/DIFF(6)
      DMDLD(7)=GGRNS(8)/DIFF(7)
      DMDLD(8)=GGRNS(9)/DIFF(8)
      GEOMD(1)=EXP(2.302585*(0.434294*ALOG(CYC2)+0.5*DIFF(1)))
      GEOMD(2)=EXP(2.302585*(0.434294*ALOG(DPC(2))+0.5*DIFF(2)))
      GEOMD(3)=EXP(2.302585*(0.434294*ALOG(DPC(3))+0.5*DIFF(3)))
      GEOMD(4)=EXP(2.302585*(0.434294*ALOG(DPC(4))+0.5*DIFF(4)))
      GEOMD(5)=EXP(2.302585*(0.434294*ALOG(DPC(5))+0.5*DIFF(5)))
      GEOMD(6)=EXP(2.302585*(0.434294*ALOG(DPC(6))+0.5*DIFF(6)))
      GEOMD(8)=EXP(2.302585*(0.434294*ALOG(0.08)+0.5*DIFF(8)))
      GEOMD(7)=EXP(2.302585*(0.434294*ALOG(DPC(7))+0.5*DIFF(7)))
      WRITE(3,506) GGRNS(1),DMDLD(1),GEOMD(1)
      WRITE(3,506) GGRNS(3),DMDLD(2),GEOMD(2)
      WRITE(3,506) GGRNS(4),DMDLD(3),GEOMD(3)
      WRITE(3,506) GGRNS(5),DMDLD(4),GEOMD(4)
      WRITE(3,506) GGRNS(6),DMDLD(5),GEOMD(5)
      WRITE(3,506) GGRNS(7),DMDLD(6),GEOMD(6)
      WRITE(3,506) GGRNS(8),DMDLD(7),GEOMD(7)
      WRITE(3,506) GGRNS(9),DMDLD(8),GEOMD(8)
      GO TO 150
   10 IF(MC3) 50,50,60
   60 IF(MS-5) 70,70,80
   70 CONTINUE
      DIFF(1)=0.434294*(ALOG(DMAX)-ALOG(CYC3))
      DIFF(2)=0.434294*(ALOG(CYC3)-ALOG(DPC(1)))
      DIFF(3)=0.434294*(ALOG(DPC(1))-ALOG(DPC(2)))
      DIFF(4)=0.434294*(ALOG(DPC(2))-ALOG(DPC(3)))
      DIFF(5)=0.434294*(ALOG(DPC(3))-ALOG(DPC(4)))
      DIFF(6)=0.434294*(ALOG(DPC(4))-ALOG(DPC(5)))
      DIFF(7)=0.434294*(ALOG(DPC(5))-ALOG(DPC(6)))
      DIFF(8)=0.434294*(ALOG(DPC(6))-ALOG(0.08))
      DMDLD(1)=GGRNS(1)/DIFF(1)
      DMDLD(2)=GGRNS(2)/DIFF(2)
      DMDLD(3)=GGRNS(3)/DIFF(3)
      DMDLD(4)=GGRNS(4)/DIFF(4)
      DMDLD(5)=GGRNS(5)/DIFF(5)
```

```
      DMDLD(6)=GGRNS(6)/DIFF(6)
      DMDLD(7)=GGRNS(7)/DIFF(7)
      DMDLD(8)=GGRNS(9)/DIFF(8)
      GEOMD(1)=EXP(2.302585*(0.434294*ALOG(CYC3)+0.5*DIFF(1)))
      GEOMD(2)=EXP(2.302585*(0.434294*ALOG(DPC(1))+0.5*DIFF(2)))
      GEOMD(3)=EXP(2.302585*(0.434294*ALOG(DPC(2))+0.5*DIFF(3)))
      GEOMD(4)=EXP(2.302585*(0.434294*ALOG(DPC(3))+0.5*DIFF(4)))
      GEOMD(5)=EXP(2.302585*(0.434294*ALOG(DPC(4))+0.5*DIFF(5)))
      GEOMD(6)=EXP(2.302585*(0.434294*ALOG(DPC(5))+0.5*DIFF(6)))
      GEOMD(7)=EXP(2.302585*(0.434294*ALOG(DPC(6))+0.5*DIFF(7)))
      GEOMD(8)=EXP(2.302585*(0.434294*ALOG(0.08)+0.5*DIFF(8)))
      WRITE(3,506) GGRNS(1),DMDLD(1),GEOMD(1)
      WRITE(3,506) GGRNS(2),DMDLD(2),GEOMD(2)
      WRITE(3,506) GGRNS(3),DMDLD(3),GEOMD(3)
      WRITE(3,506) GGRNS(4),DMDLD(4),GEOMD(4)
      WRITE(3,506) GGRNS(5),DMDLD(5),GEOMD(5)
      WRITE(3,506) GGRNS(6),DMDLD(6),GEOMD(6)
      WRITE(3,506) GGRNS(7),DMDLD(7),GEOMD(7)
      WRITE(3,506) GGRNS(9),DMDLD(8),GEOMD(8)
      GO TO 150
   80 CONTINUE
      DIFF(1)=0.434294*(ALOG(DMAX)-ALOG(CYC3))
      DIFF(2)=0.434294*(ALOG(CYC3)-ALOG(DPC(1)))
      DIFF(3)=0.434294*(ALOG(DPC(1))-ALOG(DPC(2)))
      DIFF(4)=0.434294*(ALOG(DPC(2))-ALOG(DPC(3)))
      DIFF(5)=0.434294*(ALOG(DPC(3))-ALOG(DPC(4)))
      DIFF(6)=0.434294*(ALOG(DPC(4))-ALOG(DPC(5)))
      DIFF(7)=0.434294*(ALOG(DPC(5))-ALOG(DPC(6)))
      DIFF(8)=0.434294*(ALOG(DPC(6))-ALOG(DPC(7)))
      DIFF(9)=0.434294*(ALOG(DPC(7))-ALOG(0.08))
      DMDLD(1)=GGRNS(1)/DIFF(1)
      DMDLD(2)=GGRNS(2)/DIFF(2)
      DMDLD(3)=GGRNS(3)/DIFF(3)
      DMDLD(4)=GGRNS(4)/DIFF(4)
      DMDLD(5)=GGRNS(5)/DIFF(5)
      DMDLD(6)=GGRNS(6)/DIFF(6)
      DMDLD(7)=GGRNS(7)/DIFF(7)
      DMDLD(8)=GGRNS(8)/DIFF(8)
      DMDLD(9)=GGRNS(9)/DIFF(9)
      GEOMD(1)=EXP(2.302585*(0.434294*ALOG(CYC3)+0.5*DIFF(1)))
      GEOMD(2)=EXP(2.302585*(0.434294*ALOG(DPC(1))+0.5*DIFF(2)))
      GEOMD(3)=EXP(2.302585*(0.434294*ALOG(DPC(2))+0.5*DIFF(3)))
      GEOMD(4)=EXP(2.302585*(0.434294*ALOG(DPC(3))+0.5*DIFF(4)))
      GEOMD(5)=EXP(2.302585*(0.434294*ALOG(DPC(4))+0.5*DIFF(5)))
      GEOMD(6)=EXP(2.302585*(0.434294*ALOG(DPC(5))+0.5*DIFF(6)))
      GEOMD(7)=EXP(2.302585*(0.434294*ALOG(DPC(6))+0.5*DIFF(7)))
      GEOMD(8)=EXP(2.302585*(0.434294*ALOG(DPC(7))+0.5*DIFF(8)))
      GEOMD(9)=EXP(2.302585*(0.434294*ALOG(0.08)+0.5*DIFF(9)))
      WRITE(3,506) GGRNS(1),DMDLD(1),GEOMD(1)
      WRITE(3,506) GGRNS(2),DMDLD(2),GEOMD(2)
      WRITE(3,506) GGRNS(3),DMDLD(3),GEOMD(3)
      WRITE(3,506) GGRNS(4),DMDLD(4),GEOMD(4)
      WRITE(3,506) GGRNS(5),DMDLD(5),GEOMD(5)
      WRITE(3,506) GGRNS(6),DMDLD(6),GEOMD(6)
      WRITE(3,506) GGRNS(7),DMDLD(7),GEOMD(7)
      WRITE(3,506) GGRNS(8),DMDLD(8),GEOMD(8)
      WRITE(3,506) GGRNS(9),DMDLD(9),GEOMD(9)
      GO TO 150
   50 IF(M00) 90,90,100
  100 IF(MS-5) 110,110,120
```

```
  110 CONTINUE
      DIFF(1)=0.434294*(ALOG(DMAX)-ALOG(DPC(1)))
      DIFF(2)=0.434294*(ALOG(DPC(1))-ALOG(DPC(2)))
      DIFF(3)=0.434294*(ALOG(DPC(2))-ALOG(DPC(3)))
      DIFF(4)=0.434294*(ALOG(DPC(3))-ALOG(DPC(4)))
      DIFF(5)=0.434294*(ALOG(DPC(4))-ALOG(DPC(5)))
      DIFF(6)=0.434294*(ALOG(DPC(5))-ALOG(DPC(6)))
      DIFF(7)=0.434294*(ALOG(DPC(6))-ALOG(0.08))
      DMDLD(1)=GGRNS(2)/DIFF(1)
      DMDLD(2)=GGRNS(3)/DIFF(2)
      DMDLD(3)=GGRNS(4)/DIFF(3)
      DMDLD(4)=GGRNS(5)/DIFF(4)
      DMDLD(5)=GGRNS(6)/DIFF(5)
      DMDLD(6)=GGRNS(7)/DIFF(6)
      DMDLD(7)=GGRNS(9)/DIFF(7)
      GEOMD(1)=EXP(2.302585*(0.434294*ALOG(DPC(1))+0.5*DIFF(1)))
      GEOMD(2)=EXP(2.302585*(0.434294*ALOG(DPC(2))+0.5*DIFF(2)))
      GEOMD(3)=EXP(2.302585*(0.434294*ALOG(DPC(3))+0.5*DIFF(3)))
      GEOMD(4)=EXP(2.302585*(0.434294*ALOG(DPC(4))+0.5*DIFF(4)))
      GEOMD(5)=EXP(2.302585*(0.434294*ALOG(DPC(5))+0.5*DIFF(5)))
      GEOMD(6)=EXP(2.302585*(0.434294*ALOG(DPC(6))+0.5*DIFF(6)))
      GEOMD(7)=EXP(2.302585*(0.434294*ALOG(0.08)+0.5*DIFF(7)))
      WRITE(3,506) GGRNS(2),DMDLD(1),GEOMD(1)
      WRITE(3,506) GGRNS(3),DMDLD(2),GEOMD(2)
      WRITE(3,506) GGRNS(4),DMDLD(3),GEOMD(3)
      WRITE(3,506) GGRNS(5),DMDLD(4),GEOMD(4)
      WRITE(3,506) GGRNS(6),DMDLD(5),GEOMD(5)
      WRITE(3,506) GGRNS(7),DMDLD(6),GEOMD(6)
      WRITE(3,506) GGRNS(9),DMDLD(7),GEOMD(7)
      GO TO 150
  120 CONTINUE
      DIFF(1)=0.434294*(ALOG(DMAX)-ALOG(DPC(1)))
      DIFF(2)=0.434294*(ALOG(DPC(1))-ALOG(DPC(2)))
      DIFF(3)=0.434294*(ALOG(DPC(2))-ALOG(DPC(3)))
      DIFF(4)=0.434294*(ALOG(DPC(3))-ALOG(DPC(4)))
      DIFF(5)=0.434294*(ALOG(DPC(4))-ALOG(DPC(5)))
      DIFF(6)=0.434294*(ALOG(DPC(5))-ALOG(DPC(6)))
      DIFF(7)=0.434294*(ALOG(DPC(6))-ALOG(DPC(7)))
      DIFF(8)=0.434294*(ALOG(DPC(7))-ALOG(0.08))
      DMDLD(1)=GGRNS(2)/DIFF(1)
      DMDLD(2)=GGRNS(3)/DIFF(2)
      DMDLD(3)=GGRNS(4)/DIFF(3)
      DMDLD(4)=GGRNS(5)/DIFF(4)
      DMDLD(5)=GGRNS(6)/DIFF(5)
      DMDLD(6)=GGRNS(7)/DIFF(6)
      DMDLD(7)=GGRNS(8)/DIFF(7)
      DMDLD(8)=GGRNS(9)/DIFF(8)
      GEOMD(1)=EXP(2.302585*(0.434294*ALOG(DPC(1))+0.5*DIFF(1)))
      GEOMD(2)=EXP(2.302585*(0.434294*ALOG(DPC(2))+0.5*DIFF(2)))
      GEOMD(3)=EXP(2.302585*(0.434294*ALOG(DPC(3))+0.5*DIFF(3)))
      GEOMD(4)=EXP(2.302585*(0.434294*ALOG(DPC(4))+0.5*DIFF(4)))
      GEOMD(5)=EXP(2.302585*(0.434294*ALOG(DPC(5))+0.5*DIFF(5)))
      GEOMD(6)=EXP(2.302585*(0.434294*ALOG(DPC(6))+0.5*DIFF(6)))
      GEOMD(7)=EXP(2.302585*(0.434294*ALOG(DPC(7))+0.5*DIFF(7)))
      GEOMD(8)=EXP(2.302585*(0.434294*ALOG(0.08)+0.5*DIFF(8)))
      WRITE(3,506) GGRNS(2),DMDLD(1),GEOMD(1)
      WRITE(3,506) GGRNS(3),DMDLD(2),GEOMD(2)
      WRITE(3,506) GGRNS(4),DMDLD(3),GEOMD(3)
      WRITE(3,506) GGRNS(5),DMDLD(4),GEOMD(4)
      WRITE(3,506) GGRNS(6),DMDLD(5),GEOMD(5)
```

```
      WRITE(3,506) GGRNS(7),DMDLD(6),GEOMD(6)
      WRITE(3,506) GGRNS(8),DMDLD(7),GEOMD(7)
      WRITE(3,506) GGRNS(9),DMDLD(8),GEOMD(8)
      GO TO 150
   90 IF(MS-5) 130,130,140
  130 CONTINUE
      DIFF(1)=0.434294*(ALOG(DMAX)-ALOG(DPC(2)))
      DIFF(2)=0.434294*(ALOG(DPC(2))-ALOG(DPC(3)))
      DIFF(3)=0.434294*(ALOG(DPC(3))-ALOG(DPC(4)))
      DIFF(4)=0.434294*(ALOG(DPC(4))-ALOG(DPC(5)))
      DIFF(5)=0.434294*(ALOG(DPC(5))-ALOG(DPC(6)))
      DIFF(6)=0.434294*(ALOG(DPC(6))-ALOG(0.08))
      DMDLD(1)=GGRNS(3)/DIFF(1)
      DMDLD(2)=GGRNS(4)/DIFF(2)
      DMDLD(3)=GGRNS(5)/DIFF(3)
      DMDLD(4)=GGRNS(6)/DIFF(4)
      DMDLD(5)=GGRNS(7)/DIFF(5)
      DMDLD(6)=GGRNS(9)/DIFF(6)
      GEOMD(1)=EXP(2.302585*(0.434294*ALOG(DPC(2))+0.5*DIFF(1)))
      GEOMD(2)=EXP(2.302585*(0.434294*ALOG(DPC(3))+0.5*DIFF(2)))
      GEOMD(3)=EXP(2.302585*(0.434294*ALOG(DPC(4))+0.5*DIFF(3)))
      GEOMD(4)=EXP(2.302585*(0.434294*ALOG(DPC(5))+0.5*DIFF(4)))
      GEOMD(5)=EXP(2.302585*(0.434294*ALOG(DPC(6))+0.5*DIFF(5)))
      GEOMD(6)=EXP(2.302585*(0.434294*ALOG(0.08)+0.5*DIFF(6)))
      WRITE(3,506) GGRNS(3),DMDLD(1),GEOMD(1)
      WRITE(3,506) GGRNS(4),DMDLD(2),GEOMD(2)
      WRITE(3,506) GGRNS(5),DMDLD(3),GEOMD(3)
      WRITE(3,506) GGRNS(6),DMDLD(4),GEOMD(4)
      WRITE(3,506) GGRNS(7),DMDLD(5),GEOMD(5)
      WRITE(3,506) GGRNS(9),DMDLD(6),GEOMD(6)
      GO TO 150
  140 CONTINUE
      DIFF(1)=0.434294*(ALOG(DMAX)-ALOG(DPC(2)))
      DIFF(2)=0.434294*(ALOG(DPC(2))-ALOG(DPC(3)))
      DIFF(3)=0.434294*(ALOG(DPC(3))-ALOG(DPC(4)))
      DIFF(4)=0.434294*(ALOG(DPC(4))-ALOG(DPC(5)))
      DIFF(5)=0.434294*(ALOG(DPC(5))-ALOG(DPC(6)))
      DIFF(6)=0.434294*(ALOG(DPC(6))-ALOG(DPC(7)))
      DIFF(7)=0.434294*(ALOG(DPC(7))-ALOG(0.08))
      DMDLD(1)=GGRNS(3)/DIFF(1)
      DMDLD(2)=GGRNS(4)/DIFF(2)
      DMDLD(3)=GGRNS(5)/DIFF(3)
      DMDLD(4)=GGRNS(6)/DIFF(4)
      DMDLD(5)=GGRNS(7)/DIFF(5)
      DMDLD(6)=GGRNS(8)/DIFF(6)
      DMDLD(7)=GGRNS(9)/DIFF(7)
      GEOMD(1)=EXP(2.302585*(0.434294*ALOG(DPC(2))+0.5*DIFF(1)))
      GEOMD(2)=EXP(2.302585*(0.434294*ALOG(DPC(3))+0.5*DIFF(2)))
      GEOMD(3)=EXP(2.302585*(0.434294*ALOG(DPC(4))+0.5*DIFF(3)))
      GEOMD(4)=EXP(2.302585*(0.434294*ALOG(DPC(5))+0.5*DIFF(4)))
      GEOMD(5)=EXP(2.302585*(0.434294*ALOG(DPC(6))+0.5*DIFF(5)))
      GEOMD(6)=EXP(2.302585*(0.434294*ALOG(DPC(7))+0.5*DIFF(6)))
      GEOMD(7)=EXP(2.302585*(0.434294*ALOG(0.08)+0.5*DIFF(7)))
      WRITE(3,506) GGRNS(3),DMDLD(1),GEOMD(1)
      WRITE(3,506) GGRNS(4),DMDLD(2),GEOMD(2)
      WRITE(3,506) GGRNS(5),DMDLD(3),GEOMD(3)
      WRITE(3,506) GGRNS(6),DMDLD(4),GEOMD(4)
      WRITE(3,506) GGRNS(7),DMDLD(5),GEOMD(5)
      WRITE(3,506) GGRNS(8),DMDLD(6),GEOMD(6)
      WRITE(3,506) GGRNS(9),DMDLD(7),GEOMD(7)
```

```
300          150 CONTINUE
301              RETURN
302              END
 PROG > 4K
```

APPENDIX B - EXTRACTIVE SAMPLING

Figure B1 shows our experimental setup for extracting, diluting, and drying representative aerosol samples from the duct. As shown in the schematic, a precollector cyclone is used to prevent particles from clogging the sample metering orifice. At the flow rate normally used, the cyclone has a cut point or D_{50} of about 5 μm and is oriented with the inlet nozzle downstream. Thus, this sampling method is anisokinetic and the sample withdrawn from the duct is representative of the flue gas only at diameters of about 2 μm and less.

The main probe and cyclone support is a 24 inch long section of 3/16 inch pipe. The sampling line is a length of ¼" copper tubing. The diluter body is a hollow aluminum cylinder approximately 5 inches in diameter, and 18 inches long. A perforated cone is located at one end within the diluter cavity and dilution air is forced through a number of jets arranged at various angles on the cone so that a highly turbulent mixing zone is established. The sample aerosol is drawn in at the apex of this cone.

Several taps are available on the diluter body where inlet lines to the optical and CN counters are connected. Other taps are located downstream on the diluter for return lines from these instruments. Return lines are sometimes necessary for proper operation of the aerosol sampling instruments when the diluter interior is significantly above or below atmospheric pressure because the sample flow rates will fluctuate and pneumatic valves will not function if the inlet and outlet pressures differ by more than a few inches of water.

Fine adjustments of the dilution ratio are made by opening or closing a bleed valve located on the dilution air pump. With this valve closed and return lines connected for all the aerosol sampling instruments, the air flow system is a closed

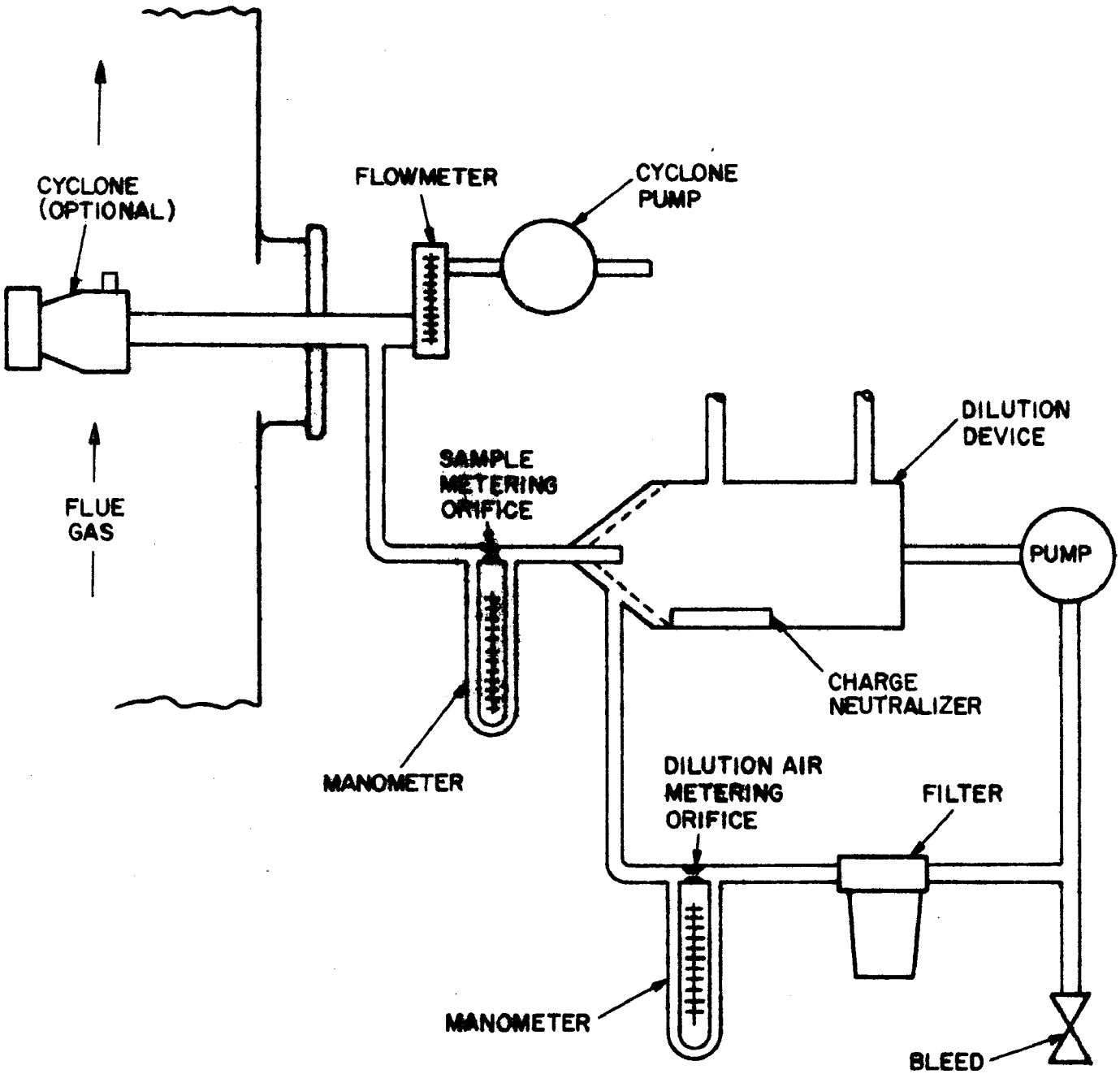

Figure B1. Extraction and Dilution system for out of stack flue gas sampling.

loop and no sample is drawn into the diluter. If, however, the bleed valve is opened, some air escapes and the sample air enters as makeup air. Using the bleed valve, the dilution ratio can be varied in a predictable fashion by about a factor of ten. For large changes in dilution, say on going from an inlet situation to an outlet, the sampling orifice is replaced with a venturi. Water manometers were adequate to monitor the orifice differential pressures.

For the sampling orifice,

$$Q_{SO} = C_{SO} \sqrt{\frac{\Delta P_{SO} T_{SO}}{P_{SO}}}$$

For the venturi,

$$Q_V = C_V \sqrt{\frac{\Delta P_V T_V}{P_V}}$$

And, for the dilution air metering orifice,

$$Q_D = C_D \sqrt{\frac{\Delta P_D T_D}{P_D}} ,$$

where

Q_{SO} = flow rate through sample metering orifice,
C_{SO} = calibration constant for sample metering orifice,
ΔP_{SO} = pressure differential across the sample metering orifice,
T_{SO} = temperature of the sample metering orifice, &
P_{SO} = the absolute pressure upstream from the sample metering orifice.

Subscripts of v and D denote these same parameters for the sample metering venturi and dilution air metering orifice, respectively.

The absolute pressure does not vary significantly from the dilution air metering orifice to the sample metering orifice, so that the dilution ratio can be calculated from:

$$D.F. = \frac{Q_D}{Q_{SO}} = \frac{C_D}{C_{SO}} \sqrt{\frac{\Delta P_D T_D}{\Delta P_{SO} T_{SO}}} \quad \text{or}$$

$$D.F. = \frac{Q_D}{Q_v} = \frac{C_D}{C_v} \sqrt{\frac{\Delta P_D T_D}{\Delta P_v T_v}}$$, depending on which sample metering arrangement is used.

The fraction of diluent air that is returned from the instruments is passed through glass condensers in an ice bath and dried. In some cases, additional drying is needed to avoid condensation in the sampling lines. Diffusional drying cylinders were used in the sampling lines to the instruments on one occasion where the flue gas contained 40% water. A diffusional dryer is shown in Figure B2. The sample aerosol is passed through the cylindrical cavity bounded by the 100 mesh stainless screen. Water molecules, having much higher mobilities than particulate, diffuse through the screen and are absorbed by the drierite. We hope that a similar device can be used to remove SO_x which also presents condensation problems when sampling. This depends upon selecting a material which will adsorb or absorb SO_x readily.

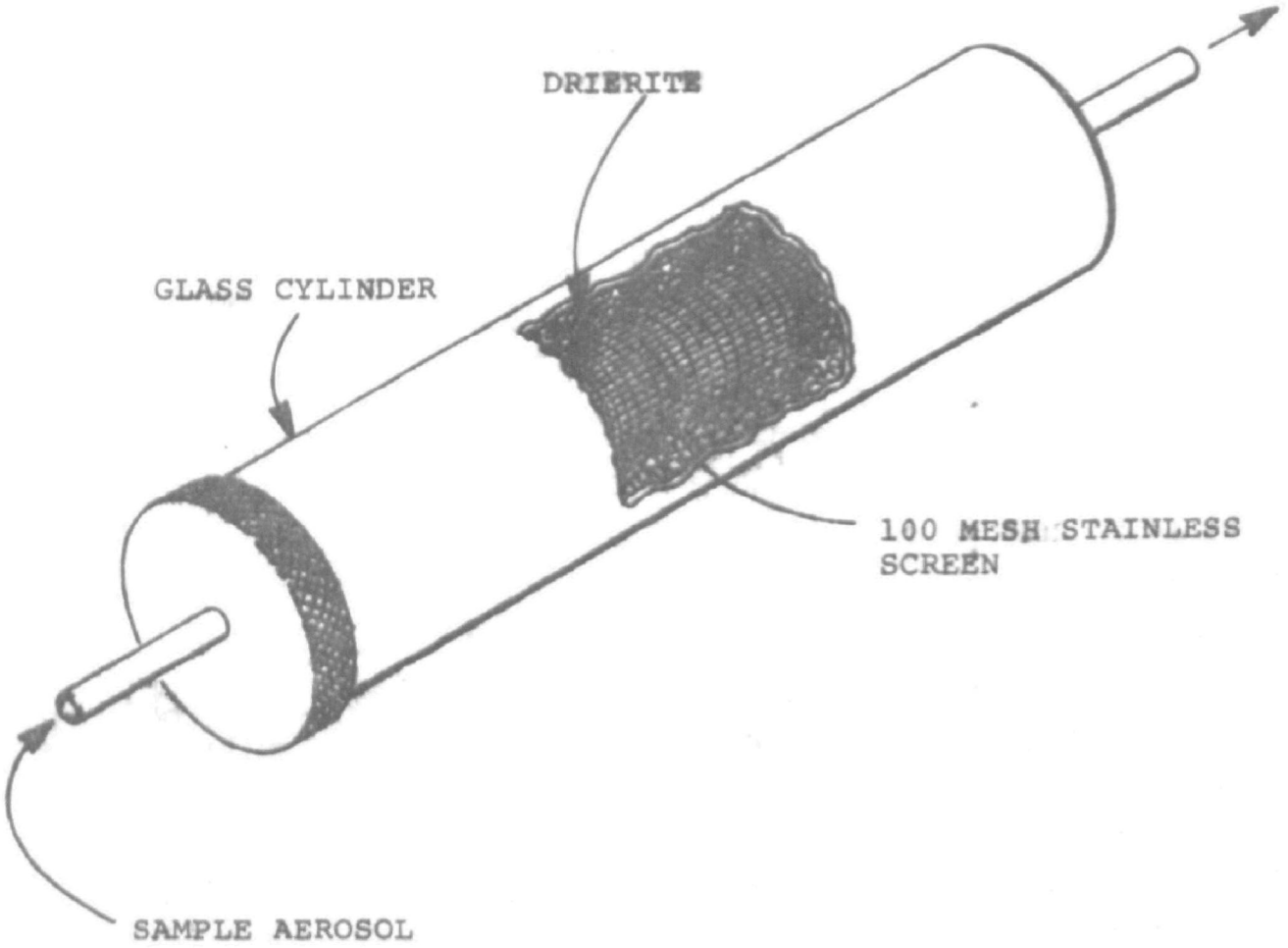

Figure B2. Diffusional Adsorption Apparatus for Removal of H_2O From Sample Aerosol.

APPENDIX C - DIFFUSIONAL PARTICLE SIZING

A. Experimental Procedure

Figure C1 is a block diagram showing the experimental set up for making particle size distribution measurements in the ultrafine range. One condensation nuclei (CN) counter is used to constantly monitor the diluted sample so that variations in particle concentration due to process fluctuations can be accounted for in the data reduction. A second CN counter, with a variable flow rate, is used to measure the particle concentration in the aerosol after passing through the diffusion batteries. The plumbing is arranged so that this CN counter reads the number concentration at the diluter outlet, or after penetrating one, two, three, or four diffusion batteries in series. The exhaust air from the CN counters is dried, filtered, and then returned to the diluter. The use of return lines minimizes pressure differentials between the inlet and exhaust section of the CN counters which might otherwise prevent proper operation. The antipulsation device shown in Figure C1 consists of a 0.005" thick surgical glove stretched over a 4½" plastic funnel as described by Sinclair.[15] These are necessary to damp out flow pulsations caused by the valving action in the CN counters and to insure laminar flow through the diffusion batteries. When calculating $\frac{n}{n_o}$, the fraction of the aerosol which penetrates a series of diffusion batteries, the transport time through the diffusion batteries must be taken into account. This is about 3½-5 minutes for each of the 100 channel diffusion batteries. Thus, with four large diffusion batteries in series, (n) at a particular time, would be related to n_o at a point 16-20 minutes earlier in time on a chart recording. Making a complete measurement of a particle size distribution takes 2-4 hours; thus, diffusional measurements are most useful on stable sources where the particle size distribution is constant in time.

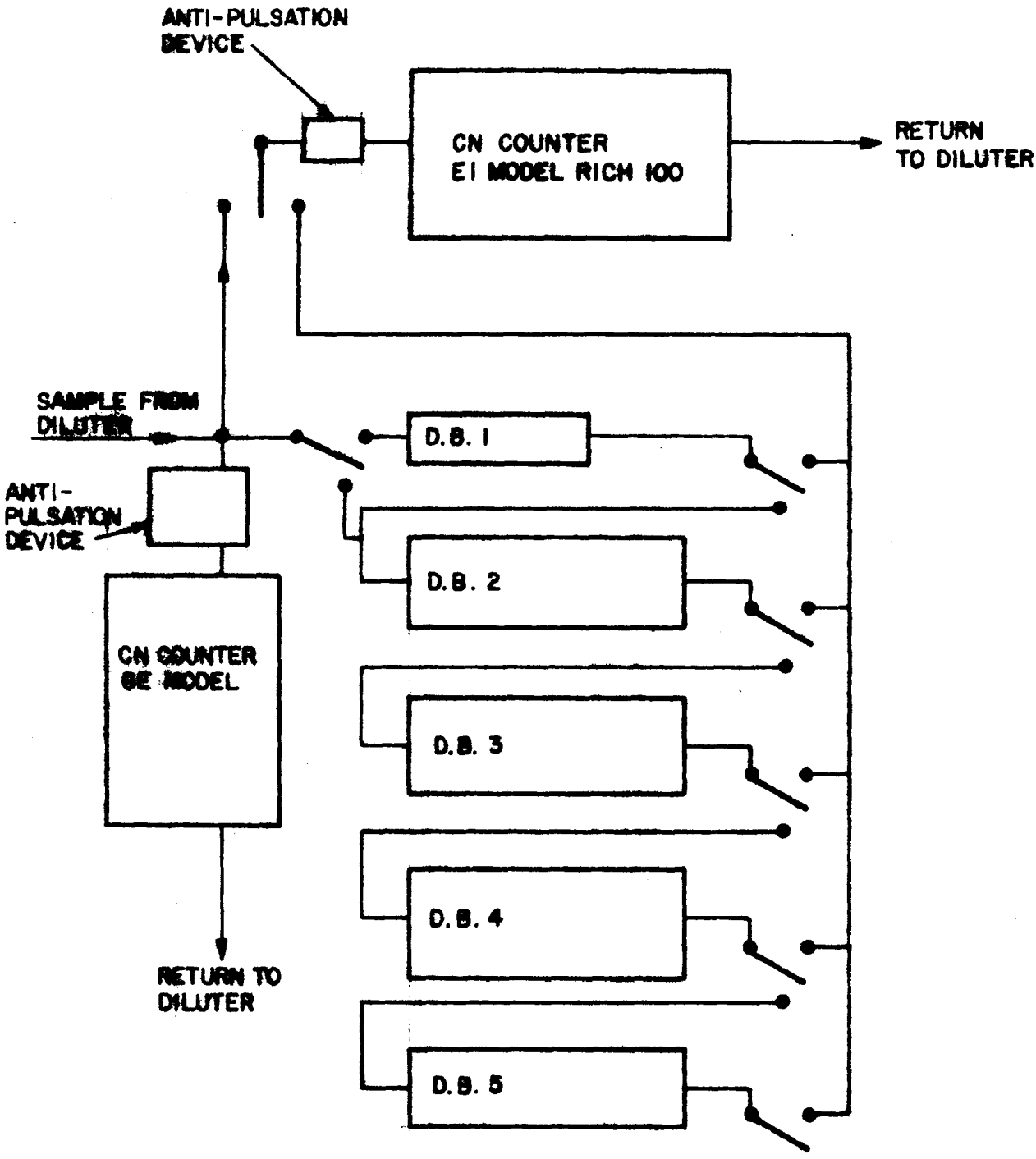

Figure C1. Diffusion battery and condensation nuclei counter lay-out for fine particle sizing.

Although the tests are normally run at a constant dilution ratio, the bleed value on the dilution air pump should be adjusted periodically to obtain a new dilution ratio and check the linearity of the diluter. Agreement between the calculated change in dilution (calculated from flow rates as measured using the calibrated orifice) and the response of the CN counters indicates that the diluter and CN counters are functioning properly.

By varying the number of diffusion batteries in series and the flow rate, it is possible to measure penetrations under a variety of conditions. In most cases, an effort is made to measure the penetration of four-100 channel diffusion batteries, one to four batteries in series and the 12 channel diffusion battery, all at three different flow rates. This yields fifteen data points from which the particle size distribution (0.01-0.2 μm diameter) can be reconstructed.

B. Data Analysis

The penetration of parallel plate diffusion batteries by a monodisperse aerosol is given by:[17]

$$\frac{n}{n_o} = 0.91e^{-xmD} + 0.053e^{-11.37xmD} + 0.051e^{-33.06xmD} + \ldots\ldots\ldots \quad (C1)$$

where

$x = 3.77\ bl/aQ$,

b = height of each rectangular slot (cm),

l = length of each rectangular slot (cm),

$2a$ = width of each rectangular slot (cm),

Q = volumetric flow rate (cm^3/sec),

m = outlet concentration (No./cm^3),

n_o = inlet concentration (No./cm^3),

D = diffusion coefficient of particles (cm^3/sec), and

m = number of rectangular channels in each diffusion battery.

Three methods were used to calculate particle size distributions from raw diffusional data. One method was to calculate a set of penetration curves similar to those in Figure 1b, and to apply the D_{50} technique which is commonly used with cascade impactors. This method was described in Appendix A. A second technique is that introduced by Fuchs et al[20] which assumes a log normal distribution. We regard this assumption as a loss of generality and this technique was not often used. The third technique, and the one which we normally use, was suggested by Sinclair.[15] Looking at equation C1, it can be seen that for a particular particle size (or diffusion coefficient), a diffusional sampling geometry can be described by the parameter xm, which involves the diffusion battery geometry and aerosol flow rate. In order to facilitate the data reduction, a nomograph is prepared, plotting $\frac{n}{n_o}$ versus xm for a number of particle sizes. Our nomograph is shown in Figure C2. The experimental data points will constitute a single curve similar to that shown in Figure C3. There is, however, some ambiguity associated with forming this experimental graph. Theoretically, the penetration of two or more diffusion batteries in series is given by the product of the penetrations of each individual battery. If all the terms in equation C1 are used, there is no unique value of the parameter xm, representing an equivalent diffusion battery geometry which is valid for all particle sizes. For the purpose of plotting the experimental data (n/n_o vs. xm), we have approximated the penetration by the first term in this equation. The error introduced by this approximation is less than two percent in all cases. Specifically, for one diffusion battery, $\frac{n}{n_o}$ is plotted versus xm; for two similar batteries,

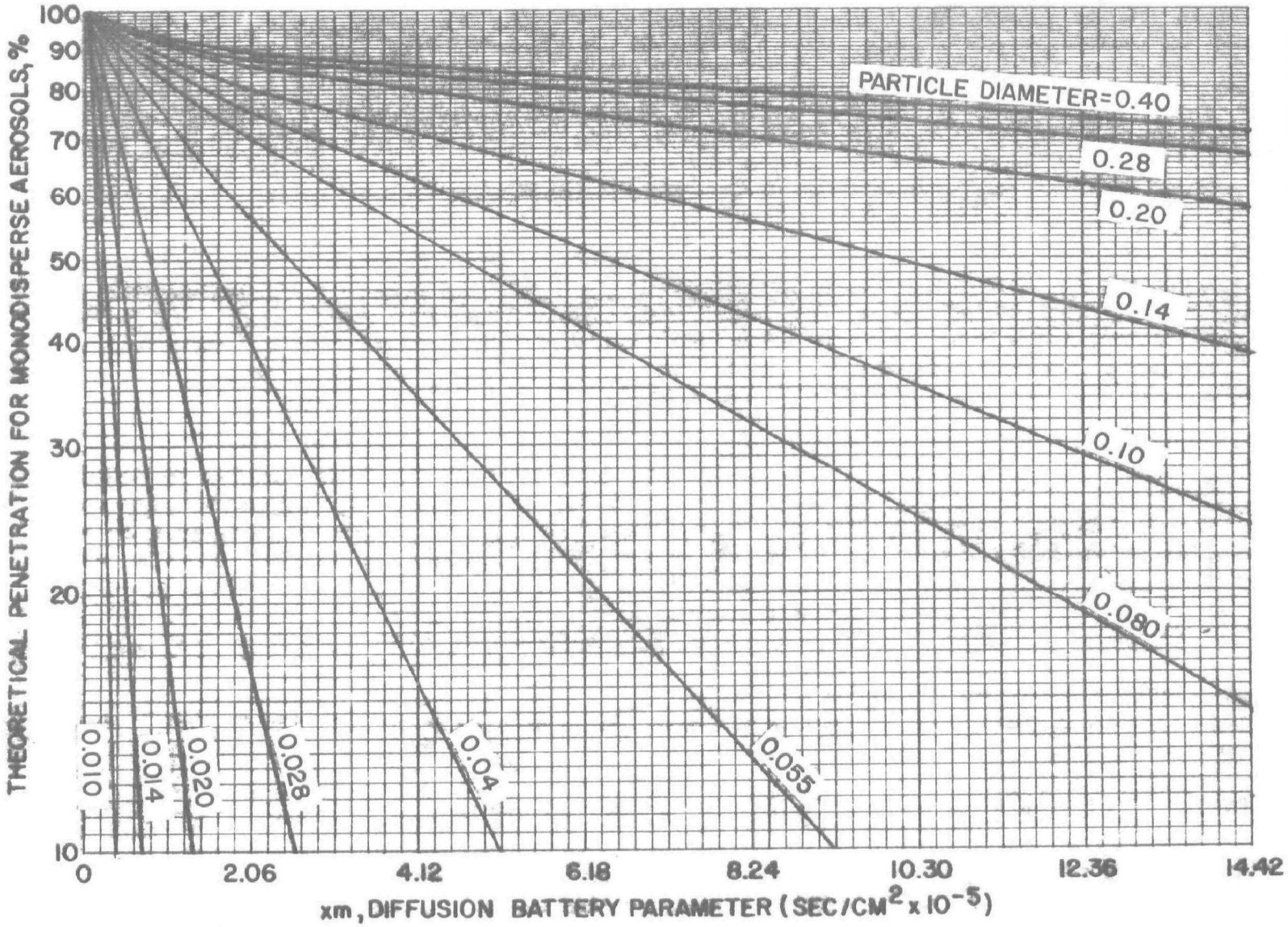

Figure C2. Nomograph for determining fine particle size distribution using diffusion battery data.

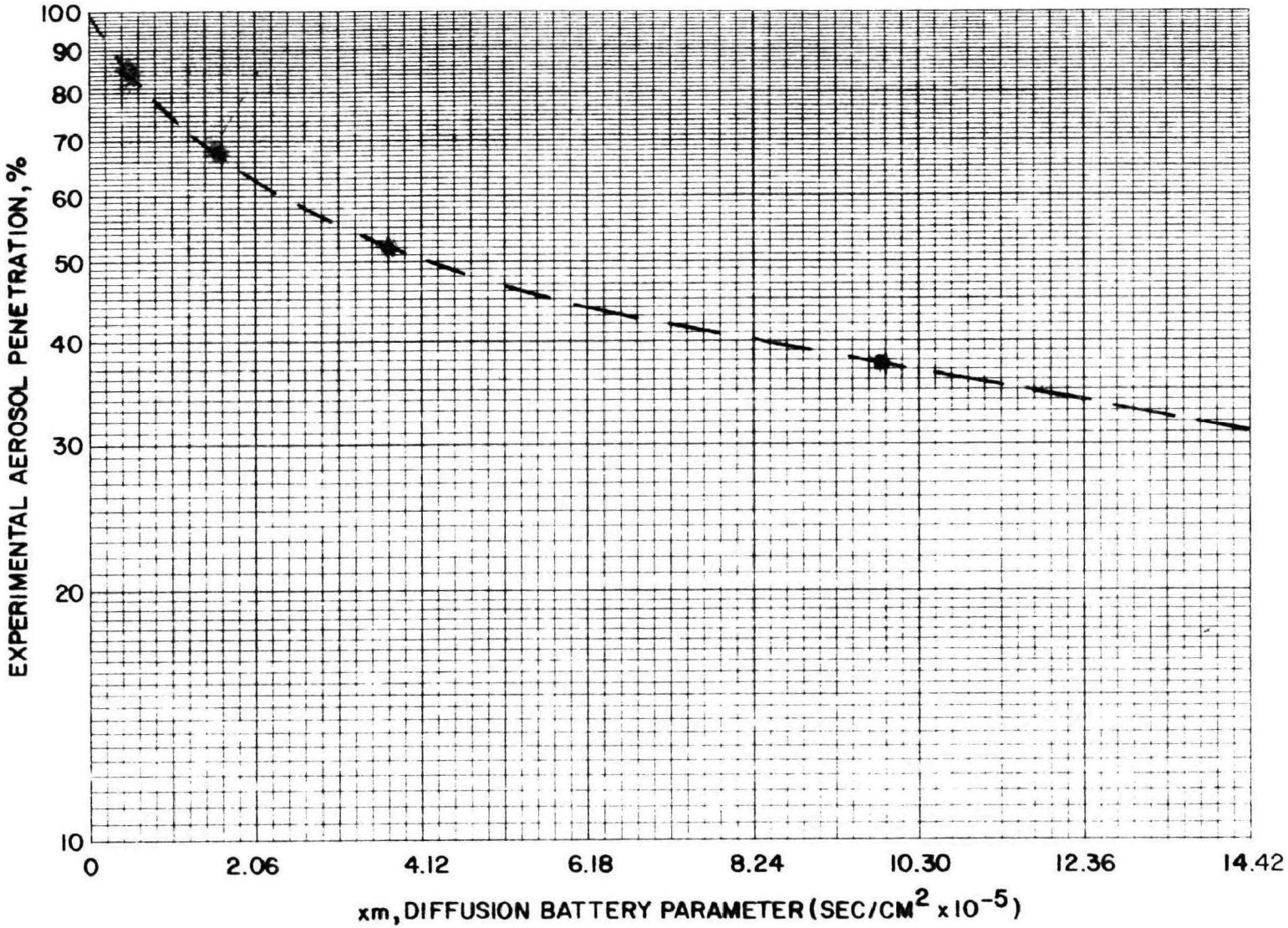

Figure C3. Experimental diffusion battery data to be used in conjunction with Figure C2 in determining fine particle size distribution.

$\frac{m/n_o}{0.91}$ is plotted versus 2xm; for three similar batteries

$\frac{n/n_o}{(0.91)^2}$ is plotted versus 3xm; etc..

The graphical stripping procedure consists of placing the experimental curve on top of the nomograph (C2) so that the ordinate axes lie along the same line. The experimental curve is then shifted vertically until it is slightly above a matching curve on the nomograph. The experimental curve should approach, but not cross, the theoretical (nomograph) curve at the extreme right hand side of the nomograph. The value on the ordinate on the experimental curve where the monodisperse penetration curve crosses (y intercept) is the fraction of the aerosol which is contained in that size (theo. curve) and larger. The theoretical curve is subtracted from the experimental curve and the result is treated as a new experimental curve. From this point, the process is repeated until a cumulative particle size distribution is obtained over the desired range.

APPENDIX D - OPTICAL TECHNIQUES

Insofar as this project is concerned, the study of aerosol size distributions by optical techniques has taken second place to impactor and diffusional sizing methods. It has been used mainly to correlate inertial and diffusional data and has not undergone as extensive a study as these other sizing techniques.

These measurements of particle size and concentration by light scattering involved the use of a Climet Particle Size Analyzer, Model CI-201. The theory of operation has been described in an earlier section. In this case, no correction was made for aerosol refractive index. The particle counter was calibrated in our laboratory using polystyrene latex spheres. The calibration curve is shown in Figure 4.

Data was obtained in two ways. The Climet has a front panel meter showing cumulative particles per cubic foot larger than an indicated size, selected as either 0.3, 0.5, 1.0, 3.0, 5.0 or 10.0 microns. Full scale on the meter is 10^6 particles/cu.ft., In normal field use, sample stream dilution was required to keep the concentration below this full scale value. The dilution system is described in the Appendix on Extractive Sampling. A size distribution was obtained by taking the differences in particle concentrations at adjacent size thresholds and plotting these values at the geometric mean of these particle sizes.

The particular Climet Analyzer received by Southern Research Institute from the Environmental Protection Agency had an Ortec digital ratemeter and an Ortec digital voltage spectrum scanner incorporated with the size analyzer. This allowed more resolution and a greater number of data points. The ratemeter also allowed for time averaging from 10 seconds to 10 minutes. This was useful at some testing locations where the concentration of large particles was quite low. Also, the scanning cycle would repeat automatically, allowing for uninterrupted data accumulation over several hours. This data was handled in the same fashion

as that acquired using the panel meter; i.e., by taking concentration differences and plotting at the particle size geometric mean.

Figure 6, found in the Experimental Methods Section, shows data acquired by the optical particle counter at a coal-fired power boiler. It correlates quite well with the impactor and diffusional data.

Birmingham, Alabama
July 12, 1974
2923-XXI
(10:1:2:15) mlm
Mr. D. B. Harris, Project Officer - 10 copies
Mr. M. P. Huneycutt, Contracting Officer - 1 copy
Mr. Robert Lorentz - 2 copies

REFERENCES

1. May, K. R., "The Cascade Impactor: An Instrument for Sampling Coarse Aerosols", J. Sci. Instr. 22 (October, 1945).

2. Andersen, A. A., "New Sampler for the Collection, Sizing, and Enumeration of Viable Airborne Particles", J. of Bacteriology, 76 (1958).

3. Brink, J. A., Jr., "Cascade Impactor for Adiabatic Measurements", Ind. and Eng. Chem., 44, No. 6 (June, 1952).

4. Rantz, W. E. and Wong, J. B., "Impaction of Dust and Smoke Particles", Ind. and Eng. Chem., 50, No. 4 (April, 1958).

5. Pilat, M. J., Ensor, D.S., and Busch, J. C., "Cascade Impactor for Sizing Particulates in Emission Sources", Am. Ind. Hygiene Assoc. J., 32, No. 8, (August, 1971).

6. Liu, B. Y. H., Whitby, K. T., and Pui, D. Y. H., "A Portable Electrical Aerosol Analyzer for Size Distribution Measurement of Submicron Aerosols", Presented at the 66th Annual Meeting of the Air Pollution Control Association, Paper No. 73-283, (June, 19730.

7. Cohen, J. J. and Montan, D. N., "Theoretical Considerations, Design, and Evaluation of a Cascade Impactor," Am. Ind. Hygiene Assoc. J., (March-April, 1967).

8. Lundgren, D. A., "An Aerosol Sampler for Determination of Particle Concentration as a Function of Size and Time", J. Air Pol. Con. Assoc., 17, No. 4, (April, 1967).

9. Gussman, R. A., Sacca, A. M., and McMahon, N. M., "Design and Calibration of a High Volume Cascade Impactor", J. Air Pol. Con. Assoc., 23, No. 9, (September, 1973).

10. Ström, L., "Transmission Efficiency of Aerosol Sampling Lines", Atmos. Env., 6, (1972).

11. Haberl, J. B. and Fusco, S. J., "Condensation Nuclei Counters: Theory and Principles of Operation", General Electric Technical Information Series, No. 70-POD 12 (1970).

12. Hodkinson, J. R., "The Optical Measurement of Aerosols", Aerosol Science, Academic Press (1966) ed. by C. N. Davies.

13. Berglund, R. N., "Basic Aerosol Standards and Optical Measurements of Aerosol Particles," Ph.D. dissertation, Mech. Eng. Dept., U. of Minnesota, (1972).

14. Fuchs, N. A., The Mechanics of Aerosols, The MacMillan Co., 60-5th Avenue, N. Y. (1964).

15. Sinclair, D., "A Portable Diffusion Battery", Am. Inst. Hygiene Assoc. J., (November, 1972).

16. Breslin, A. J., Guggenheim, S. F., and George, A. C., "Compact High Efficiency Diffusion Batteries", Staub-Reinhalt, Luft, Vol. 31, No. 8 (August, 1971).

17. Twomey, S., "The Determination of Aerosol Size Distributions from Diffusional Decay Measurements", J. F. I. (February, 1963).

18. Sansone, E. B. and Weyel, D. A., "A Note on the Penetration of a Circular Tube by an Aerosol with a Log-normal Size Distribution", Aerosol Science, Vol. 2 (1971).

19. Gormley, P. G. and Kennedy, M., Proc. Roy. Irish Acad., Vol. 52A (1949).

20. Fuchs, N. A., Stechkina, I. B., and Starasselskii, V. I., "On the Determination of Particle Size Distribution on Polydisperse Aerosols by the Diffusion Method", Brit. J. Appl. Phys., 13, pp. 280-281 (1962).

21. Liu, B. Y. H., Mechanical Eng. Dept., University of Minnesota, private communication.

22. Berglund, R. N. and Liu, B. Y. H., "Generation of Monodisperse Aerosol Standards", Environmental Science and Technology, Vol. 6, No. 2, 1973.

23. Lindblad, N. R. and Schneider, J. M., "Production of Uniform-Sized Liquid Droplets", J. Sci. Instr., Vol. 42, 1965.

24. Ström. L., "The Generation of Monodisperse Aerosols by Means of a Disintegrated Jet of Liquid", Rev. Sci. Instr., Vol. 40, No. 6, 1969.

25. Stober, W. and Flachsbart, H., "An Evaluation of Ammonium Fluorescein as a Laboratory Aerosol", Atmos. Environ., Vol. 7, 1973.

26. Picknett, R. G., "A New Method of Determining Aerosol Size Distributions From Multistage Sampler Data", Aerosol Science, 1972.

TECHNICAL REPORT DATA
(Please read Instructions on the reverse before completing)

1. REPORT NO. EPA-650/2-74-102	2.	3. RECIPIENT'S ACCESSION NO.
4. TITLE AND SUBTITLE Particulate Sizing Techniques for Control Device Evaluation		5. REPORT DATE October 1974
		6. PERFORMING ORGANIZATION CODE
7. AUTHOR(S) Wallace B. Smith, Kenneth M. Cushing, and Joseph D. McCain		8. PERFORMING ORGANIZATION REPORT NO. SORI-EAS-74-138
9. PERFORMING ORGANIZATION NAME AND ADDRESS Southern Research Institute 2000 Ninth Avenue, South Birmingham, Alabama 35205		10. PROGRAM ELEMENT NO. 1AB012; ROAP 21ADM-011
		11. CONTRACT/GRANT NO. 68-02-0273
12. SPONSORING AGENCY NAME AND ADDRESS EPA, Office of Research and Development NERC-RTP, Control Systems Laboratory Research Triangle Park, NC 27711		13. TYPE OF REPORT AND PERIOD COVERED Summary: 7/73-6/74
		14. SPONSORING AGENCY CODE
15. SUPPLEMENTARY NOTES		

16. ABSTRACT The report gives results of a study that has proven the feasibility of measuring particle size distributions in stack gases (and fractional efficiencies) from 0.01 to 15 μm. It describes a first-generation system that represents a viable package that can be improved and will continue to be useful in making these extremely important measurements related to the control of fine particles. Three techniques were used to measure particle size distributions in industrial plant environments under a variety of conditions: cascade impactors, in the particle size range 0.5-20 μm; diffusion batteries and CN counters, 0.01-0.2 μm; and optical counters, 0.3-2 μm. The stage collection efficiencies of several impactors and cyclones were also measured in the laboratory. A vibrating-orifice aerosol generator was used for calibration. With careful use, cascade impactors can give reliable particle size information; however, no single impactor was versatile enough to measure accurately under the extreme grain loading variations found between control device inlets and outlets. Stage collection efficiencies of all impactor stages tested (except one) agreed fairly well with the theory of Rantz and Wong. Diffusional sizing was practical with diluted samples; although it is tedious and time consuming: it is most accurate for sources with relatively stable particle size distribution and concentration.

17. KEY WORDS AND DOCUMENT ANALYSIS

a. DESCRIPTORS		b. IDENTIFIERS/OPEN ENDED TERMS	c. COSATI Field/Group
Air Pollution	Optical Measurement	Air Pollution Control	13B
Measurement	Cyclone Separators	Stationary Sources	07A
Flue Gases		Fine Particulate	21B
Particle Size Distribution		Cascade Impactors	
		Diffusion Batteries	14B
Industrial Plants		CN Counters	13H

18. DISTRIBUTION STATEMENT Unlimited	19. SECURITY CLASS (This Report) Unclassified	21. NO. OF PAGES 127
	20. SECURITY CLASS (This page) Unclassified	22. PRICE

EPA Form 2220-1 (9-73)